EEFIT

Earthquake Engineering Field Investigation Team

EEFIT Project Report

2015 Nepal Earthquake: Seismic Performance and Post-Earthquake Reconstruction of Stone Masonry Buildings

Rohit Kumar Adhikari and Dina D'Ayala

Department of Civil, Environmental and Geomatic Engineering,

University College London

UCL

October 2019

ACKNOWLEDGEMENT

Cover Photos: Stone in mud mortar masonry houses: damaged due to the 2015 Nepal earthquake (left) and a newly built house (right), photos from Sindhupalchowk district.

Credits are given to the original sources for the photos and figures used in this report. All other photos, for which source is not mentioned, are taken by the first author.

TABLE OF CONTENTS

LIST OF FIGURES

LIST OF TABLES

ABSTRACT

Despite economic and human losses, disasters teach us very important lessons. It is hence important to collect, document, analyse and understand the causes and impacts of natural disasters such as an earthquake to minimize losses in future disastrous events. This report is an outcome of the analysis of data and information related to the damage and post-earthquake reconstruction of residential buildings, collected during the field survey by the authors, in light of 2015 Nepal earthquake sequence. First, the extent of damage sustained by the residential buildings in 2015 Nepal earthquake sequence is presented, focusing on stone in mud mortar masonry typology as this was the highest contributor to the seismic damage. As the reconstruction is currently ongoing and the Nepal government aims to use this opportunity to increase the seismic resilience of communities, some pressing issues in the post-earthquake reconstruction in rural mountainous areas such as building usability/functionality, code-compliance and construction quality are discussed. Then, the range of prevalent typologies of pre- and post-earthquake residential houses and their distribution is presented. Since uncoursed random rubble stone masonry in mud mortar is the most common construction type in the country, even in the post-earthquake reconstruction, the construction characteristics of these typologies are discussed in detail. The results of non-linear seismic analysis on the pre- and post-earthquake stone in mud mortar masonry typologies are then presented and discussed in terms of capacity curves and failure mechanisms. As per the seismic design code of Nepal, site specific seismic performance assessment is conducted to understand the seismic design levels of these constructions. Finally, seismic performance assessment for a number of ground motions is conducted on both pre- and post- earthquake stone in mud mortar masonry typologies in order to derive seismic fragility and vulnerability functions, considering the uncertainty in ground motions and material quality, which are useful tools in understanding the associated seismic risk as well as for developing effective seismic strengthening measures to reduce risk in future earthquakes.

1   INTRODUCTION

Nepal is one of the most earthquake prone countries in the world and has experienced several devastating earthquakes of magnitude exceeding Mw7.5 (i.e. in 1255, 1408, 1505, 1833, 1934 and 2015) (Thapa and Wang, 2013). The most recent earthquake of moment magnitude Mw 7.8, occurred in the central region of Nepal on April 25, 2015, at 11:56 Nepal Standard Time with the epicentre (28.147°N, 84.708°E) located in the village of Barpak, Gorkha district, approximately 78 km northwest of Kathmandu (Figure 1) with a focal depth of 15 km (USGS, 2015). Hundreds of aftershocks with Mw greater than 4.0 were recorded during more than a year after the earthquake (NSC, 2016), with some significant seismic events having Mw 6.7 on April 26, 2015, and Mw 7.3 on May 12, 2015 (Figure 1). The earthquake resulted in a Maximum Modified Mercalli Intensity of IX (Violent) with about 8,790 deaths and nearly 22,300 injuries (NPC, 2015). The earthquake sequence hit the residential houses severely, affecting about 800,000 houses, thereby leaving about 8 million people homeless (NPC, 2015). The seismic sequence resulted in an economic loss of about $7 billion half of which was contributed by the housing sector damage (NPC, 2015).
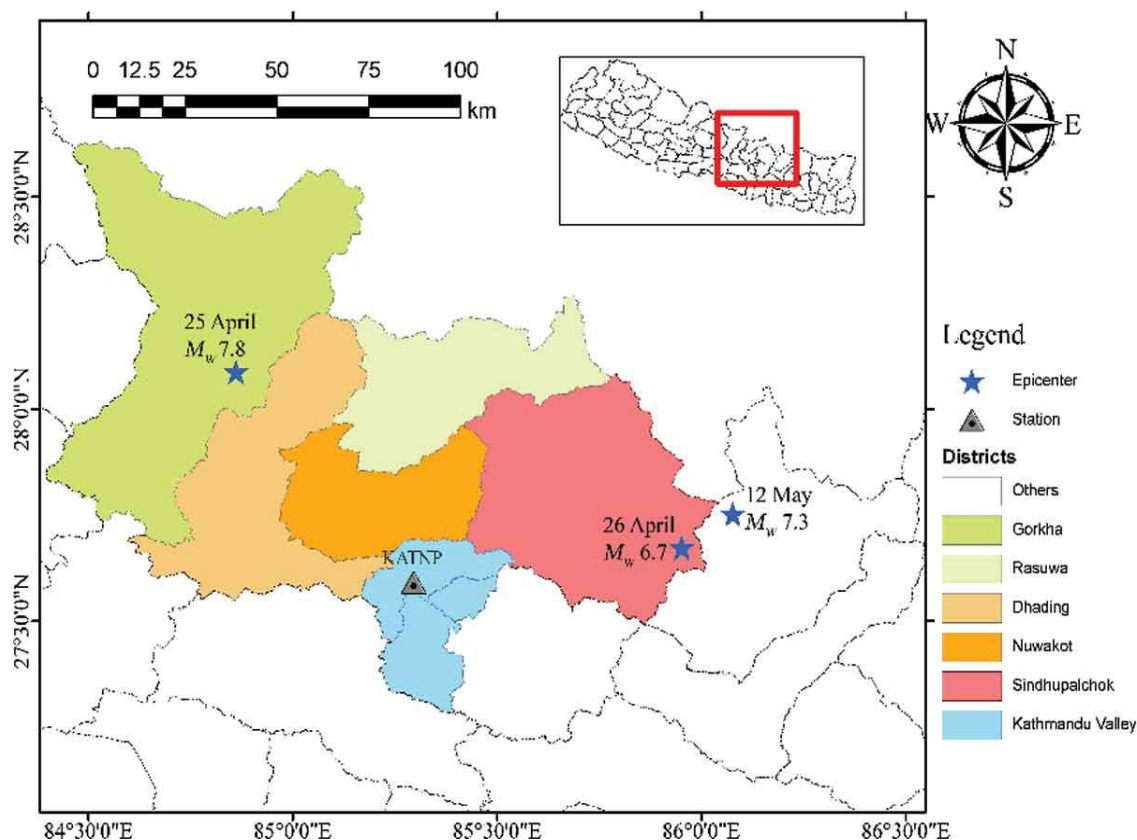
Figure 1. Location of the mainshock and major aftershocks of the 2015 Nepal earthquake (Bhagat et al., 2018).

After the 2015 earthquake sequence, several post-earthquake damage surveys were conducted by different groups of researchers focusing on the extent and type of damage sustained by the building structures (e.g. Goda et al., 2015; Parajuli and Kiyono, 2015; Adhikari et. al., 2015; Varum et al., 2017; Bhagat et al., 2018, Wilkinson et al., 2019). All of these survey missions reported that the significant damage was sustained by low-strength masonry buildings (i.e. stone and brick masonry buildings

with mud mortar) which lacked seismic resistant features while the reinforced concrete buildings suffered little damage. As the seismic design and building code implementation were poorly practiced in the country, the heavy damage was inevitable.

Recently, several studies are being published focusing on different aspects of the post-earthquake reconstruction. Sharma et al. (2018) discusses the challenges of reconstruction such as the political issues, lack of coordination, shortage of manpower and materials etc. HRRP (2018) presents several examples of newly built houses of different typologies in the affected districts reporting the status of construction, technical issues such as code-compliance and level of technical assistance received by the house-owners. The same document also reports the median cost of construction of each different typology, based on the survey of several hundred households, which ranges from about $6,000 USD for stone masonry houses to $20,000 for RC constructions. There are more urgent issues which needs attention and immediate actions from NRA and other stakeholders as well as the communities such as the workmanship and quality of construction, layouts/functional requirements of newly built houses etc. which will be discussed in this report.

In the context of Nepal, the construction characteristics, seismic capacity and strengthening needs of the urban constructions such as RC buildings and Newari constructions in Kathmandu valley have been studied by many researchers in the past (e.g. D'Ayala and Bajracharya, 2003; D'Ayala, 2004; Chaulagain et al., 2013; Chaulagain et al., 2015, Gautam et.al., 2016). However, the construction characteristics and seismic capacity of rural vernacular constructions, for instance stone masonry-based typologies, practiced for centuries, have not been studied in detail. Although it is known that these are seismically vulnerable, it is necessary to quantify their seismic capacity and understand deficiency and possible failure mechanisms so that the construction practice of these traditional building types can be improved in order to make these seismic resistant. The main obstacles to the analytical/numerical study of these masonry buildings are the modelling issues related to the heterogenous nature of masonry and the uncertainties in the input parameters such as material properties which can vary greatly from one building to the next. Furthermore, as these constructions lack quality control measures, the uncertainties further increase.

In literature, there are few experimental studies exploring the effective strengthening methods for stone masonry in mud mortar buildings. Pun (2015) studied the applicability of galvanized steel wire (GSW) for improving the seismic performance of coursed semi-dressed stone in mud mortar masonry buildings by conducting static and dynamic shake table tests on unreinforced and reinforced masonry walls. Although, the masonry bond pattern of the tested walls doesn't well represent the Nepalese uncoursed random rubble stone masonry construction, this study showed that the external steel wire mesh reinforcement could considerably improve the strength as well as ductility of stone in mud mortar masonry walls. In light of 2015 Nepal earthquake, Wang et al. (2018) conducted several in-plane cyclic tests on full-scale walls, without and with retrofitting, to study the effectiveness of low-cost and affordable retrofitting options. This study proved that the fragile behaviour of rubble stone masonry walls can be effectively improved in terms of stiffness, strength, integrity and ductility with carefully designed low-cost retrofitting options using locally available materials such as wood, gabion wires and tarpaulin. Bothara et al. (2019) conducted shake table tests on scaled models of semi-reinforced stone in mud mortar masonry school buildings. The reinforcement included horizontal

bands and steel mesh on both sides of all masonry walls. This study demonstrated that such reinforcements can prevent collapse of these buildings even under intense seismic shaking with peak ground acceleration (PGA) as high as 1.0g.

Recently, in order to develop effective retrofitting options for existing rubble stone masonry in Nepal (both damaged and undamaged due to the 2015 earthquake sequence), Build Change (2019) conducted an experimental campaign to characterize the material properties as well as the lateral in-plane behaviour of Nepalese random rubble stone masonry walls. The hysteretic response under cyclic shear-compression loading results showed that the strength and ductility of rubble stone in mud mortar masonry walls can be substantially improved by the use of through concrete and cement plaster. The results of the material characterizations tests are very useful inputs in the numerical modelling and analysis of Nepalese random rubble stone in mud mortar masonry constructions.

However, very few studies have investigated the global building level seismic performance and behaviour of Nepalese stone masonry in mud mortar building typology. Guragain (2015) conducted non-linear time history analyses of common typologies of single and two-storied stone masonry buildings to derive analytical fragility functions using the applied element method. As there were no reliable tests results available on Nepalese stone masonry buildings for mechanical characterization, this study lacks to report the relevant inputs in their numerical analyses and hence its reliability is limited. Similarly, Bothara et al. (2018) studied the analytical seismic performance of unreinforced and semi-reinforced single-storied stone masonry buildings using finite element method in order to show the benefits of minimal reinforcement on improving the seismic performance. However, rectangular elements are used in this study to characterise the random rubble stone masonry walls and the key inputs of material properties used for rubble stone masonry are very high, again limiting the reliability of the reported capacity curves and failure modes.

Since studies on seismic capacity, collapse mechanisms or reliable fragility functions for traditional as well as newly built Nepalese stone masonry typologies are currently lacking, this study focuses on addressing and answering these issues. For the numerical analysis presented in this study, as the material properties are key inputs, the results of recent test campaign on Nepalese stone masonry walls conducted by Build Change (2019) are used. Furthermore, advanced non-linear analysis using element by element modelling technique is conducted in the present study in order to account for the randomness of the masonry fabric. The outcomes of this study will be beneficial in a number of ways: to appreciate the seismic design levels, to understand the seismic vulnerability and failure mechanisms, to develop effective strengthening measures and to improve the construction practice of both pre-earthquake and post-earthquake stone masonry building typologies so that the rural communities can be made more resilient to seismic hazard.

The report is organized as follows. First, the extent of damage sustained by the residential building hit by the 2015 Nepal earthquake sequence is discussed. As the reconstruction is currently ongoing, some pressing issues in the post-earthquake reconstruction in rural mountainous areas such as building usability/functionality, code-compliance and construction quality are discussed. Then the range and distribution of different typologies of pre- and post-earthquake residential houses in the affected districts is presented. Since uncoursed random rubble stone masonry in mud mortar (referred as SMM hereafter) is the most common construction type in the country, even in the post-

earthquake reconstruction, the construction characteristics of these buildings are discussed. The results of advanced non-linear seismic analyses on the representative index buildings of the pre- and post-earthquake SMM typologies is then presented in terms of capacity curves and failure mechanisms. As per the seismic design code of Nepal, site specific seismic performance assessment is also conducted to understand the seismic design levels of these structures. Then, seismic performance assessment for a number of ground motions is conducted on both pre- and post-earthquake SMM typologies in order to derive seismic fragility and vulnerability functions, considering the uncertainty in ground motions and material quality, which are useful tools in understanding the associated seismic risk as well as for developing effective seismic strengthening measures to reduce risk in future earthquakes.

2 DAMAGE TO RESIDENTIAL BUILDINGS

Extensive damage to many public and private buildings was observed in the 2015 Nepal earthquake sequence. The residential houses were hit hard by the earthquake and its aftershocks resulting in about half a million houses destroyed and more than 250,000 houses partially damaged (NPC, 2015). In several cases, whole villages were turned into rubble in areas where old vernacular constructions such as stone masonry in mud mortar (SMM) houses with minimal seismic resistant features were mostly present. In some of the severely hit districts (Figure 2) such as Sindhupalchowk, as high as 90% of the total houses suffered heavy damage to complete collapse (HRRP, 2017).
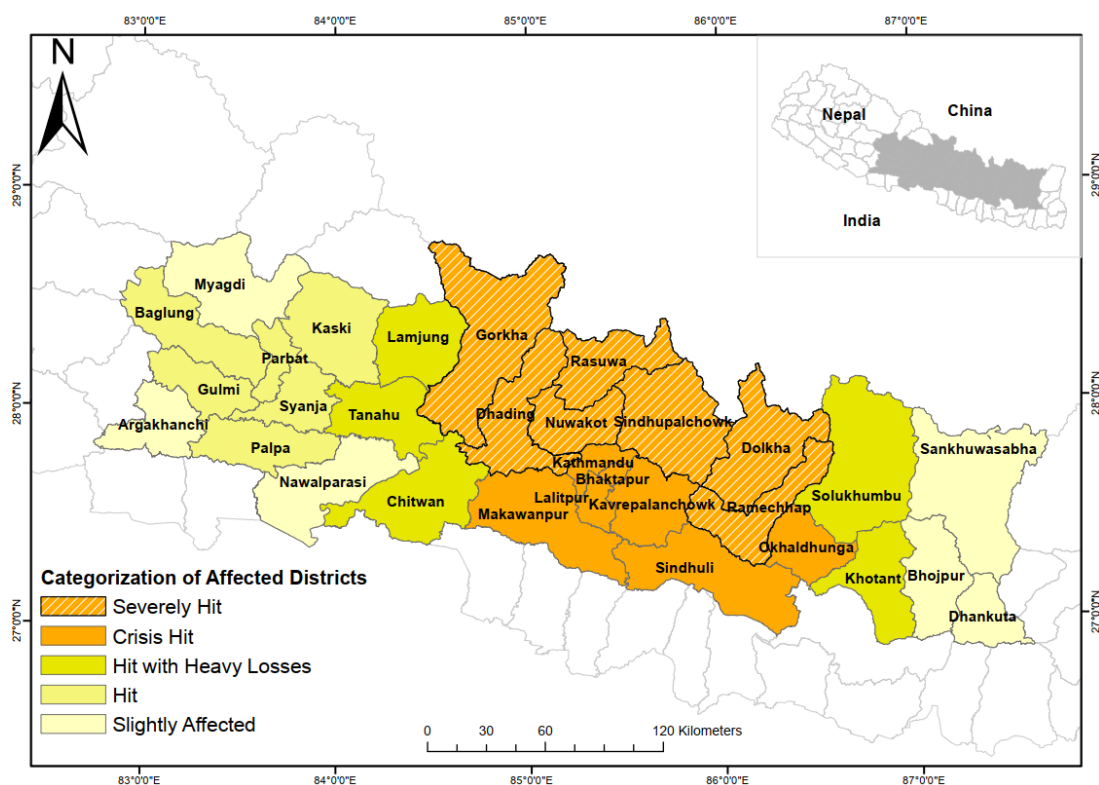
Figure 2. Map showing the categorization of earthquake-affected 31 districts (NPC, 2015).

4

House Damage Grading by Districts:

District	Grade 1	Grade 2	Grade 3	Grade 4	Grade 5	Total
Bhaktapur	1,045	1,132	4,647	13,128	10,968	30,920
Dhading	4,951	7,526	15,218	26,080	35,346	89,121
Dolakha	1,353	2,993	6,520	14,409	35,364	60,639
Gorkha	4,351	8,555	15,507	22,536	27,125	78,074
Kathmandu	1,918	2,173	6,106	16,099	24,835	51,131
Kavrepalanchowk	8,330	11,726	25,130	28,974	23,859	98,019
Lalitpur	1,746	2,125	5,282	11,152	12,788	33,093
Makwanpur	32,540	21,135	18,525	10,928	7,866	90,994
Nuwakot	2,615	2,745	8,209	23,284	40,295	77,148
Okhaldhunga	7,961	8,605	9,220	7,946	5,620	39,352
Ramechhap	2,127	7,151	16,945	20,910	11,490	58,623
Rasuwa	277	343	782	2,064	9,178	12,644
Sindhuli	13,089	14,468	17,086	15,918	8,191	68,752
Sindhupalchowk	1,233	2,009	3,271	10,796	71,432	88,741
TOTAL	83,536	92,686	162,448	224,224	324,367	877,261

Note:

This map highlights the areas by Damage Grade present in 14 most affected districts of Nepal.

Legend
- Damage Grade 1
- Damage Grade 2
- Damage Grade 3
- Damage Grade 4
- Damage Grade 5

| Creation Date: | 26 DEC 2016; | Projection: | WGS 84; | Map Data Source: | NRA; | | Web Resource: | www.nra.gov.np; |
| Map Doc Name: | DamageGrade | Datum: | EVEREST 1830; | Geo Data Source: | DoS, MoFALD; | | Feedback: | ict@nra.gov.np |

Figure 3. Damage grade distribution of residential houses in 14 most affected districts (NRA, 2016a).

5

As can be seen from Figure 3 which presents the distribution of damage grade at building level in the affected districts, the highest damage grade i.e. 'damage grade 5' is mostly concentrated in the rural mountainous region where the SMM typology is most common, and in the Kathmandu valley where the traditional Newari construction in adobe/brick in mud mortar construction was most common. Among the damaged buildings in all the affected districts, about 96% were of load bearing masonry typology and only 4% of the damaged buildings were RC constructions (NPC, 2015). Figure 4 shows example photographs of typical damage sustained by low-strength masonry and non-engineered RC construction during the 2015 earthquake sequence. Typical damage to different typologies of residential buildings, cultural heritage structures as well as school buildings due to the 2015 earthquake sequence can be found in more detail in Bhagat et al. (2018).

(a)

(b)

(c)
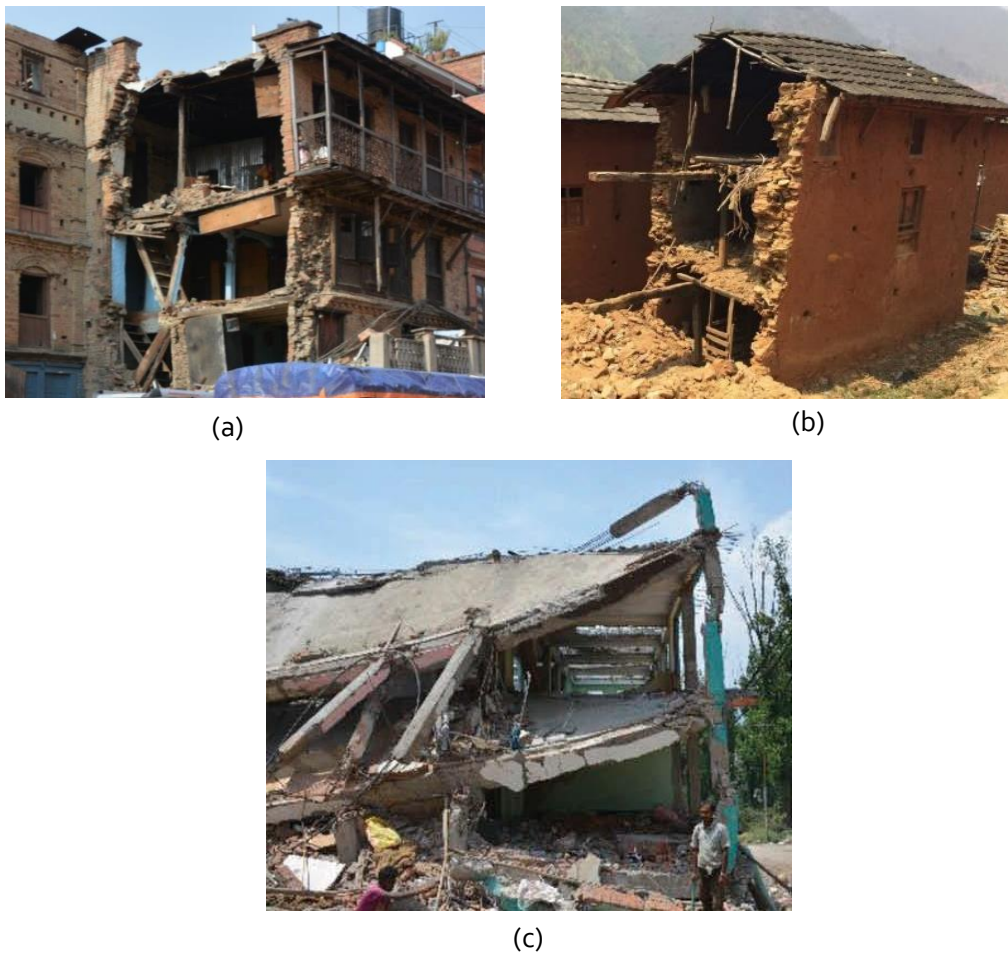
Figure 4. Damage sustained by residential buildings in the 2015 Nepal earthquake: (a) out-of-plane collapse of brick in mud mortar masonry wall in traditional Newari construction (Photo from Bhaktapur), (b) out-of-plane collapse of SMM masonry (Photo credit: Build Change) and (c) Complete collapse of non-engineered RC construction.
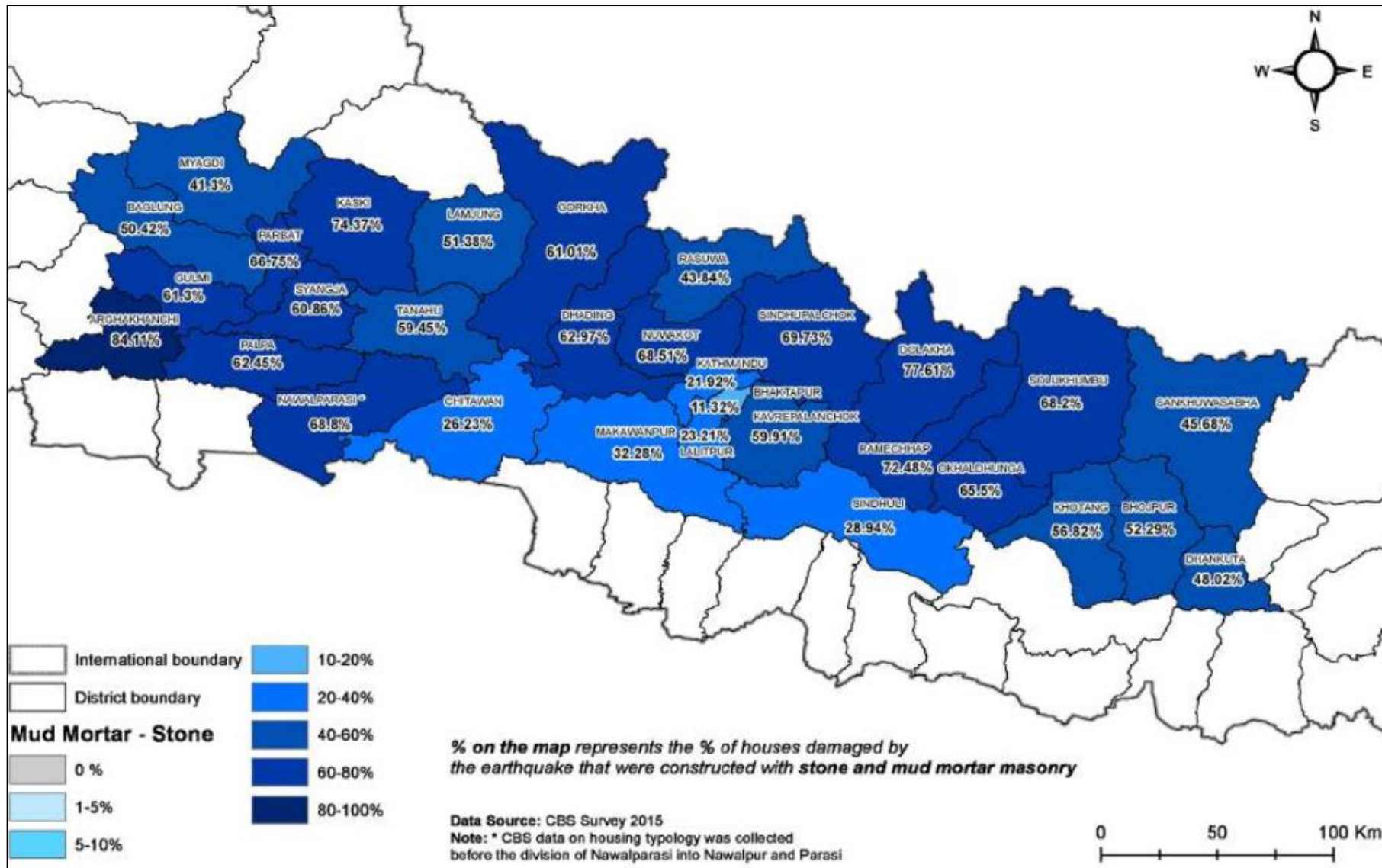
Figure 5. Distribution of damage to SMM typology in the affected districts (HRRP, 2018).

The damage suffered by the existing stone in mud mortar masonry (PRE-SMM) typology during the 2015 Nepal earthquake was extensive and contributed significantly to both economic and human losses due to the earthquake. Figure 5 shows the distribution of damage to SMM buildings in the affected districts due to 2015 earthquake sequence (HRRP, 2018). The damage sustained by the PRE-SMM buildings in the remote mountainous districts such as Dolakha and Sindhupalchowk was very heavy such that the damage contribution of such buildings to the total damage was as high as 77%. Typical damage patterns sustained by the PRE-SMM buildings in the 2015 Nepal earthquake has been reported in several literature (Dizhur et al., 2016; Parajuli and Kiyono, 2015 etc.) and the recurring failure modes are: vertical separation of wall, complete out-of-plane overturning collapse, gable collapse, shear damage in the in-plane walls with openings, out-of-plane bulging and delamination etc. Similar failure modes were reported for stone masonry buildings by Spence and D'Ayala (1999) after the 1997 Umbria-Marche Earthquakes in Italy. Figure 6 presents the photographs of these main damage patterns experienced by PRE-SMM buildings in the 2015 Nepal earthquake

(a) Separation of short wall at cross-wall connection

(b) Complete out-of-plane collapse (Photo: Build Change)

(c) Collapse of gable (Photo: Build Change)

(e) Out-of-plane bulging and debonding

(d) Shear damage in in-plane walls with openings

Figure 6. Main failure mechanisms of PRE-SMM typology observed in the 2015 Nepal earthquake.

This section presented the extent and type of damage suffered by the residential buildings in the 2015 Nepal earthquake sequence in which the SMM construction contributed to the highest seismic loss. Lack of seismic design practice and code-compliance were the main reasons of such poor seismic performance of the residential building stock. As Nepal is aiming to increase the seismic resilience of built infrastructure by adopting 'build back better' principle in the post-earthquake reconstruction, in the next section, some pressing issues in the reconstruction of residential buildings is reported.

3 SOME ISSUES IN POST-EARTHQUAKE RECONSTRUCTION

In this section, some important issues in the ongoing post-earthquake reconstruction in Nepal are discussed. These information and discussions presented herein are based on the observations, data collection and interviews conducted by the author during (and after) his field visit to the affected districts in December 2018.

3.1 State of Reconstruction

Almost a year after the devastating earthquake sequence, the National Reconstruction Authority (NRA) of Nepal developed and started the implementation of a Post Disaster Recovery Framework (PDRF) (NRA, 2016b) based on the findings of the Post Disaster Needs Assessment (NPC, 2015). One of the key objectives of the PDRF is the reconstruction of disaster resilient residential houses in the affected areas. According to the PDRF, in the 31 earthquake affected districts (14 of which classified as highly affected districts, see Figure 2), owners are being provided with financial assistance in tranches (total of $3000 approx.), supported by timely provision of technical assistance, training and facilitation, so that people can rebuild their own houses as soon as possible. Introduction and duties of key stakeholders, including NRA, in the post-earthquake reconstruction can be found in Sharma et al. (2018). As of 1st October 2019, about 56% of the identified housing grant beneficiaries have completed the construction of their new houses (NRA, 2019b). This indicates that even 4 years after the earthquake, about half of the total beneficiaries haven't finished the complete reconstruction of their houses. The reasons for the regional variations in the rate of reconstruction and overall slower reconstruction process are several, such as unstable government, transition into federalism, economic hardships, coordination issues between stakeholders, issues related to the availability of construction materials and skilled labour etc. (see also Sharma et al., 2018).

3.2 Usability/Functional Aspects of Reconstruction

The main purpose of building a house is to serve its basic functions and every day uses of the occupiers, as totally integrated to their culture, well beyond the need to withstand strong earthquakes. In the rural mountainous areas where the transportation of modern construction materials is difficult, POST-SMM typologies have been built while in the peri-urban setting, brick in cement mortar houses are frequently constructed. Sadly, many residential houses (particularly load bearing masonry houses) have been built without planning the current and future space requirements and the new houses do not blend with the socio-cultural scenario of the communities. These houses lack typical layouts of houses that include living rooms, bed rooms, bathrooms, kitchen etc. although the design catalogue published by NRA (2015) includes such provisions in the suggested layouts (see Figure 7). Furthermore, as most of the rural mountainous households are farmers, no provisions for storage spaces for harvests, overhangs for drying of crops, livestock sheds etc. can be seen in most of the new construction. As observed and surveyed by the author during his field trip in Sindhupalchowk district, many of the newly built houses are substantially under dimensioned, with respect to the needs of their occupiers. Figure 8 compares the typical pre-earthquake and post-earthquake masonry house typologies in rural mountainous district. The footprint of both existing

and newly built houses is comparable at about 36 m² (refer to Figure 38 for dimensions). However, while the existing houses were mostly two storied with an attic making available gross floor area of about 108 m², newly built houses (both POST-SMM and POST-BCM (Brick in Cement Mortar) typologies) are mostly single storied with only the usable ground floor area of about 36 m² which is as only as one third of the floor area of the common PRE-SMM buildings. Figure 9 shows further examples of single-storied POST-SMM houses with one to two-rooms, some of which have been already abandoned.
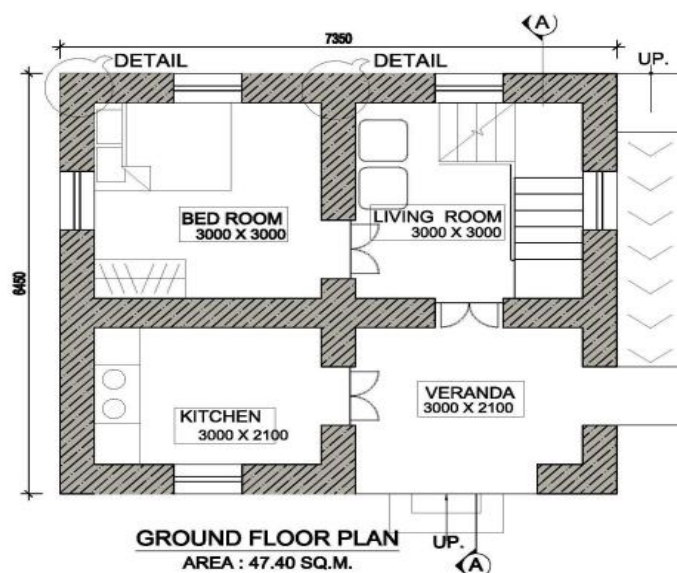
Figure 7. Layout of a SMM model house included in NRA design catalogue (NRA, 2015).

(a)

(b)

(c)

Figure 8. Photographs of typical (a) PRE-SMM, (b) POST-SMM and (c) POST-BCM buildings (Photos from Chautara, Sindhupalchowk).

10

Figure 9. Examples of newly built small 'box-type' POST-SMM houses around the Chautara area of Sindhupalchowk district. Plan area of these houses is smaller than 35 m^2.

From the interviews in the affected communities conducted by the author during his field trip, it emerged that there are several reasons behind the selection of such small houses for the reconstruction by the house owners:

- **Economic hardships** – some of the house owners mentioned that this was the only size of house they could build with the financial assistance ($3000 approx.) provided. The median total cost of construction of different typology of houses can be seen in Figure 10 which is based on the survey of several hundred households in the affected districts (HRRP, 2018).

- **Lack of adequate technical information and assistance** – some of the owners were informed that small plan single-storied houses were seismically stronger than larger and multi-storeyed houses, which is true but seismic resistance is secondary factor in house construction, as explained earlier, the primary purpose being to provide usable space commensurate to life requirement. Furthermore, the NRA engineers are not well trained for providing technical support for multi-story SMM constructions, as reported by several households (see HRRP, 2018).

- **Temporary solution** – some of the households replied that they constructed these houses as temporary solutions and will build another house in near future after saving enough money.

- **Monetary interest** – few of the neighbours mentioned that the house owners built these small houses compromising further on the quality and workmanship only to get the financial assistance from the government.

- **Financial tranche deadlines –** in several cases, the beneficiaries ended up erecting a single room sheds to claim tranches by the deadlines set by NRA (e.g. see Nepali Times, 2018a).
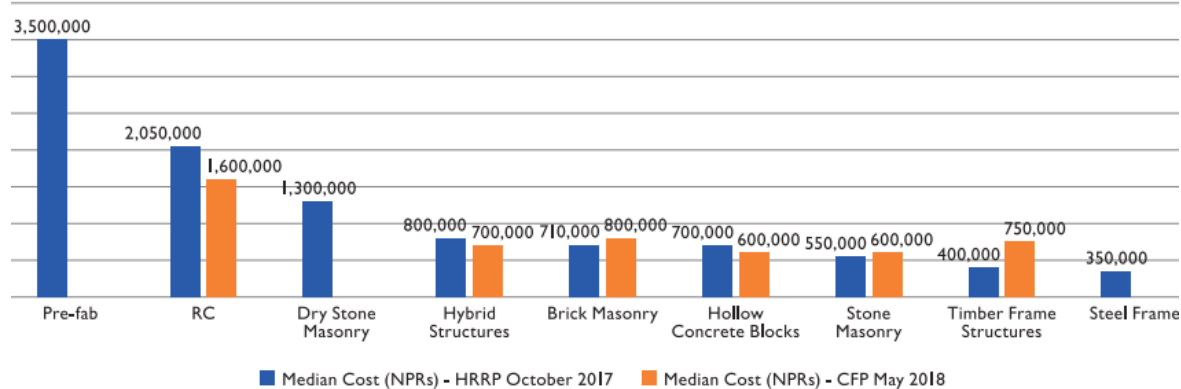
Figure 10. Median construction cost for different typologies of newly built houses in Nepal after the 2015 seismic sequence (HRRP, 2018).

Did the affected communities forget to build 'home' by being encircled inside the ring of 'seismic resistant designs' resulting in 'box-type' houses? Ramifications of such constructions has already started and will increase further in the coming future adversely affecting the livelihood of the communities. Whatever be the reasons behind, the construction of such houses with inadequate space is not a sensible policy. At the beginning of reconstruction process, NRA and all the stakeholders to be involved in reconstruction should have thought, planned and discussed the requirements and preferences of the affected communities about the functional and space requirements in their new houses. During the construction phase as well, NRA should have had stricter regulations for assessing the size/type of houses being constructed against the housing space requirements of each households.

3.3 Quality/Workmanship/Non-Compliance Issues

There are several cases where use of poor-quality material, poor workmanship and non-compliance issues (e.g. related to the size and shape of buildings, positioning and size of openings, size and positioning of seismic bands etc.) have been identified in the newly built houses (HRRP, 2018). Although NRA issued a correction/exception manual in 2017 (NRA, 2017), the implementation in the field doesn't seem effective. As the construction of these houses were carried out by local masons, the workmanship in several cases were found to be poor (see Figure 11, for example) particularly in case of RC bands where rebars can be seen exposed and cross-sections at some locations hardly reaching 50 mm while the requirement is 75 mm (NRA, 2016c). In spite of these defects, such houses have passed the inspections by the NRA engineers. Furthermore, due to the lack of quality control measures on site for mortar preparation, concrete mixing etc., the uncertainty in the material properties and hence the lateral capacity of walls is high. However, these issues are hard to overcome in rural areas. The non-compliant issues (such as incorrect positioning of seismic bands, larger attic heights etc.) are frequent in multi-storied constructions with larger plan areas which were built with

limited technical assistance from the NRA field engineers as they themselves lacked relevant trainings (HRRP, 2018, see Figure 12).

| (a) | (b) |
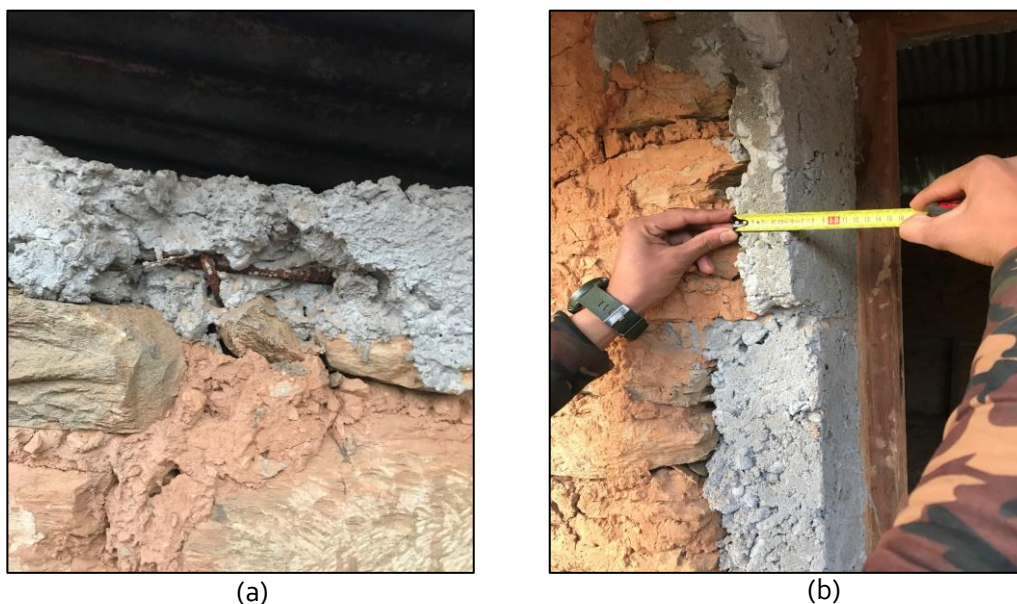
Figure 11. Poor workmanship and/or poor-quality concreting in the seismic bands in POST-SMM constructions.

(Photo from Sindhuli)   (Photo from Solukhumbu)

Figure 12. Photographs of multi-storied non-compliant houses built without technical assistance because NRA engineers were unable to provide timely technical guidance as they didn't receive training for multi-storied SMM constructions (HRRP, 2018).

It is interesting to note that, after the heavy damage sustained by the traditional masonry typologies in the 2015 seismic sequence, a misbelief has spread that the use of modern construction materials such as concrete and steel make houses seismic resistant. However, with engineering-based minimal improvements of local crafts, practiced and developed over centuries, seismic resistant structures can be constructed with traditional materials such as stone and timber (see D'Ayala, 2013 and Figure 13 for example). Hence, improving the existing traditional construction methods such as timber band and lacing with which the masons are familiar should have been promoted in the reconstruction. Nevertheless, seismic resistant features of timber elements have been used in SMM constructions in some rural locations where transportation of cement and reinforcement bars is difficult (Figure 14).
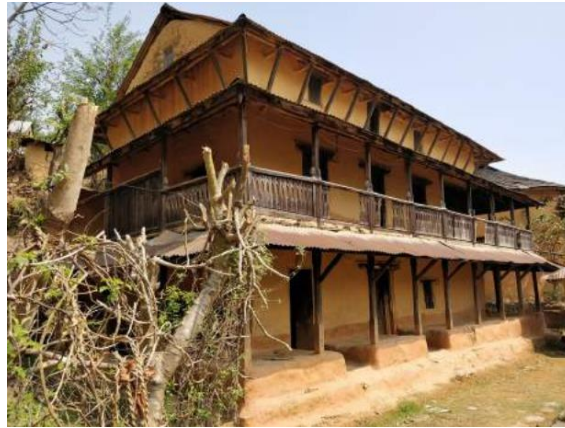
Figure 13. An 80 years old vernacular SMM house in Syangja that has survived three major earthquakes: one in 1934, one in 2011 and the recent 2015 seismic sequence. This house has traditional seismic resistant features of timber elements such as bands (two per story), lacing, vertical posts and timber roofing system that includes keys and compression struts (HRRP, 2018).

Figure 14. Photograph of a POST-SMM house with seismic resistant features of timber elements (HRRP, 2018).

Figure 15. An under-construction RC framed building with tilted columns (left) and poor workmanship of a joint resulting in offset of beams (right) (Photos from Bhaktapur district).

Even in urban areas and in modern RC constructions, workmanship issues can be observed. Figure 15 shows photographs of an under-construction RC framed building in which the tilted columns can be seen. In the same building, some of the beams were at an offset from the column lines resulting in weaker beam-column joints.

3.4 Loss of Vernacular Construction and Architecture

The 2015 Nepal earthquake sequence caused very heavy damage and loss to the cultural heritage and architecture that existed for centuries in Kathmandu valley (Bhagat et al., 2018). Although efforts have been made to recover and preserve the cultural heritage in urban areas i.e. Kathmandu valley, several facets of cultural and architectural heritage have been lost in the destruction/reconstruction in rural areas after the 2015 Nepal earthquake. For example, Barpak village (see Figure 16), the epicentre of the mainshock of 25th April 2015 used to be a beautiful village with stone masonry buildings with tile roofs that blended well with the nature and attracted tourists to this remote area (Nepali Times, 2018b). As almost everything was turned into rubble by the earthquake, a haphazardly constructed settlement of mostly reinforced concrete structures has now replaced the picturesque beauty of Barpak before the earthquake.

Sustainable construction materials such as timber and stone have been replaced by modern materials such as concrete and steel (see section 3.3). The beautiful timber roof structure (see Figure 13, Figure 23) in the existing stone masonry buildings i.e. PRE-SMM typology, which also provides stiff diaphragm action during seismic loading, can no more be seen in the newly constructed POST-SMM houses.

In the long run, all of these issues will reduce the socio-cultural values associated with the vernacular constructions and architecture and will affect the economy as a result of reduced attraction to the tourism.
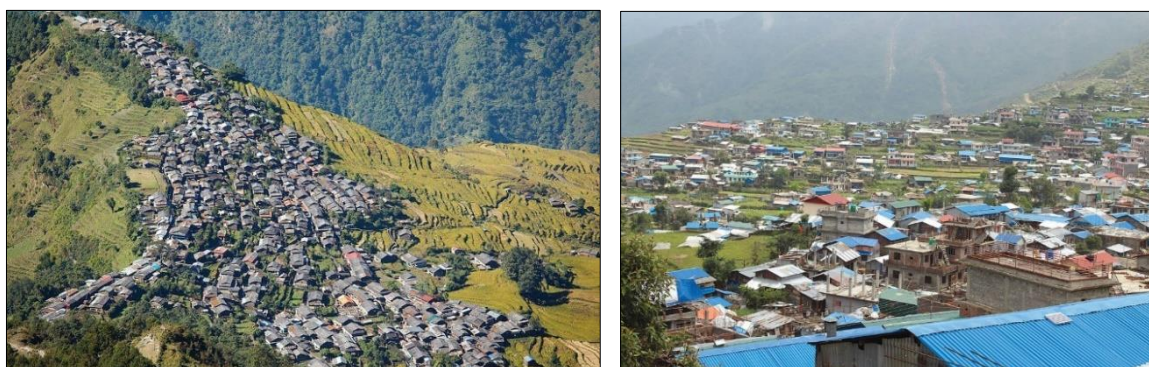
Figure 16. View of Barpak village before the earthquake (left) and present view of Barpak village with haphazard construction of houses with modern materials (right) (Photo credit: Shiva Uprety, Nepali Times).

As there exist thousands of PRE-SMM houses (undamaged and partially damaged), the retrofitting of these houses is currently ongoing (Build Change, 2017). This is a commendable effort which will not only strengthen and upgrade the seismic capacity of these buildings but will also preserve the vernacular construction and associated cultural aspects of the rural mountainous communities.

4   RESIDENTIAL BUILDING TYPOLOGIES IN THE AFFECTED DISTRICTS

In this section, the range of material and construction typologies present in Nepal before the 2015 earthquake sequence as well as being constructed after the earthquake are discussed. Traditional construction types mainly include stone masonry in rural mountainous areas (Figure 17(a)), traditional Newari constructions in the Kathmandu valley (Figure 17(b)) and, timber-framed (Figure 17(c)) and brick masonry (both adobe and burnt clay brick) in plain and urban areas (Gautam et al., 2016). Nepalese vernacular construction types are mostly built by local experienced masons without the use of seismic engineering principles, although aseismic feature can be identified, which the craft has developed over the centuries (D'Ayala, 2004). Accordingly, no 'engineered' codes or standards were followed in the construction of most of these buildings. Although codes for seismic design and building construction (for load bearing masonry as well as RC construction) were first drafted in 1994, the implementation side is found to be very poor in the construction of residential buildings which was reflected in the 2015 earthquake sequences. Since the early 1990s, RC framed construction (Figure 17(d)) has been increasingly used in urban areas as well as in peri-urban areas of rural districts. Common construction deficiencies of different typologies of Nepalese houses are discussed in detail in Gautam et al. (2016).

Figure 18 presents the distribution of building typology in the affected districts before the 2015 earthquake sequence. Except in Kathmandu valley, the most common typology is by far the SMM which represents more than 50% of the total building stock in most of the districts.
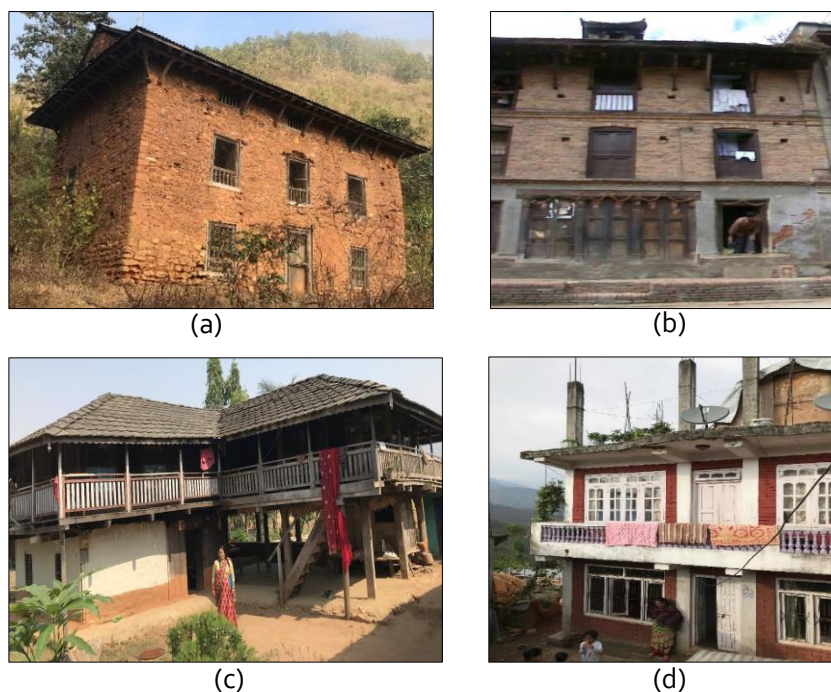
Figure 17. Photographs of main typologies of residential houses in the affected districts: (a) stone in mud mortar masonry construction (Photo from Sindhupalchowk), (b) traditional Newari construction (D'Ayala and Bajracharya, 2003), (c) timber-framed construction (Photo from Sindhuli), and (d) non-engineered RC construction (Photo from Sindhupalchowk).
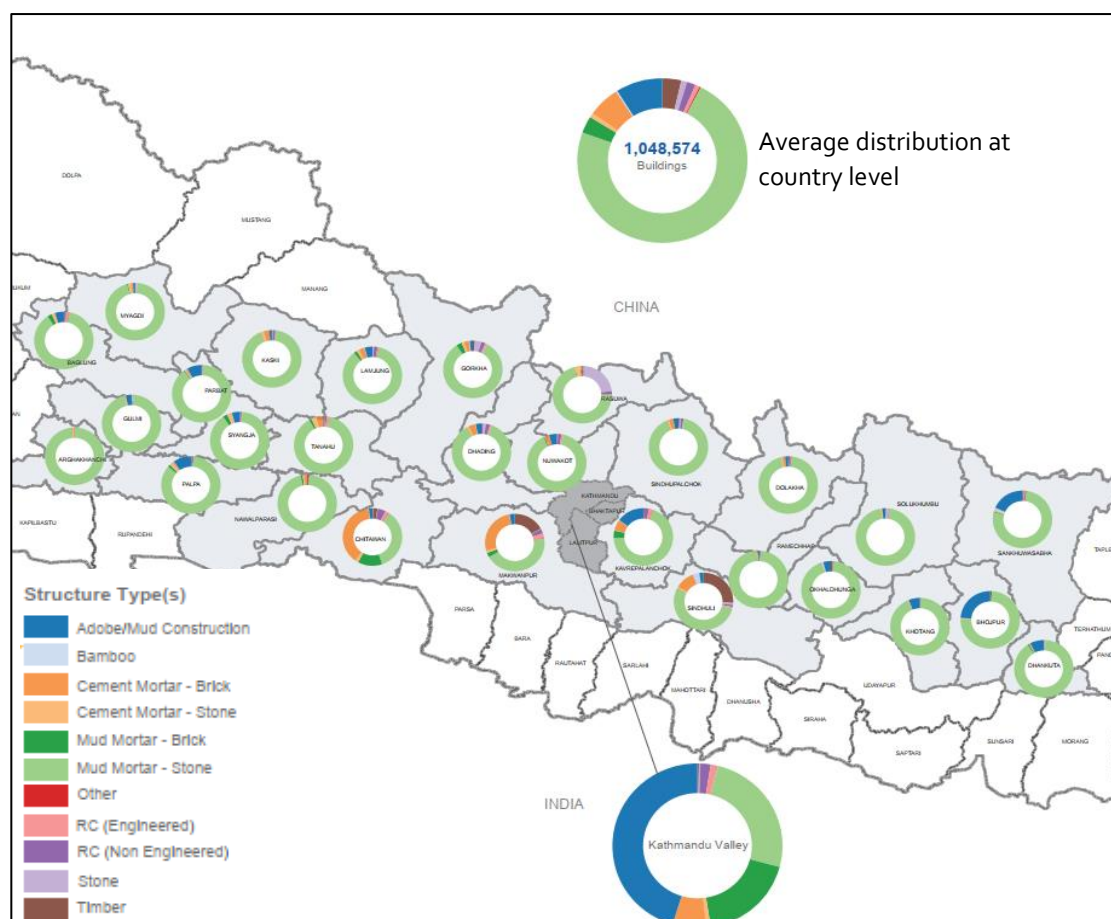
Figure 18. Distribution of pre-earthquake residential building types in the most affected districts. Light green colour represents the stone in mud mortar masonry construction. (Central Bureau of Statistics, Nepal).

In the post-earthquake reconstruction, typically multi-storey RC buildings (see Figure 20(a)) are being constructed by the economically able house-owners in the urban areas while in the peri-urban and rural mountainous areas, load bearing masonry constructions i.e. stone/brick masonry in mud/cement mortar with seismic resistant features (Figure 20(b)) are mostly constructed (HRRP, 2018). Despite being the highest contributor to damage houses, even after the earthquake, the SMM typology remains the most commonly used in the reconstruction effort. Figure 19 presents a comparison of construction typologies in the earthquake affected districts before and after the 2015 earthquake (HRRP, 2018). It should be noted that the percentage of pre-earthquake housing typologies shown in the figure is computed over the entire population of houses that existed, which was collected during post-earthquake survey by the Central Bureau of Statistics (CBS), Nepal, for identifying reconstruction and retrofit grant beneficiaries. However, the data related to post-earthquake typologies is based on a sample of about 500 newly constructed houses in different districts. Nevertheless, Figure 19 provides an indicative comparison of the pre-earthquake and post-earthquake housing typologies and the primary construction type in the affected districts both before and after the earthquake remains the SMM typology which constitutes to as much as half of the total houses. This is mainly due to difficulty of transportation of modern construction materials such as cement or steel to rural areas; readily available stone, mud etc. in these locations, available skill-set of masons and carpenters trained in traditional construction, as well as the lower cost of construction

compared to other typologies (see also Bothara et al., 2018a). The reason for many households choosing SMM typology (i.e. the cheapest solution) in reconstruction can also be linked to the economic status as well as the value of financial grant (approximately 3,000 USD in total) provided by the government for each household for house reconstruction. RC framed construction represents a low proportion of the total building population. In Sindhupalchowk, one of the hard-hit districts, as high as 46% of the post-earthquake built houses are of SMM typology (NRA, 2019a).
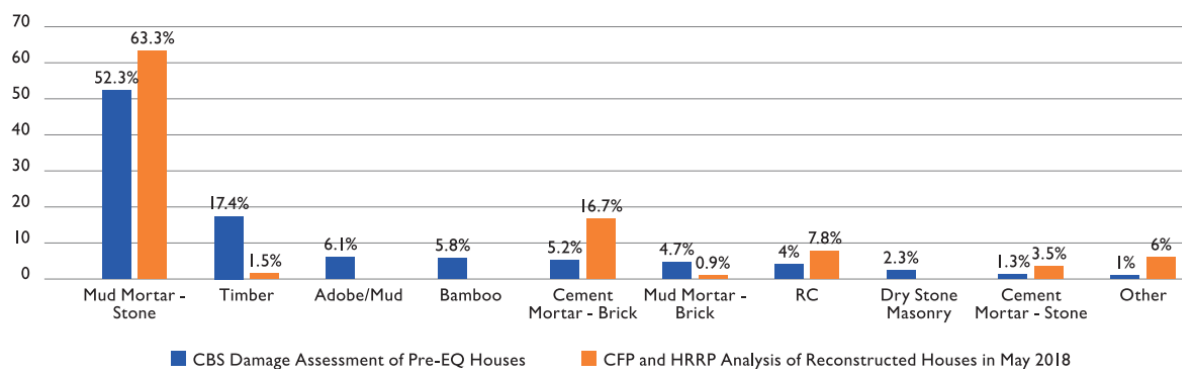
Figure 19. Comparison of prevalence of pre- and post-earthquake housing typologies in the affected districts (HRRP, 2018).

(a)   (b)
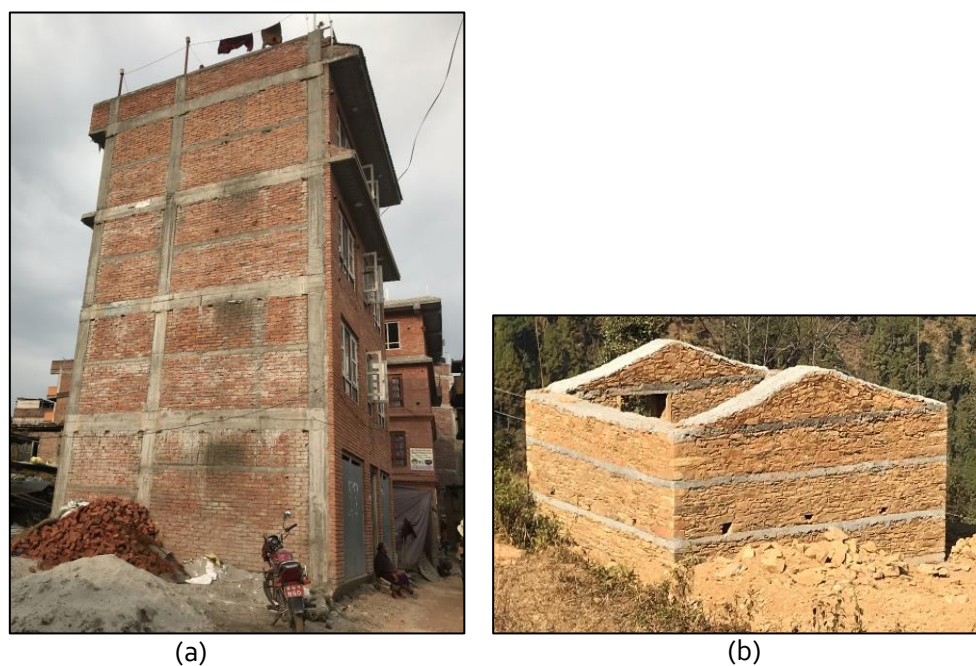
Figure 20. Photographs of newly constructed buildings (a) RC construction in Bhaktapur and (b) stone in mud mortar masonry construction in Sindhupalchowk.

The construction characteristics and seismic design level of residential building have significantly improved after the 2015 earthquake sequence. For the owner-driven reconstruction of houses, NRA has published several guidelines including building design catalogue (NRA, 2015; 2017) in order to promote the 'Build Back Better (BBB)' principle and to increase the awareness level on seismic design of houses. The design catalogue offers different typologies ranging from RC framed to SMM constructions, incorporating the seismic design requirements prescribed in recent version of Nepal

national building code (e.g. NBC 203: 2015). However, it is not necessary to adopt the prescribed design layouts offered in these documents, as beneficiaries can use different designs/layouts as long as the code-prescribed provisions are met during the inspections at different stages conducted by NRA. The staged release of the financial aid is tied to the successful outcome of each inspection. One of the major improvements in the construction of low-strength masonry typology is the provisions of seismic bands (see section 5.2) which improve the integrity and 'box-like' behaviour under seismic action. There is noticeable improvement in the design practice of RC buildings as well. Most of the common RC buildings before the earthquake were 'non-engineered' that were built with 9" x 9" columns reinforced with 4 nos. of reinforcement bars and a single shear tie. After the 2015 earthquake, NRA has made it compulsory to use 12" x 12" columns with 8 nos. of 12 to 16 mm dia. reinforcement bars tied with double shear ties and beam-column joints are well detailed so as to obtain ductile seismic response (NRA, 2016c, see Figure 21). Furthermore, the masonry infill walls are provided with intermediate RC bands which prevents the diagonal shear failure of the masonry infill walls (see Figure 20(a)).
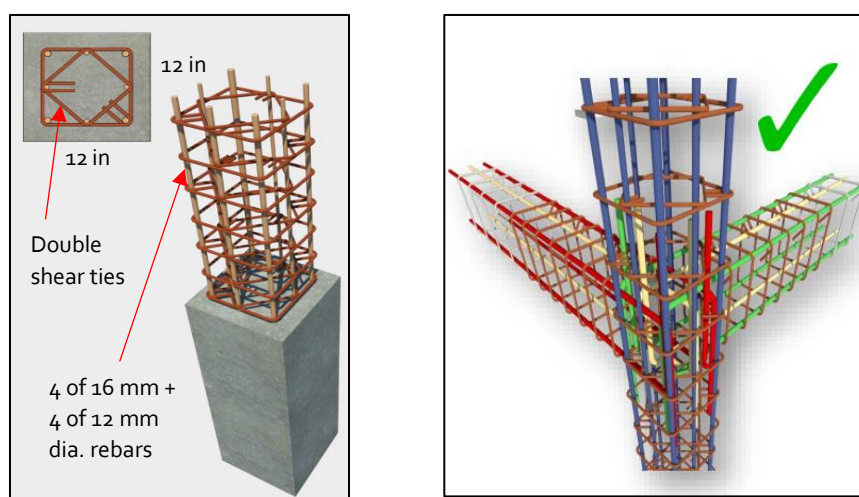
Figure 21. Reinforcement detailing in newly built RC constructions: column size and reinforcement detailing (left) and beam-column joint reinforcement detailing (right) (NRA, 2016c).

Since the SMM construction is the most common typology of residential building, both before and after the 2015 seismic sequence, the next sections will discuss the construction characteristics of these buildings in detail which will be followed by advanced numerical analysis and seismic performance assessment of PRE-SMM (existing SMM constructions) and POST-SMM (newly built SMM constructions) typologies.

5 CONSTRUCTION CHARACTERISTICS OF STONE MASONRY BUILDINGS

In order to understand the comparative seismic vulnerability of different construction typologies as well as to develop reliable numerical models for detailed analytical seismic vulnerability assessment, careful inspection of the construction characteristics at wall and building level is crucial. This includes

the detailed information and knowledge of masonry bond pattern, cross-wall connections, floor and roof structures and their connections, plan and opening layouts, dimensions etc. Before presenting the construction characteristics of PRE- and POST-SMM typology at building level, the masonry bond pattern of Nepalese SMM walls is discussed. The stone units used are from various nearby sources such as river (fairly round shaped), naturally fractured from rock or quarry site. The mud mortar used in the wall construction is prepared from locally available soil. These stone masonry walls are made up of two to three wythes of uncoursed random stones, the shape of stone varying from highly irregular to semi-dressed flat stone depending on the source, workability of the stone and skills of the mason. The void between the wythes are filled with rubbles and through stones are used to connect the wythes. Figure 22 presents photographs of the SMM bond pattern from 4 different buildings collected by the author in Sindhupalchowk district of Nepal. In some buildings the stones are flat and tend to form horizontal courses along the height while in others the shape is random, and no distinct horizontal courses can be identified. Similarly, the stone size also varies from building to building. These irregularities affect the amount of mortar used in the walls i.e. if there are larger voids in case of irregular shape of units, mortar layers are thick while if the stone are fairly flat forming horizontal courses, the mortar thickness is modest. Thus, due to such variations and uncertainties and lack of quality control measures, Nepalese SMM walls have a great variability in terms of mechanical properties and hence the lateral seismic resistance. More detailed discussions on types of stone masonry wall constructions found in South Asia including Nepal can be found in Bothara and Brzev (2011) and Pun (2015).

Figure 22. Stone masonry bond pattern from 4 different Nepalese SMM buildings.

5.1 PRE-SMM Typology

Most of the SMM buildings constructed before the 2015 earthquake (named hereafter as PRE-SMM) are traditionally constructed by local masons, unreinforced and often built with uncoursed random rubble stone in mud mortar thus displaying poor tensile and shear strength. The rubble stone masonry walls are usually thick (400 mm – 600 mm) and the wythes are not properly inter-connected using adequate amount of through stones (Bothara et al., 2018a). However, the cross-wall connections are usually made stronger by providing fairly rectangular shaped corner stones. The number of stories varies from one to three stories and the storey height is typically low at about 2 m. Figure 23 presents photographs of a typical house in the rural mountainous districts and the same is used as an index building representative of the PRE-SMM typology in the present study (in section 6.2). These are usually two-storied buildings with an attic floor covered in multi-pitched timber roof structure. Besides the SMM wall loading bearing system, the vertical load bearing structure consists of a timber frame centrally placed in the longitudinal direction, see Figure 23 (b). The longitudinal girder, resting over the short walls, at each floor level supports a number of transverse joists that span in the transverse direction, resting on the long walls and providing the support for the mud topped timber floor structure.

The timber roof structure is supported by a system of compression struts locked to the masonry by timber keys as seen in Figure 23(c) which improves the floor-wall connections thus favouring global behaviour and provides in-plane stiffness at the attic floor level.

(a)   (b)

(c)
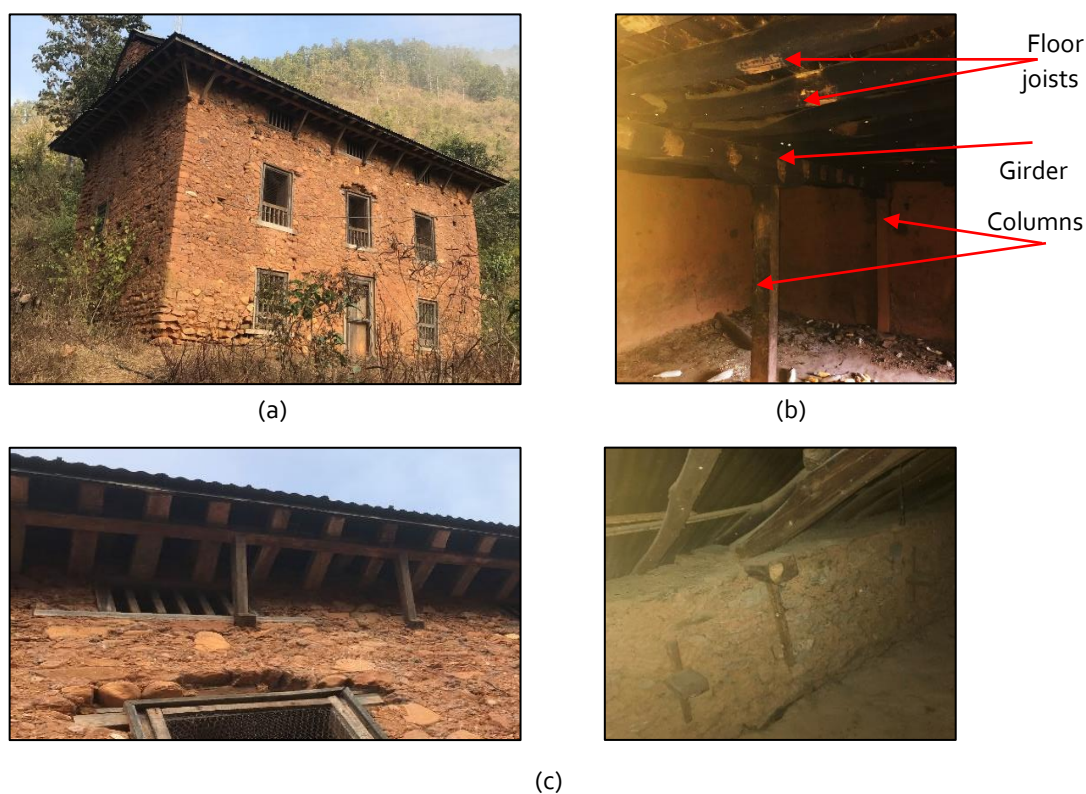
Figure 23. Construction characteristics of a typical PRE- SMM building in Sindhupalchowk district: (a) 3-D view of the building, (b) timber framing structure, (c) timber roofing system with timber keys and compression struts: outside view (left) and inside view (right).

5.2 POST-SMM Typology

The SMM buildings constructed after the 2015 earthquake (named hereafter as POST-SMM buildings) follow the seismic design requirements as per Nepal building codes for low strength masonry (NBC 203: 2015). The uncoursed random rubble stone masonry walls are $400 - 600$ mm thick as in the PRE-SMM construction. Most of the POST-SMM constructions are single storied with one to two rooms only, as already discussed in section 3.2, although the code allows multi-storied construction of up to two stories plus an attic (NBC 203: 2015). The storey height is typically low at about 2 m and the room size is also small at about 16 m². The seismic enhancement measures applied in these buildings are as below, as prescribed in NBC 203: 2015 (see Figure 24 and Figure 25).

- Through stones (or wooden dowel or precast concrete or steel rod) in walls at a spacing of 1.2 m horizontally and 0.6 m vertically
- Rectangular corner stones at cross -wall connections
- Vertical reinforcement bars (12 mm to 16 mm dia.) at the corners and both ends of openings
- Seismic bands: at roof level, lintel level, window sill level and intermediate level
- Confining elements around the openings
- Light gables of corrugated galvanized iron (CGI) sheets.

These features can be seen in the photograph of a newly built house as shown in Figure 26 which is used as an index building representative of the single-storied POST-SMM typology in the numerical analysis and seismic performance assessment (see section 6.2). The seismic bands are typically 75 to 100 mm deep and extend through the thickness of the masonry walls. The roof is mostly gable type and is made of timber structure with light roofing material (corrugated iron sheet).
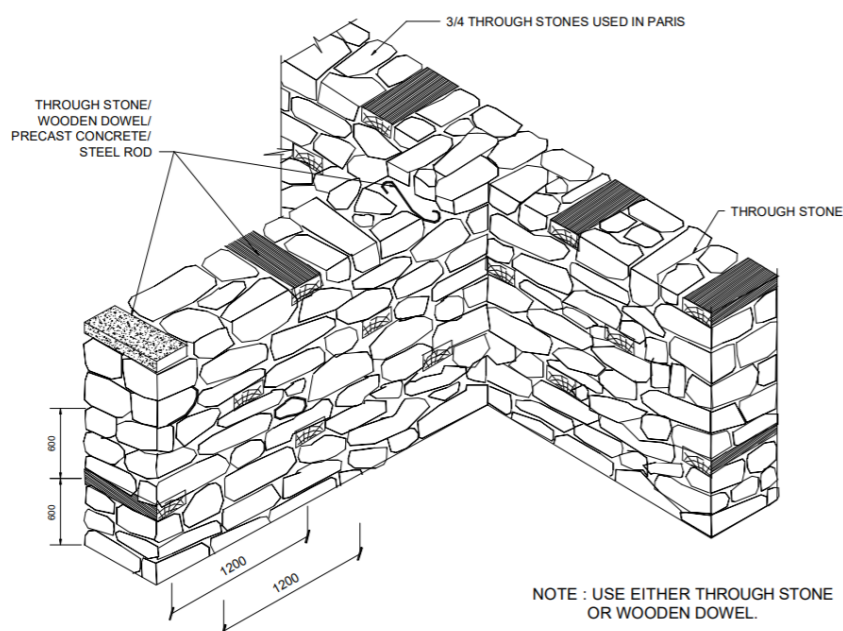
Figure 24. Stone masonry wall construction detail as per NBC 203: 2015.
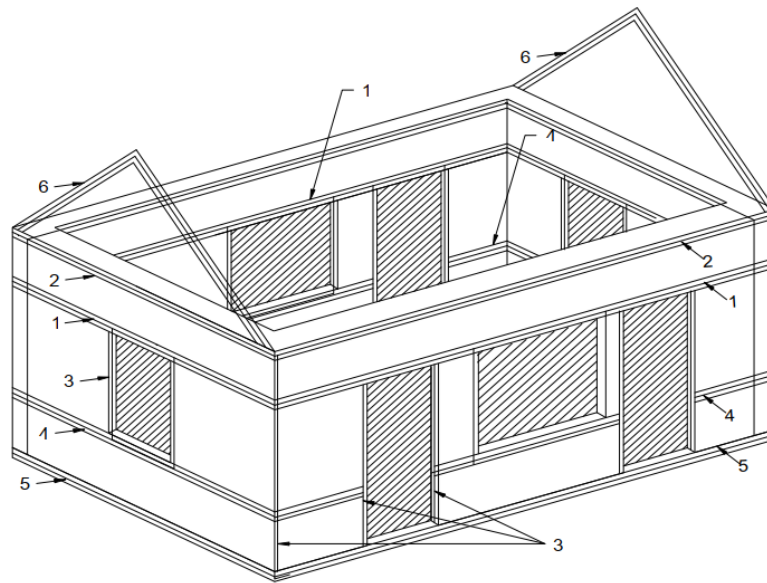
1 - Lintel Band
2 - Roof Band (only for pitched roofs and under roofs and floor)
3 - Vertical steel.
4 - Sill Band.
5 - Plinth Band.
6 - Gable Band.

Figure 25. Seismic-resistant components in load bearing masonry buildings as per NBC 203: 2015.

Figure 26. Construction characteristics of typical POST-SMM buildings (Photo from Sindhupalchowk district).

Although some households have constructed more than one storied SMM buildings (see Figure 12), these buildings often have issues such as lack of technical assistance, non-compliance etc. as the NRA engineers are not well trained for providing technical assistance in multi-storied SMM construction as discussed in section 3.3 (see also HRRP, 2018).

6 NUMERICAL MODELLING AND ANALYSIS OF SMM TYPOLOGIES

Since it is very difficult to conduct the full-scale building level experimental tests to characterize the seismic behaviour, and with the advancement of modelling approaches, software tools and computational capabilities; analytical seismic assessment methods are widely used within the engineering community (e.g. D'Ayala and Speranza, 2003; Lagomarsino et al., 2013; D'Ayala et al., 2015). Furthermore, analytical and numerical models have flexibility in altering the input parameters (e.g. dimensions, material properties etc.) and the behaviour under several ground motions with different characteristics can be studied which is not feasible to carry out using experimental tests. This section thus presents a discussion on the numerical modelling approach, results of validation and calibration studies for SMM masonry and the results of non-linear pushover analyses conducted on representative index buildings of the PRE-SMM and POST-SMM typologies. The failure mechanisms and capacity curves for both typologies are presented and discussed to shed some light on the seismic capacity of existing buildings and seismic resilience of the post-earthquake reconstruction.

6.1 Applied Element Modelling of Rubble Stone Masonry: Validation and Calibration

Modelling of masonry is complex because of the heterogenous nature of masonry due to the presence of units and mortar having different elastic and non-linear properties. Several methods have been used for studying the structural behaviour of masonry: e.g. limit analysis based methods (e.g. D'Ayala and Speranza, 2003) and numerical methods such as finite element based methods (e.g. Bothara et al., 2018b), discrete element based method (e.g. Lemos and Costa, 2017) and applied element based methods (e.g. Guragain, 2015). Three modelling approaches can be followed for numerical modelling and analysis: micro-modelling, simplified micro-modelling and macro-modelling (Lourenco, 1997). In simplified micro-modelling approach, the mortar layer and the two unit-mortar interfaces are lumped into a zero-thickness joint while the units are slightly expanded on all sides to accommodate the mortar thickness. Simplified micro-modelling approach using the applied element method has been chosen for this study as the complete lateral behaviour of masonry from the initiation of cracking to the ultimate collapse state can be studied using this approach. This section thus presents a discussion on the numerical modelling strategy for random rubble stone masonry using the applied element method.

Extreme Loading for Structures (ELS) software (ASI, 2018), based on applied element method (AEM), is used in the present study. In this method, structures are discretized into 3D-elements which are connected at the interface by a number of deformable springs that represent all the force-deformation and non-linearity. Two types of springs are used for modelling masonry, 'unit' or 'element' springs connecting the 3D applied elements of the units, and 'interface' springs connecting the individual applied elements to represent the equivalent properties of mortar and mortar-unit interface. A detailed overview of the formulation, constitutive laws, failure criteria etc. for masonry modelling in AEM can be found in Malomo et al. (2018).

In this study, to account for the random irregular shape of rubble stone, a triangular 3-D mesh is first created, and then random shaped units are generated by clustering these triangular applied elements by means of the 'unit' springs. Figure 27 is self-explanatory where different coloured cluster represents each single stone unit. It should be noted that such modelling technique inherently presents some uncertainty as the wall construction itself presents great variability in terms of shape and size of units and the resulting bond pattern (also refer to Figure 22)

Triangular meshing and clustering of SMM wall (note that clustering is done such that fairly horizontal courses are obtained)

Unit springs (establishing the continuity within the stone units)

Stone unit

Applied (rigid) elements

Interface springs (representing the mortar plus unit-mortar interface)

Stone unit
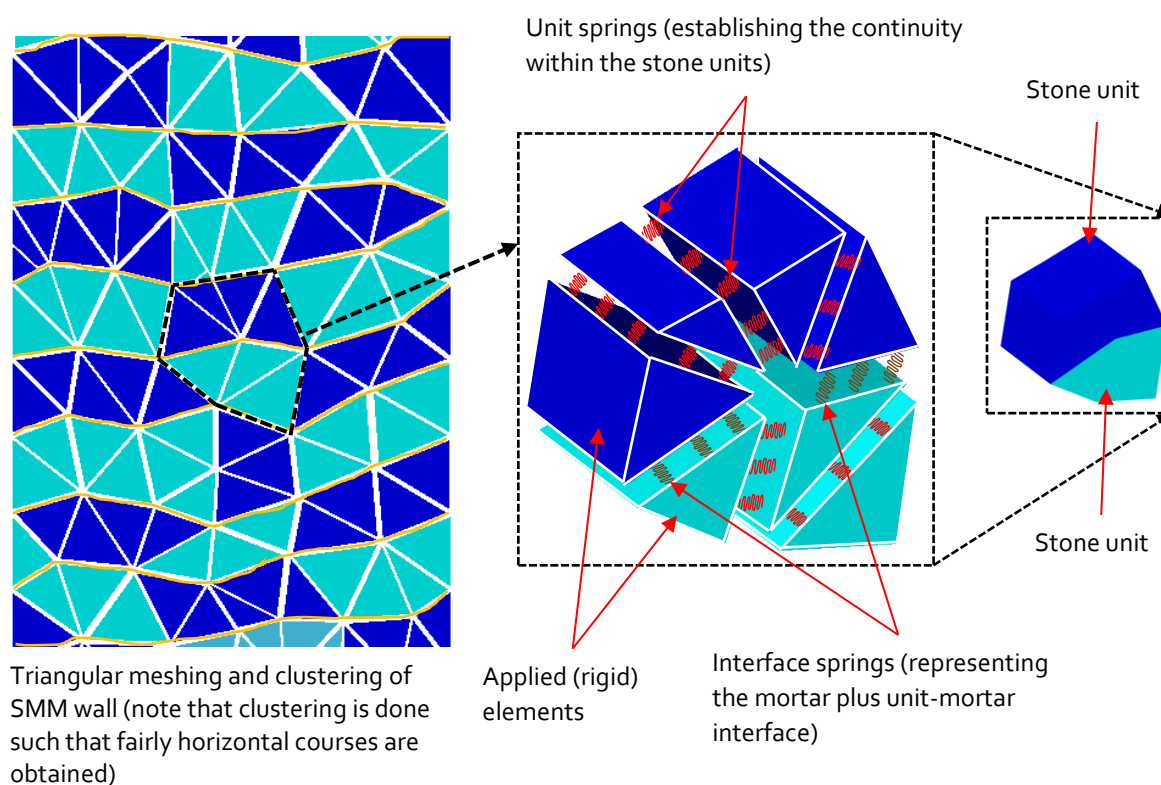
Figure 27. Schematic of simplified micro-modelling of random rubble stone masonry using AEM.

For the validation and calibration of the proposed numerical modelling strategy using AEM method, numerically obtained compressive and lateral behaviour of SMM walls are compared against experimental test results. Three distinct experimental tests are numerically reproduced for validation and calibration of AEM method for rubble stone masonry: uniaxial compression behaviour, in-plane shear-compression behaviour and out-of-plane bending behaviour. It should be noted that there are very few experimental test campaigns conducted on SMM masonry from Nepal, and the size and shape of stone, as well as workmanship in the available experimental tests (presented herein) might not represent all different SMM constructions in different locations because of the variability of source and the level of skills of masons (as explained in section 5).

6.1.1   Uniaxial Compression Behaviour

The uniaxial compression test on random rubble stone masonry conducted by Build Change (2019) is numerically reproduced. The test specimen of size 450 mm (width) x 350 mm (thickness) x 540 mm (height) is built by local masons using local stone and mud mortar from rural Nepal which is well representative of the buildings considered in this study for numerical analysis (see section 6.2). Key

material properties from the mechanical characterization tests conducted in the same experimental campaign are presented in Table 1. The average compressive strength of eight stone sample from rural mountainous area (Kavre district) is found to be 30.4 MPa (CoV = 68%). Strength of mortar cubes is not reported in the Build Change (2019) report, however, experimental tests by Pun (2015) reported average compressive strength of mud mortar cubes and stone units to be 1.56 MPa and 37.91 MPa, respectively.

Table 1. Material properties for Nepalese rubble stone masonry in mud mortar (Build Change, 2019).

Material properties	Average value	CoV (%)
Unit weight	2200 kg/m^3	-
Young's modulus	65.10 MPa	31
Compressive strength	2.40 MPa	13
Tensile strength	0.02 MPa	16.5
Cohesion	0.013 MPa	16.5

Figure 28 and Figure 29 compare the numerical crack patterns and the stress-strain diagram to the experimental results for the SMM wallete subjected to vertical uniaxial compression. Vertical and inclined cracks are observed which mainly pass through the mud mortar joints, both in the experiment and numerical analysis result. In terms of load-deformation behaviour, apart from a slight discrepancy in the initial stiffness, the average Young's modulus as well as peak strength and strain are well predicted by the numerical analysis. The difference in the initial stiffness is most probably due to the fact that the test specimen presented some voids and hence showed non-linearity at the beginning of testing.
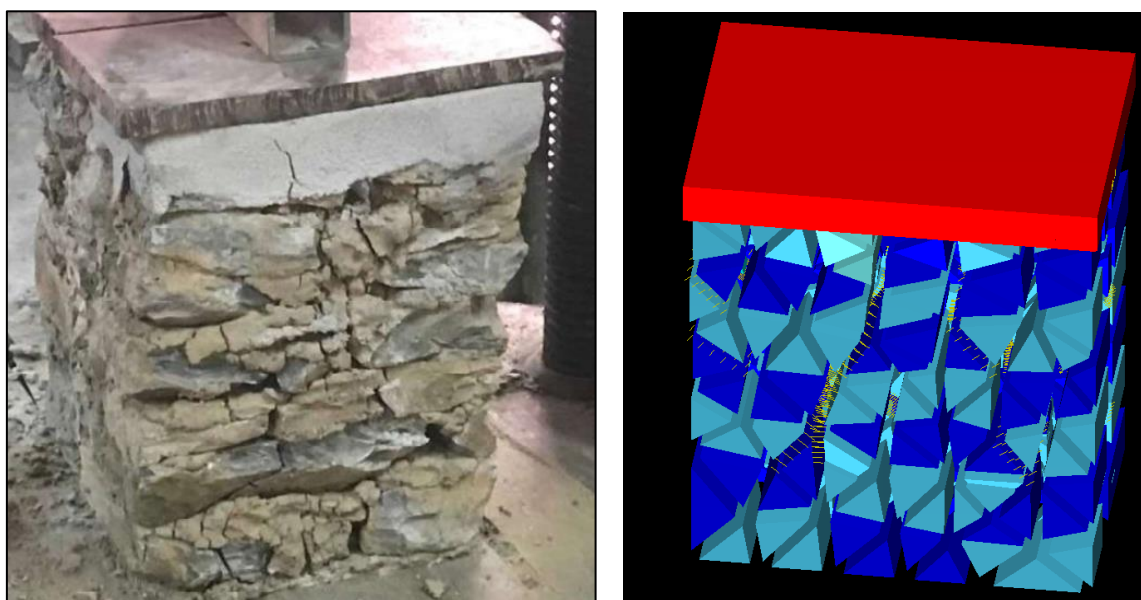
Figure 28. Experimental and AEM analysis results comparison: failure pattern under uniaxial compression.
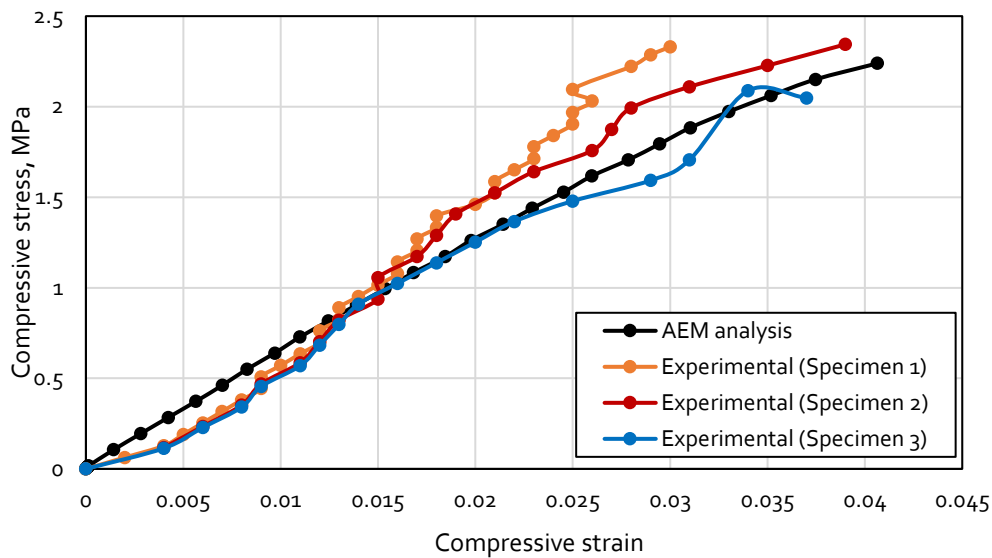
Figure 29. Experimental and AEM analysis results comparison: stress-strain curve under uniaxial compression.

6.1.2 Lateral Shear-Compression Behaviour

For the validation of in-plane behavior of random rubble stone masonry wall, the cyclic shear-compression test conducted by Build Change (2019) is modelled using AEM. The wall specimen has a size of 1.2 m (length) x 1.2 m (height) x 0.45 m (thickness) and is built by local masons. Since this test is also from the same campaign, the same material properties as listed in Table 1 are applicable. The wall is subjected to a cyclic (loading-unloading) displacement history up to a maximum lateral displacement of 48 mm under a vertical pre-compression of 0.011 MPa (see Figure 30).
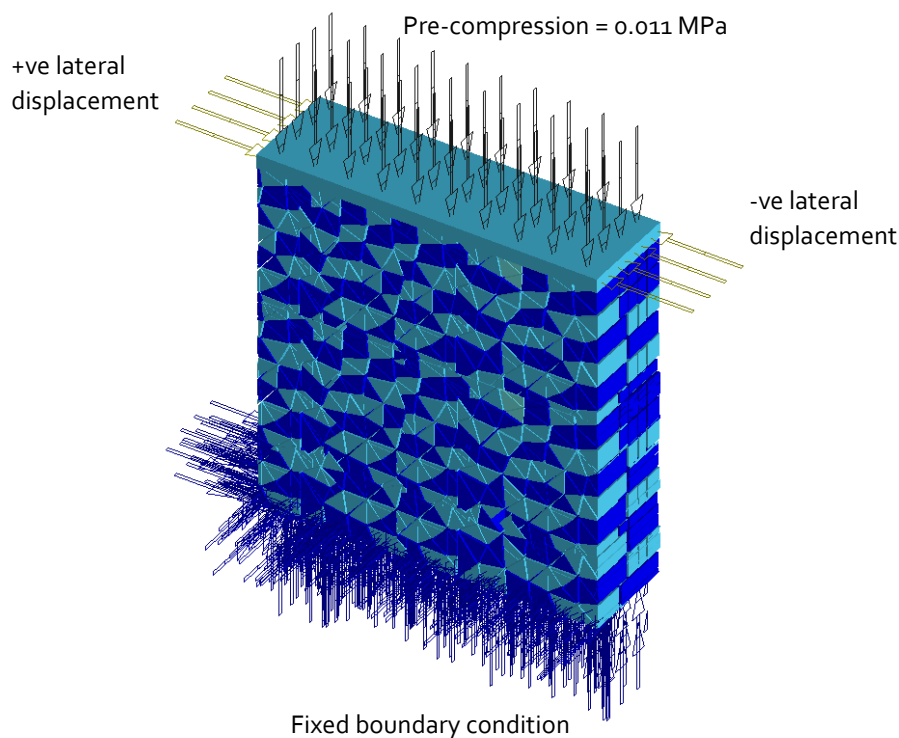
Figure 30. AEM numerical model of the SMM wall showing the boundary condition and loading condition.

Figure 31 shows the ultimate crack pattern under cyclic shear-compression loading. As the cyclic displacement level increases, the cracks become widely distributed all over the wall surface, passing mostly through the mud mortar joint/interfaces. Similar crack patterns were obtained in another test on a larger wall conducted on Nepalese random rubble stone masonry wall (Wang et al., 2018), see Figure 32. As the pier was tested until complete collapse in the experiment, out-of-plane delamination (see Figure 33) of the wall was observed at ultimate state of cyclic loading (48 mm top lateral displacement). However, the AEM numerical analysis became unstable after reaching a top lateral displacement of about 36 mm (i.e. 3%) due to the conrentration of displacement in one crack leading to numerical instability. However, such out-of-plane debonding is triggered mainly after the in-plane cracks become wide and hence loose frictional interlocking.

(a) Experimental (Build Change, 2019)

(b) AEM analysis
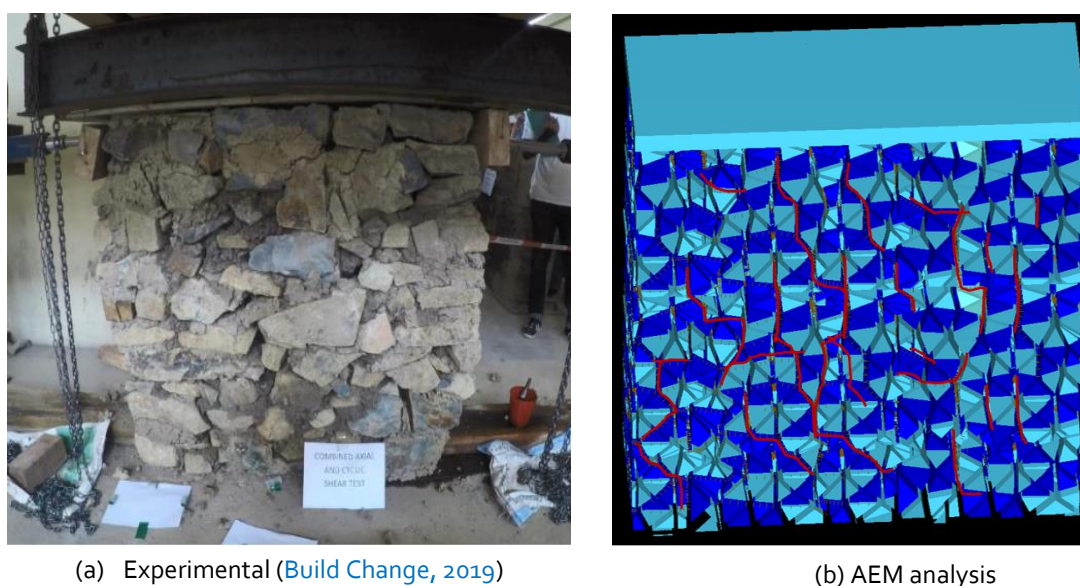
Figure 31. Crack patterns comparison under cyclic shear-compression loading (maximum crack opening is 20 mm).

Specimen W1
Green: 8mm
Yellow: 14mm
Orange: 22mm
Red: 28mm
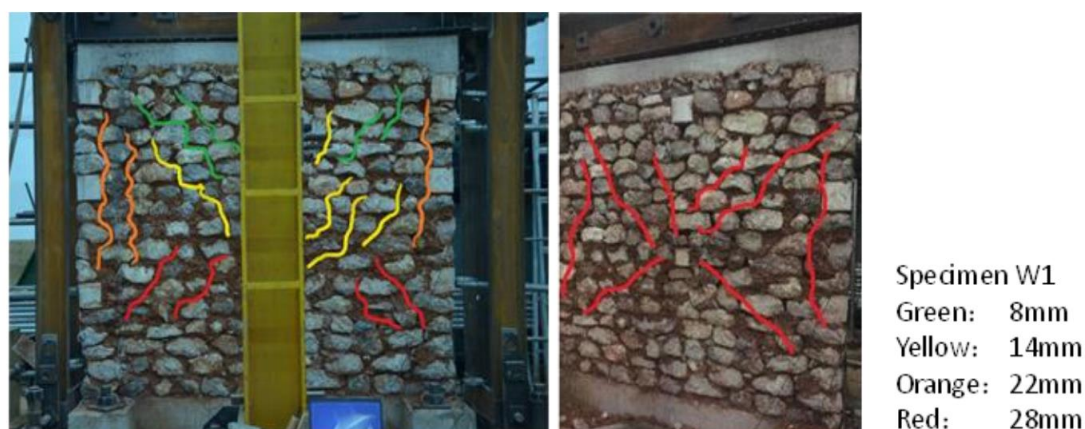
Figure 32. Ultimate crack pattern for random rubble stone masonry wall in mud mortar (Wang et al., 2018).

28

Figure 33. Delamination of the SMM wall specimen at ultimate state (Build Change, 2019).

Figure 34 presents the comparision of hysteretic load-deformation behavior from the AEM analysis and the experiment. Overall, the cyclic lateral loading and unloading stiffnesses as well as the peak capacity is well reproduced by the AEM analysis, although it slightly overestimates the hysteretic behaviour.
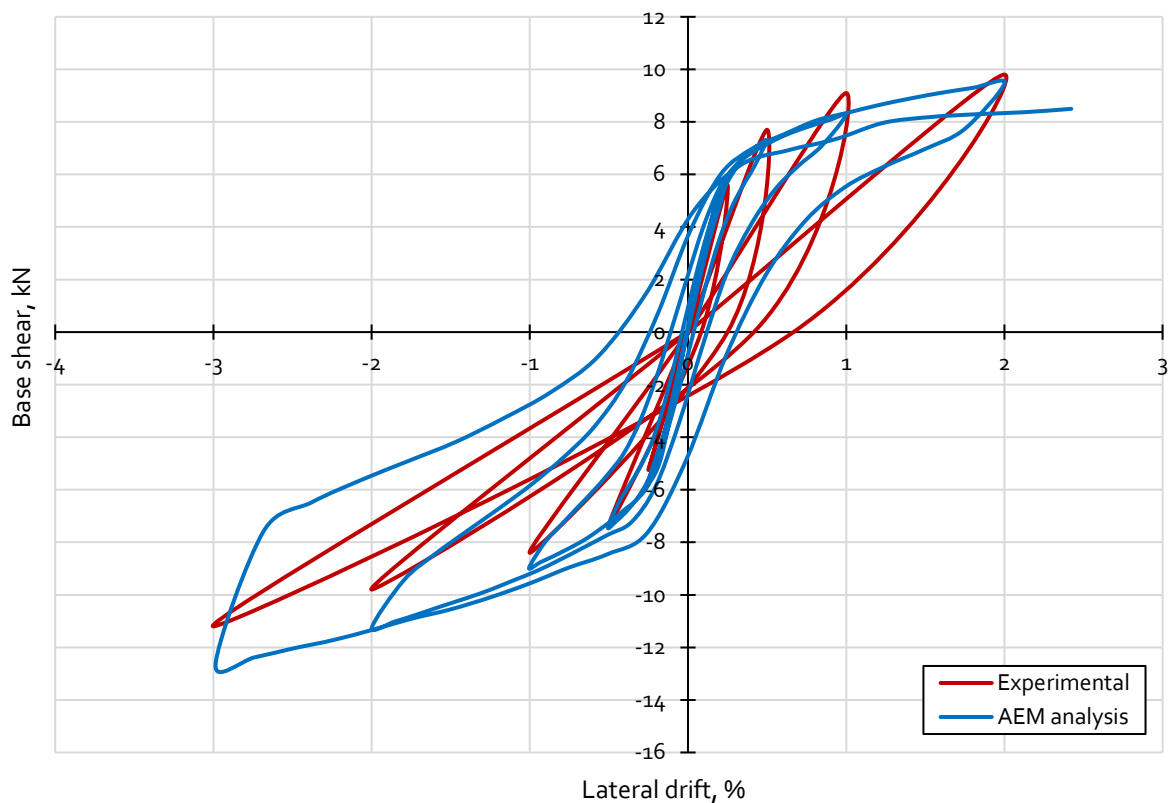
Figure 34. Comparison of experimental and AEM analysis cyclic hysteretic response under shear-compression loading.

6.1.3   Lateral Bending Behaviour
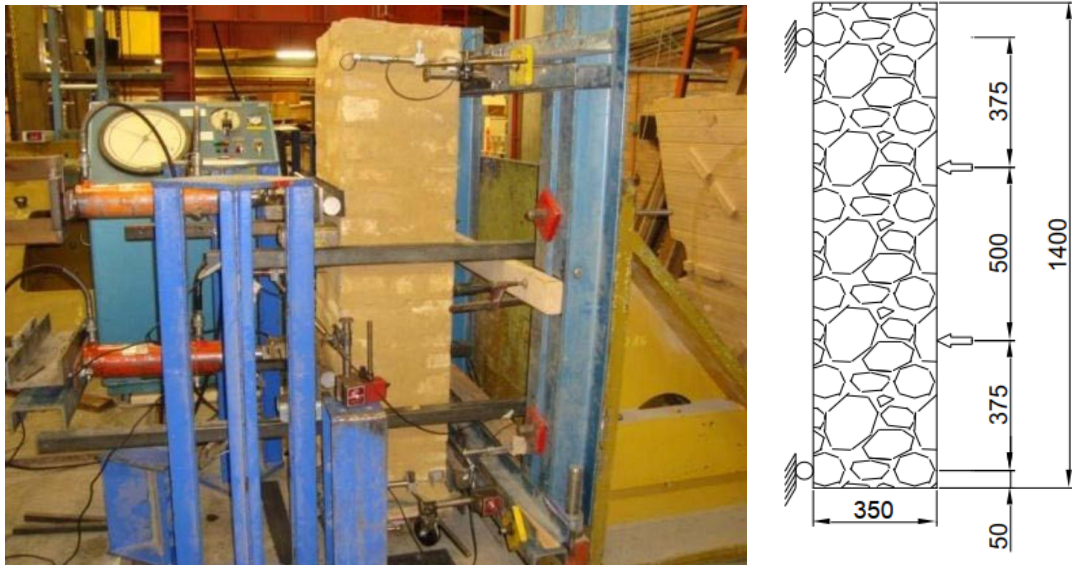
Figure 35. Wall specimen and test setup for four-point bending test (units in mm) (Pun, 2015).

In order to validate the vertical bending behaviour of mud mortar masonry walls, the experimental tests on a semi-dressed stone masonry pier conducted by Pun (2015) is considered. Figure 35 shows the details of the four-point vertical bending test setup for a SMM pier. The location of crack at ultimate stage (which is at a height of 925 mm from the bottom, as shown in Figure 36) as well as the load-deformation behaviour (Figure 37) are well reproduced by AEM analysis.

Experimental crack location at failure (Pun, 2015)
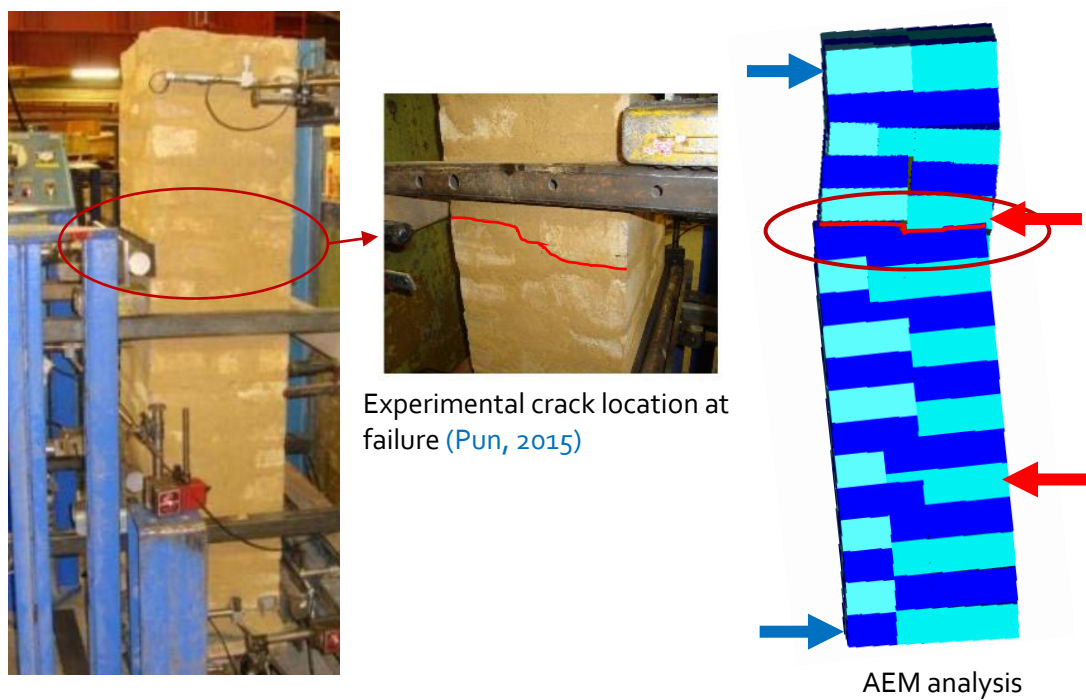
AEM analysis

Figure 36. Comparison of experimental and AEM analysis results: location of crack at ultimate stage.
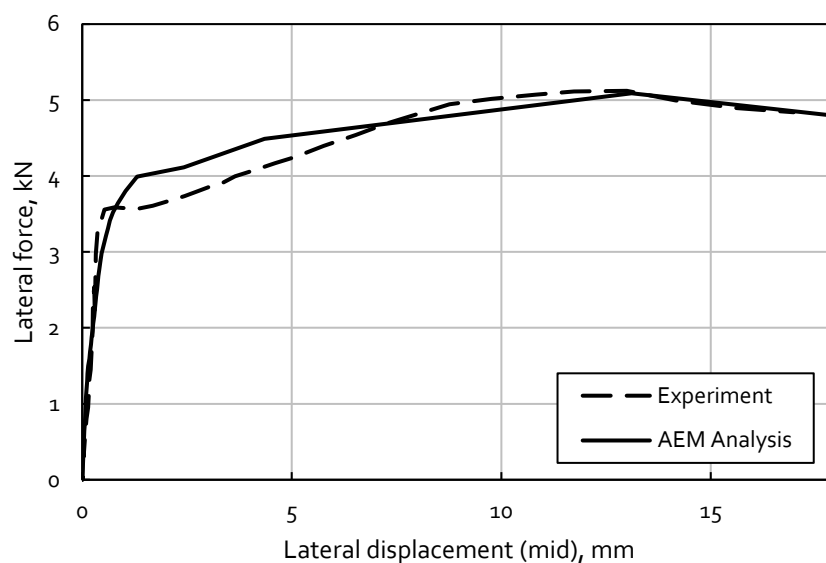
Figure 37. Comparison of AEM analysis and experimental results: load-deformation curves.

Thus, these analyses results confirm that AEM can be effectively used for the gravity and lateral load analysis of SMM structures. As the shear modulus as well as friction coefficient values were not obtained in the above presented experimental campaigns, these values were also calibrated from the AEM numerical analyses. An average shear modulus of about 0.35 times the elastic modulus is found for Nepalese SMM construction, which is in good correlation with the recommended relationship, shear modulus equal to 0.4 times the elastic modulus, in most modern codes/standards, e.g. FEMA 356 (FEMA, 2000), Eurocode 6 (EN 1996-1-1), ACI 530-11 (MSJC, 2011). Similarly, a friction coefficient of about 0.4 is found from the numerical calibration study.

6.2 Non-Linear Pushover Analysis of Index Buildings

One of the major issues that increases the difficulty in modelling the seismic response of masonry is the uncertainty associated with the material properties of its constituents. Furthermore, in older constructions such as PRE-SMM typology, the present material condition is influenced by deterioration, history of maintenance etc. and hence the uncertainty further increases. For the present study, results of experimental campaigns conducted by Build Change (2019) on Nepalese SMM walls to characterize various elastic and non-linear material properties as listed in Table 2 are used. For reinforced concrete bands in the POST-SMM typology, concrete is assumed to be M15 grade and the reinforcement bar has a yield strength of 415 MPa (NRA, 2016c).

Although the coefficient of variation for different properties in the test results is low because of the small number of sample size (three), the properties of masonry can vary greatly depending on the mortar quality, stone type and shape, type of bonding and the workmanship. Thus, a sensitivity analysis is conducted by considering good quality (assumed 50% better than the average) and poor quality (assumed 50% lower than the average) material properties in order to study the effect of 'good quality' and 'poor quality' material in the seismic capacity, fragility and vulnerability function of the SMM typologies as discussed in Section 6.3 and 7.2.

31

Table 2. Material properties for Nepalese rubble stone masonry in mud mortar (Build Change, 2019).

Material properties	Average value	CoV (%)
Unit weight	2200 kg/m^3	-
Young's modulus	65.10 MPa	31
Shear modulus[1]	22.40 MPa	-
Compressive strength	2.40 MPa	13
Tensile strength	0.02 MPa	16.5
Cohesion	0.013 MPa	16.5
Coefficient of friction[1]	0.40	-

It is interesting to note that some studies have used elastic modulus for these Nepalese SMM typologies as high as 850 MPa (Bothara et al., 2018b) in their numerical study which is an order of magnitude higher than the recent test results (Table 2).

In ELS, 3-D numerical models (Figure 38) of the index buildings representative of the PRE-SMM and POST-SMM typologies are created using the modelling strategy discussed in the previous section. For computational efficiency, stone units are modelled as rigid elements i.e. the cracks are assumed to develop through the mortar joints only. This assumption is justifiable from the results of the experimental and numerical studies presented in section 6.1 that most of the cracks develop through the mortar joint and interfaces in SMM masonry due to the substantial difference in stiffness and strength of mortar and units. For the joint springs, the failure criterion is defined by specifying a separation strain equal to 0.025 which is obtained from the validation and calibration studies reported in section 6.1. Once this strain limit is exceeded in a spring, this has no further tensile capacity, however contact can occur between the adjacent applied elements depending on the loading condition. In the PRE-SMM index building model, the timber lintels above the openings as well as the timber frame elements around the openings are modelled as elastic elements. The timber framed roof structure, including the keys and compression struts are also modelled to reproduce their structural action in confining and constraining the top of the walls. Corner stones are created as rectangular elements at all corners and through stones are provided in the wall at a spacing of 1.2 m and 0.6 m in horizontal and vertical directions respectively (as per NBC 203: 2015). The building is assumed to be fixed at the base. It is worth noting that the building is non-symmetric in the longitudinal direction due to the typical distribution of opening (backside long wall is solid without any openings).

In case of POST-SMM model, masonry walls are simulated in the same way as in the PRE-SMM model. The RC bands, confining elements around the openings and the corner reinforcements are all explicitly modelled so that their contribution towards the improvement of global seismic behaviour can be reproduced. The RC elements are meshed such that the size of meshing is comparable to the size of stone units. Although it could add some benefits to the global behaviour of the building, the

---

[1] Found from validation and calibration study using AEM analyses.

light timber roof structure is not modelled, instead, the equivalent gravity load (although minimal) is applied on the top of masonry walls.
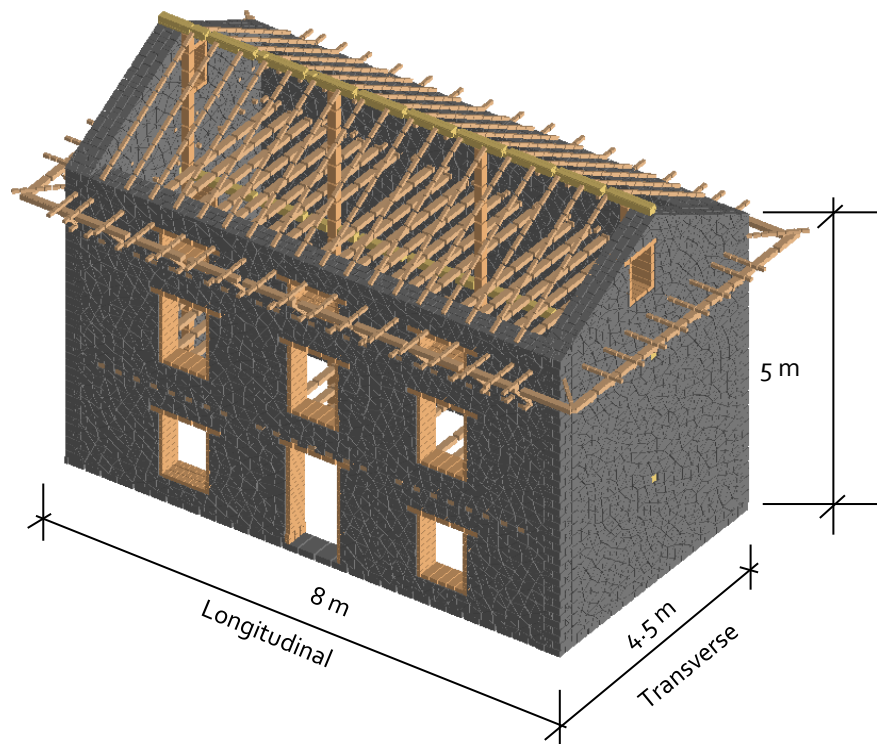
(a) PRE-SMM numerical model
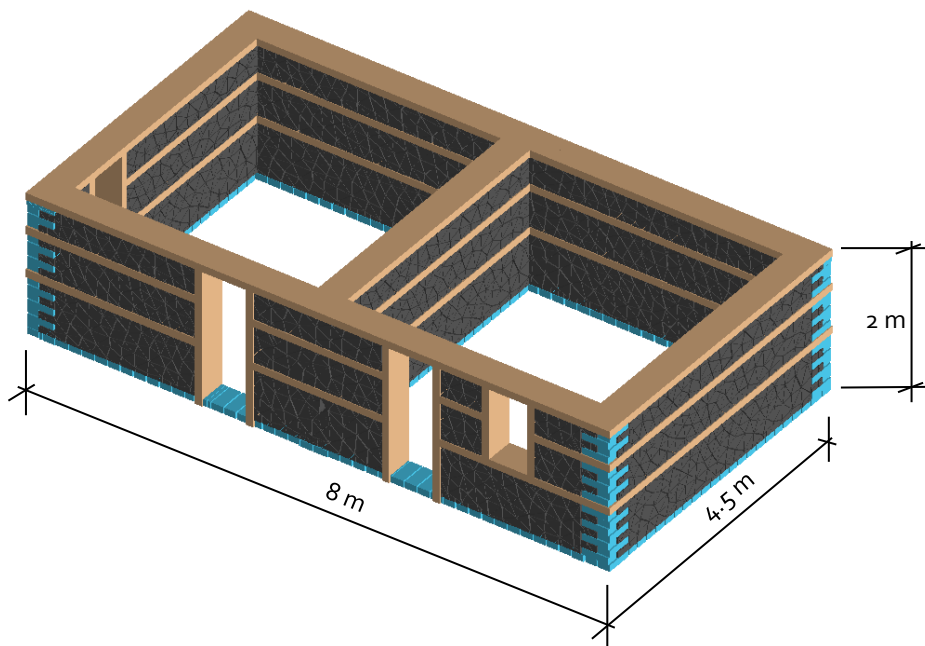
(a) PSOT-SMM numerical model

Figure 38. Numerical models of the index buildings of (a) PRE-SMM typology and (b) POST-SMM typology.

Conventional pushover analysis of masonry structures modelled using element-by-element modelling technique, with discontinuous joint represented by finite-strength springs, is complex as the application of pushover force or displacement imposed on the structure often causes stress concentration on a particular element or region thereby causing local failure without affecting the

33

rest of the structure. Thus, a different approach for applying pushover loading is proposed in which the numerical model is subjected to a linearly increasing ground acceleration, rather than a force pattern on the structure, until collapse. This works by applying an increasing 'effective earthquake force' on the structure which is mass proportional. More on this approach can be found in Adhikari and D'Ayala (2019).

6.3 Results and Discussion

6.3.1 PRE-SMM Typology

Figure 39 compares the capacity curves of an index building of the PRE-SMM typology in the longitudinal and transverse directions. For the damage scale, FEMA 356 (FEMA, 2000) performance levels i.e. Operational, Immediate occupancy, Life safety and Collapse prevention are used. The peak lateral capacity attained by the building is 0.12g and 0.08g in longitudinal and transverse direction, respectively. An analytical study by D'Ayala and Kishali (2012) also found typically low lateral capacity (0.07g - 0.19g) for two-storey Turkish SMM buildings. Due to the poor strength of mortar as well as the random shape of the stone units, the non-linear response starts at a drift as low as 0.05% and the ultimate drift capacity is only about 0.4% in both principal directions. Figure 39 also shows the roof drift thresholds representative of the four different performance levels. These will be used in the seismic performance assessment and fragility analyses in section 7.2.

Figure 40 compares the capacity curves for the PRE-SMM typology for different material quality. Substantial changes in the lateral capacity and ductility as well as in the threshold of damage states (particularly for the immediate occupancy limit) can be observed. It is thus important to improve the practice of material preparation as well as workmanship in the wall construction since both of these affect the resulting bond and hence the material properties. The poor-quality case (50% reduction in material properties i.e. elastic moduli as well as strengths) has more severe reduction in the lateral capacity than the increment due to good quality material (50% increment in material properties).
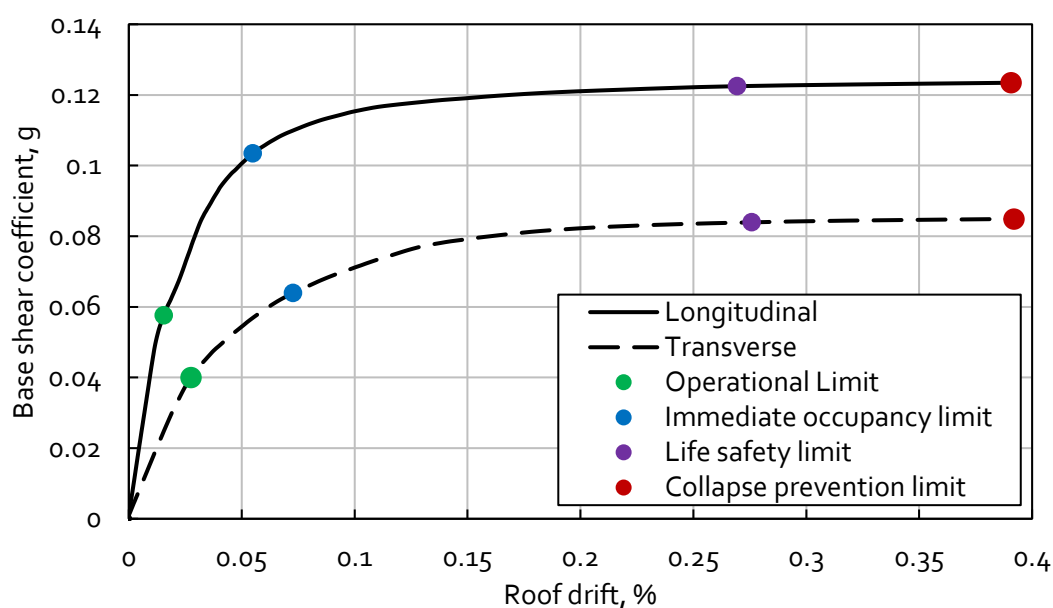
Figure 39. Capacity curves for the PRE-SMM typology in two principal directions.
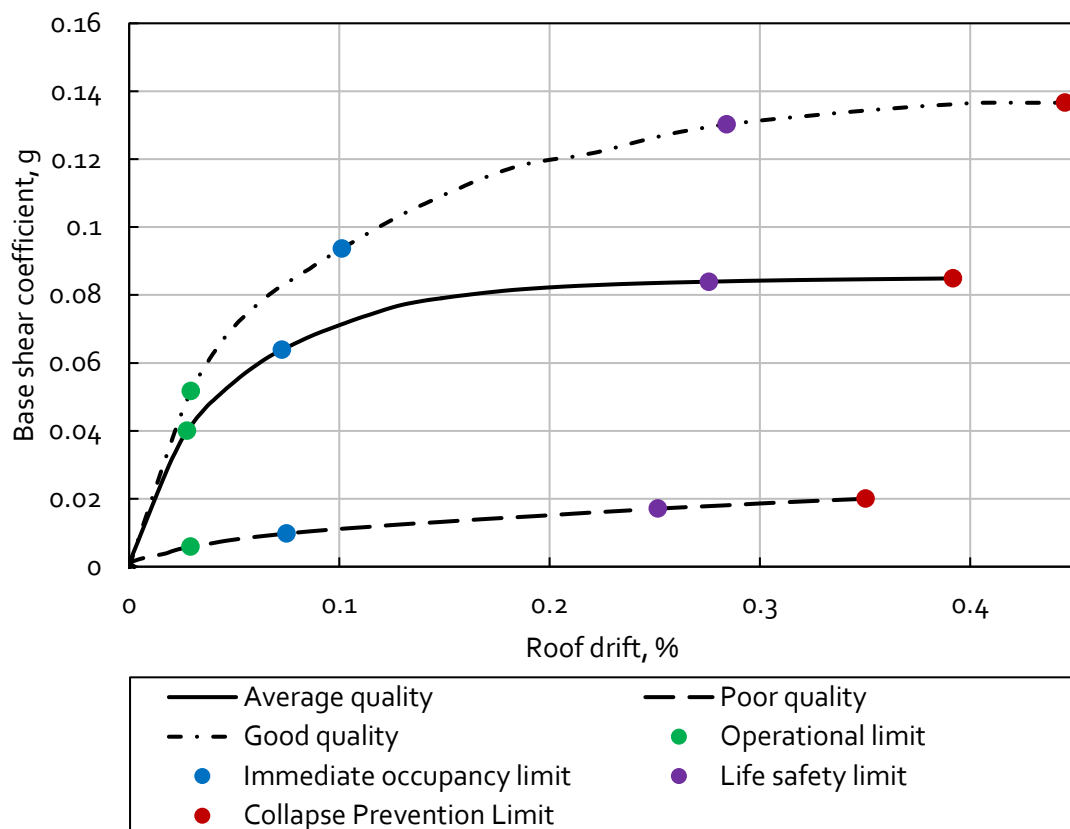
Figure 40. Effect of material quality on the PRE-SMM capacity curve (note that the capacity curves in the transverse i.e. weakest direction are compared).

Figure 41 presents the ultimate collapse mechanisms of the PRE-SMM typology when loaded in longitudinal and transverse directions. In the case of longitudinal loading, the building suffers torsional action due to the irregular distribution of openings and hence the damage starts at the weakest corner triggering the collapse of the short wall. The long wall with openings also suffers in-plane shear damage which ultimately activate the delamination in the transverse direction. In the case of transverse direction loading, in-plane shear damage originates at the opening corners of the short wall and again the corner failure of the weak cross-wall connection occurs. In both cases the ultimate collapse mechanism involves the collapse of the short walls. These damage patterns are similar to the typical damages experienced by these building in the 2015 earthquake (see Figure 6). These collapse modes also confirm that the building has sufficient rigid diaphragm action at floor and roof level.

Corner failure leading to the collapse of short wall

In-plane shear damage and delamination

Loading direction

(a)

Gable damage

In-plane shear damage and corner failure leading to the collapse of short wall

(b)
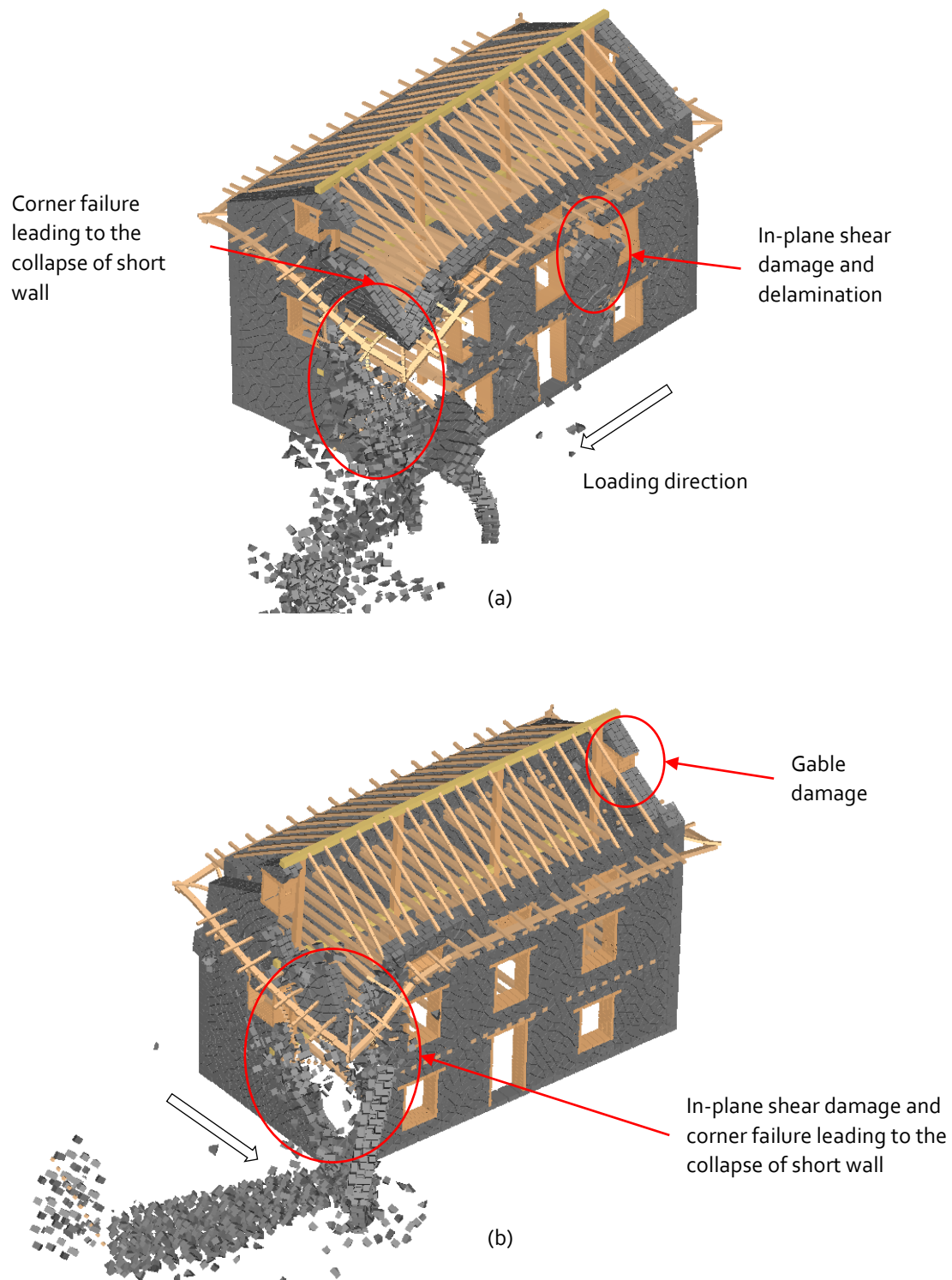
Figure 41. Ultimate collapse mechanism of PRE-SMM typology when loaded along the (a) longitudinal and (b) transverse direction.

Front

Loading direction

Back
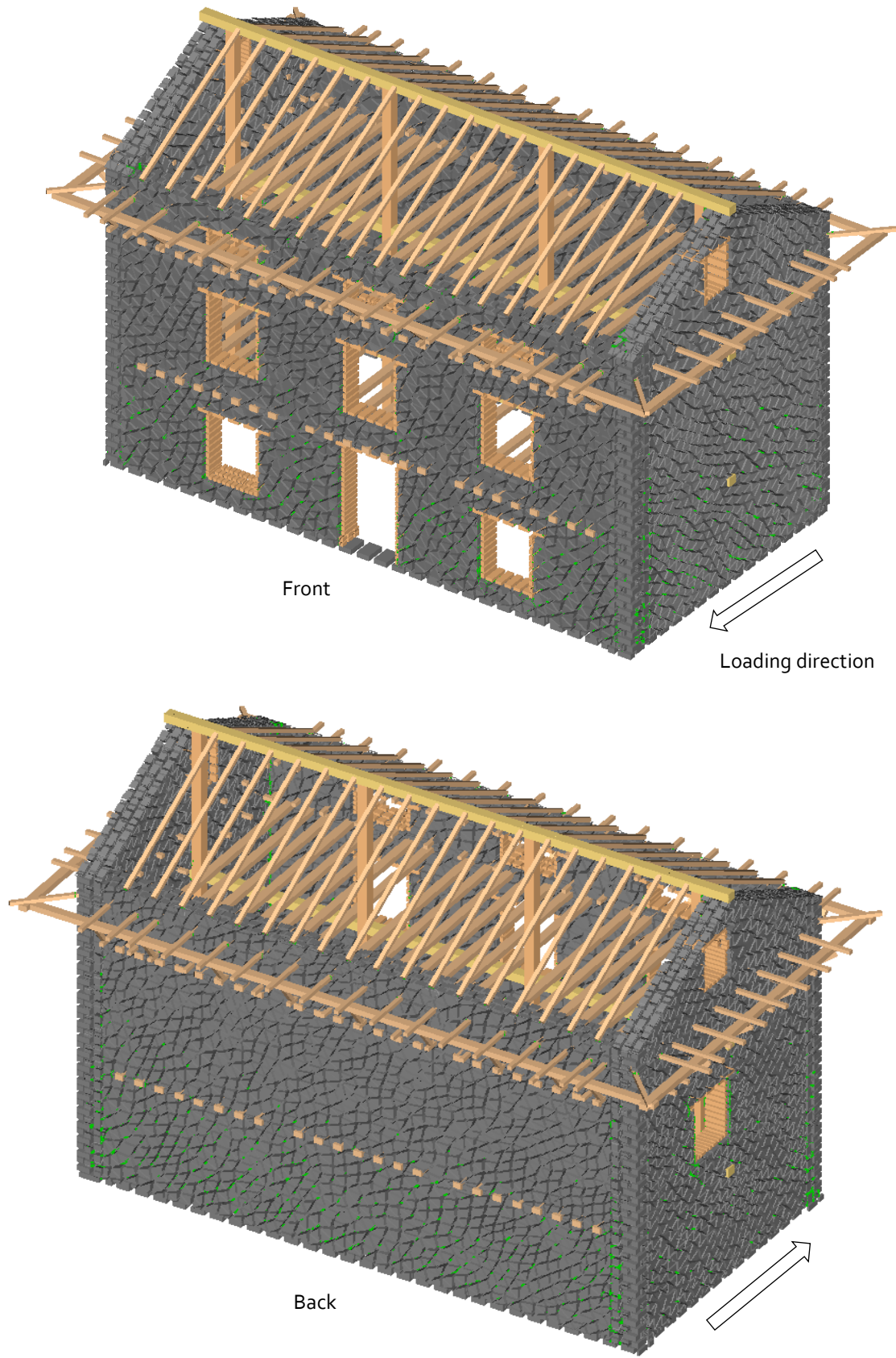
(a) **Operational limit**: Hairline cracks appear at corners of openings and wall-connections. Green cracks represent hairline cracks. Maximum crack opening is less than 0.5 mm.

Front

Back
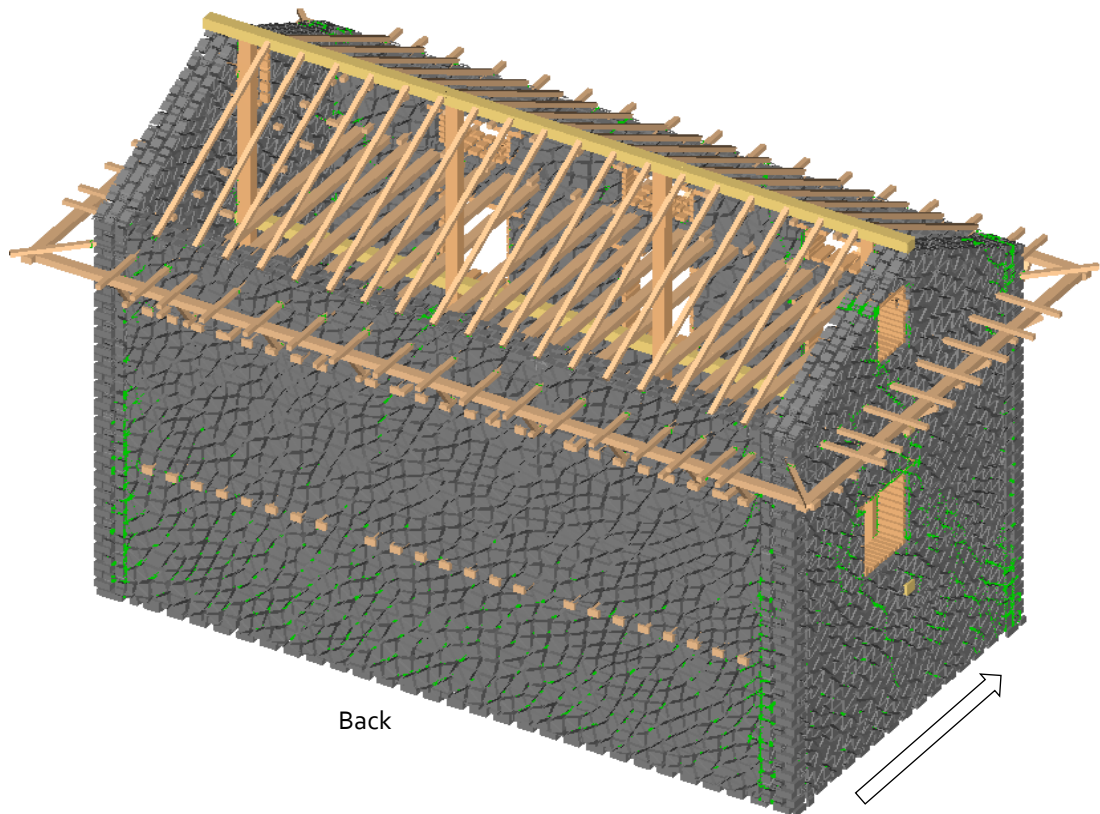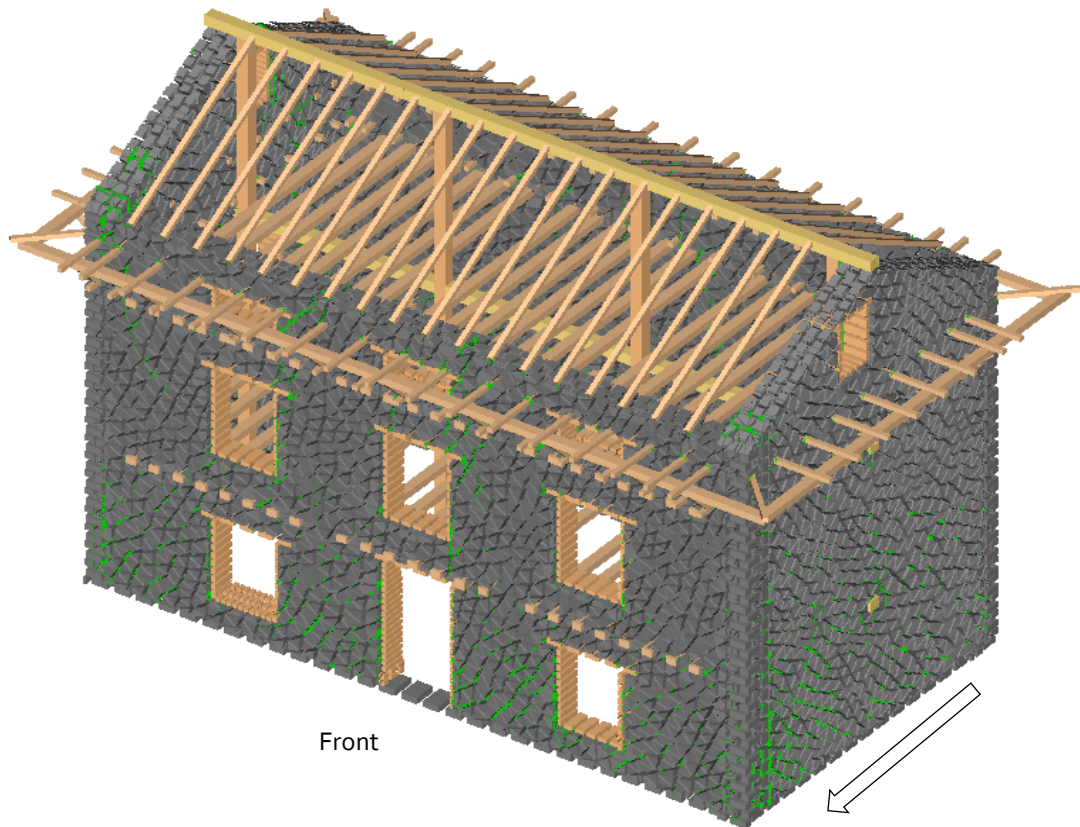
(b) **Immediate occupancy limit**: Hairline to minor cracks all over the wall surface, minor separation cracks appear at cross wall-connections. Green cracks represent hairline to minor cracks. Maximum crack opening is 5 mm. Structure reaches maximum elastic capacity and starts losing stiffness substantially (see also Figure 39).

Front

Back
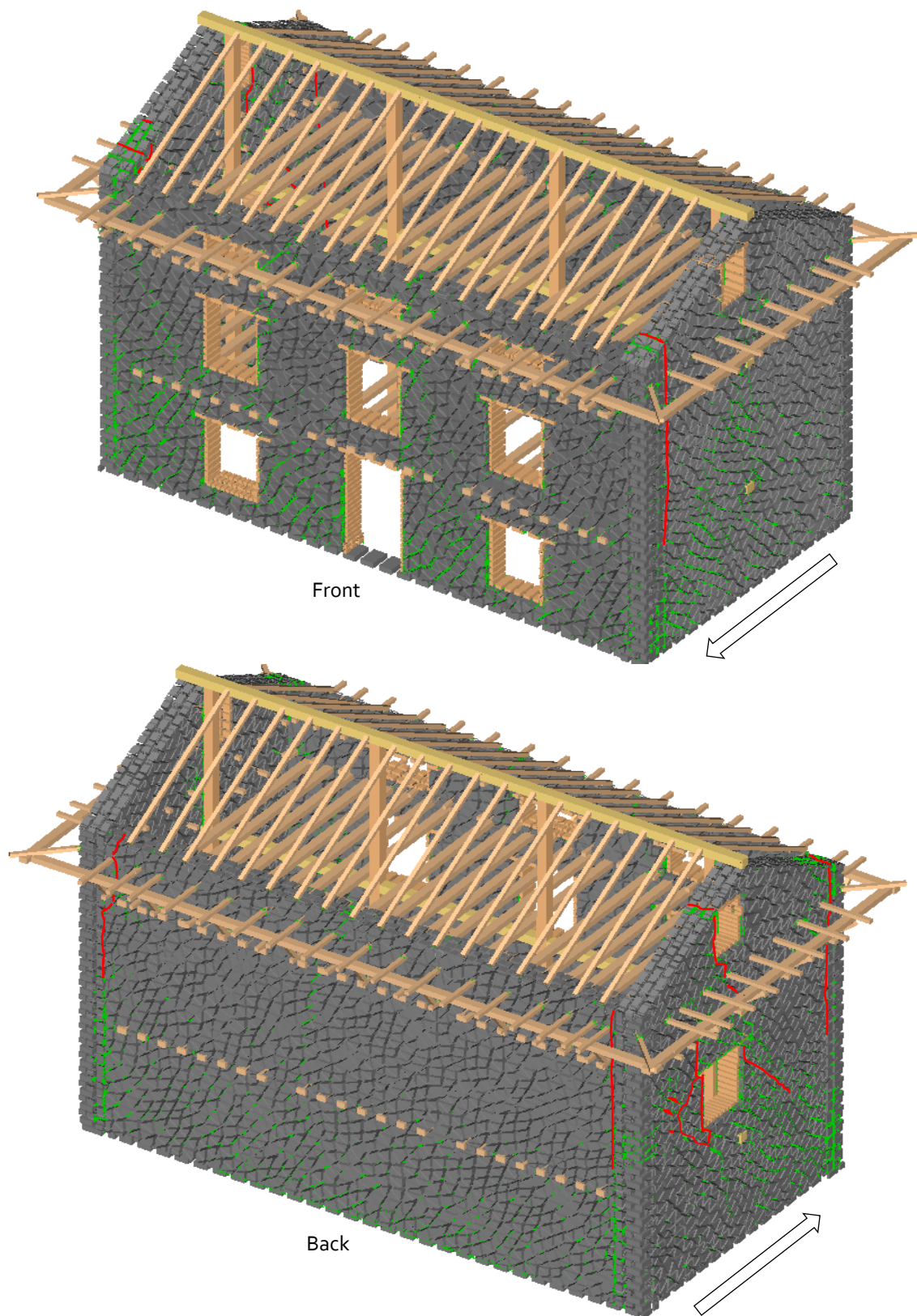
(c) **Life safety limit**: Minor to major shear cracks developed through all the masonry wall surface. The vertical separation cracks (red) become extensive (maximum crack opening of 10 mm) at the top. Visible shear damage (red) in the short in-plane wall with openings.

Front

Maximum crack
width = 15 mm

Back
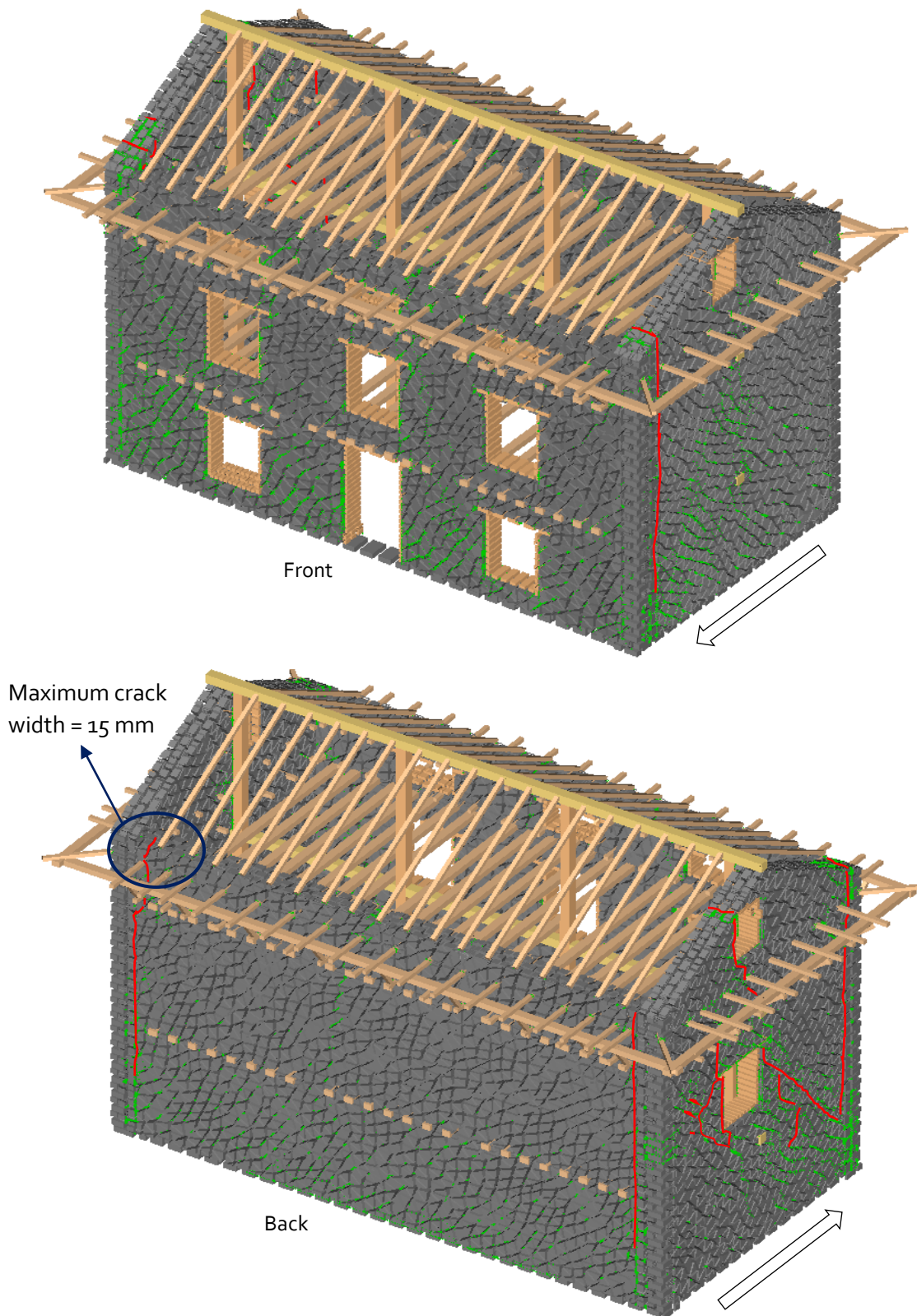
(d) **Collapse prevention limit**: Widely distributed major cracks in all the wall surfaces. The vertical separation cracks (red) and the shear cracks (red) in the short wall with openings become extensive with maximum crack opening of more than 15 mm.

Figure 42. Damage levels in the PRE-SMM building at the limits of different performance levels.

Figure 43 shows the actual damage state of the case study building (i.e. the index building used for the numerical study which was surveyed by the author during his field trip). Major vertical separation cracks (maximum crack width of about 20 mm) in both direction walls can be seen suggesting that the building was subjected to bi-directional effect of ground motion. Although the building suffered irreparable damage, it survived collapse due to the presence of stiff floor and roof diaphragms.

Figure 43. Actual damage due to the 2015 earthquake in the case study PRE-SMM building from Sindhupalchowk district. Vertical separation cracks have a maximum width of about 20 mm.

Both in the numerical analysis as well as in the observed damage, excessive out-of-plane overturning of the walls is prevented, and the ultimate collapse mechanisms involves the corner failure and damage of short walls. This indicates that the timber floor system and the roof system which includes the arrangement of timber keys and struts, provide sufficient level of in-plane stiffness for the diaphragm action.

6.3.2 POST-SMM Typology

Figure 44 compares the capacity curves of an index building of the POST-SMM typology in the longitudinal and transverse directions. The capacity curves in both longitudinal and transverse direction are similar reaching to peak lateral capacity as high as 0.6g. Figure 44 also shows the roof drift thresholds representative of the four different performance levels. These will be used in the seismic performance assessment and fragility analyses in section 7.2.

Figure 45 compares the capacity curves for the POST-SMM typology for different material quality. Although there is change in the lateral capacity, the thresholds of damage states are more or less similar. The difference due to the poor and good quality material has almost similar effect in the lateral capacity, unlike the case of PRE-SMM typology. The increment/reduction in both strength and ductility can be observed due to the good/poor quality material.
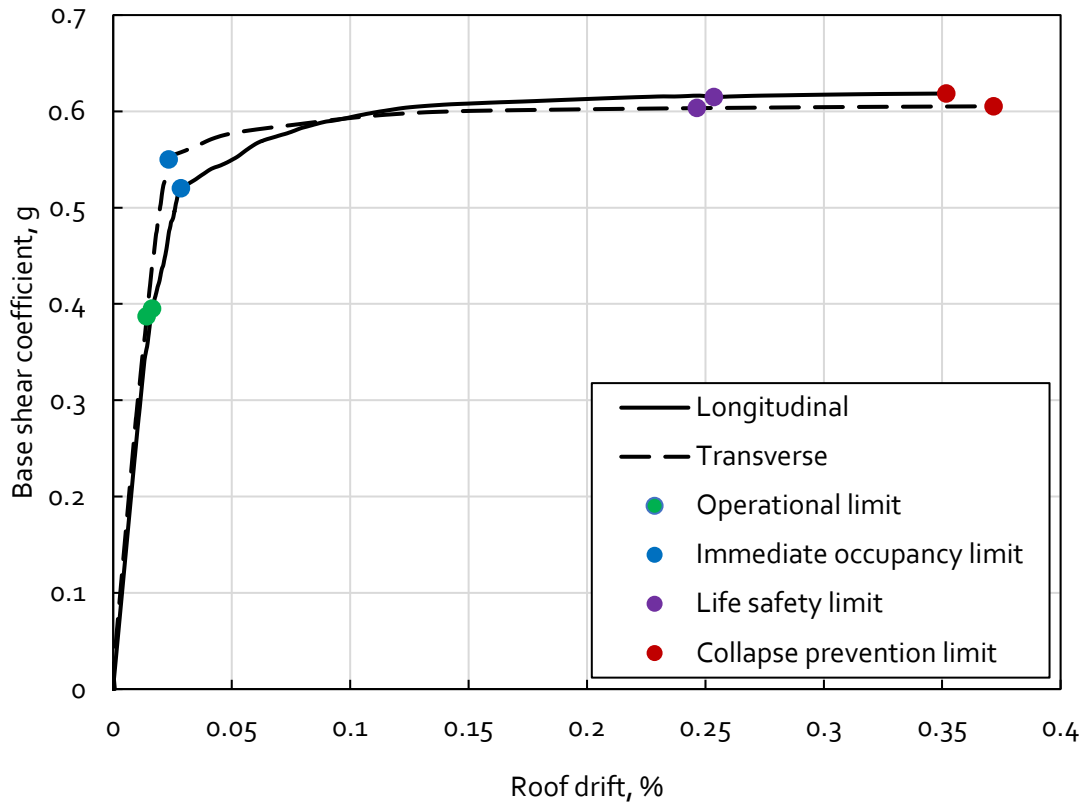
Figure 44. Capacity curves for the POST-SMM typology in two principal directions.
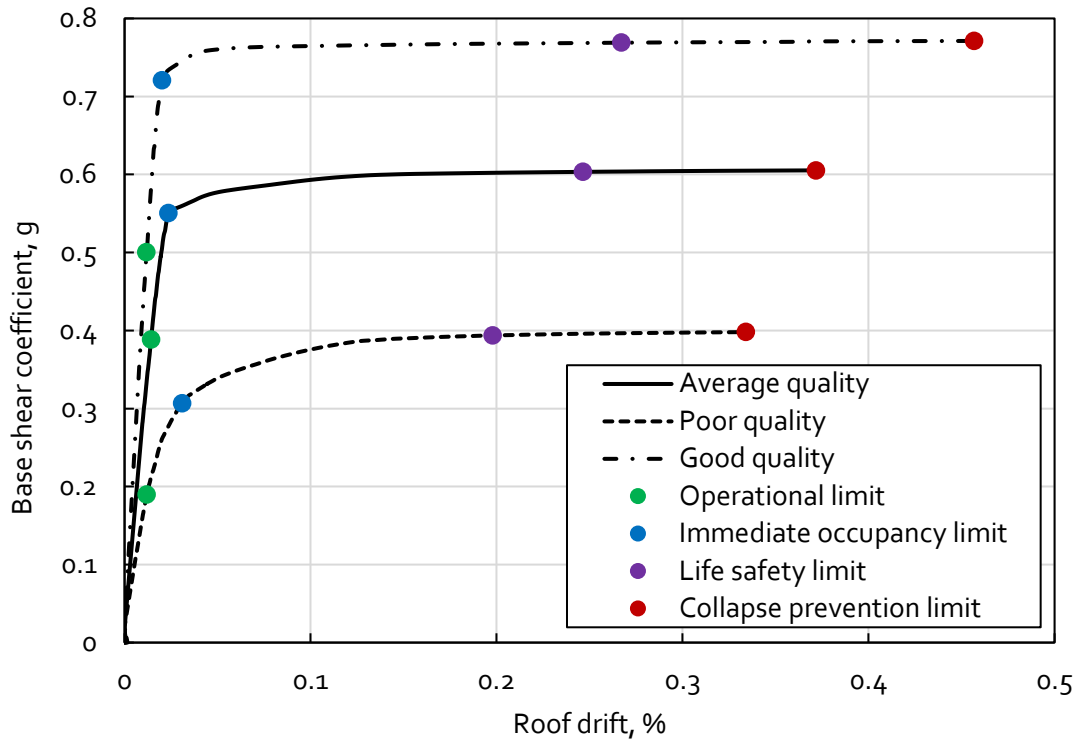
Figure 45. Effect of material quality on the POST-SMM capacity curve (note that the capacity curves in the transverse direction are compared).

A recent study by Bothara et al. (2018b) also found typically high lateral capacity (about 1.0g) for single-storied SMM school buildings from Nepal. Higher initial stiffness in our study is justified by the layout of openings in two constructions i.e. the school building has several openings in the back wall as well (see Bothara et al., 2018b) although very high (an order of magnitude higher) elastic modulus was used in their study. In contrast, due to higher value of tensile strength and shear modulus (and possibly higher value of friction coefficient, although not reported) in their analysis, the yield as well as ultimate strength capacity is considerably higher than the same from the present study. It is also worth noting that the modelling approach used (triangular elements in our study and rectangular elements in their study) could also have affected the load-deformation response.
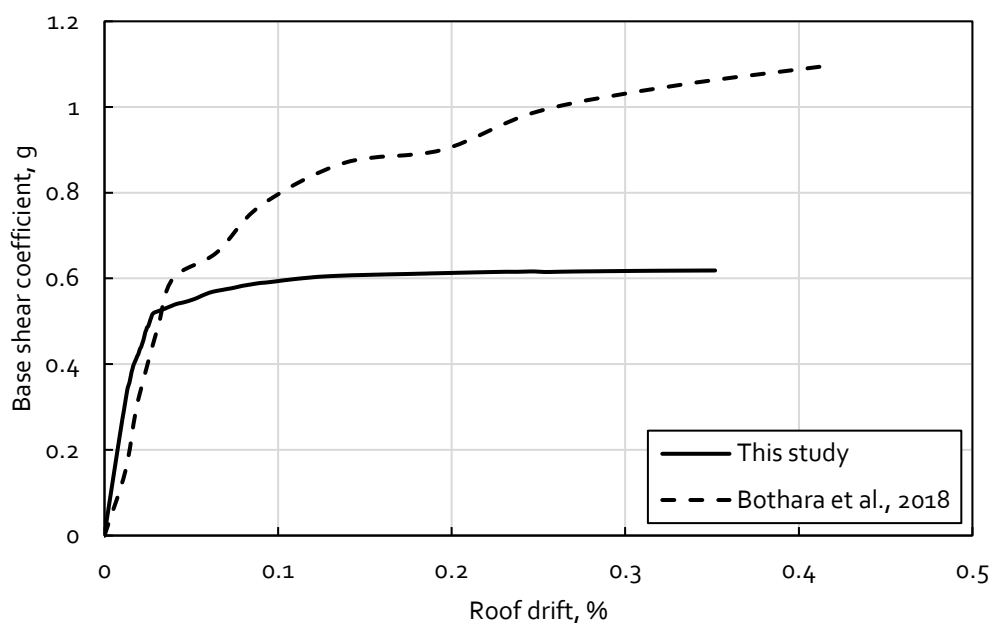
Figure 46. Comparison of capacity curve for the POST-SMM typology from this study and from literature (i.e. Bothara et al., 2018b).

Figure 47 presents the damage levels at the limits of different performance levels when loaded in the transverse direction. The seismic bands and the confining elements around the openings successfully contain and prevent the diagonal shear failure of masonry wall portions. The final collapse mechanism in POST-SMM buildings is shear sliding failure of masonry portions at the wall-band horizontal interfaces resulting in the compression failure at the corner (see Figure 47(d)). Such shear-sliding failure modes are typical when there is low vertical pre-compression and poor-quality mortar (Tomazevic, 1999). The design of POST-SMM constructions could be further improved by providing vertical confining elements at all the cross wall-connections along with dowels connecting these to the walls, which would restrict the compression failure at corners as well as improve the overall ductility.
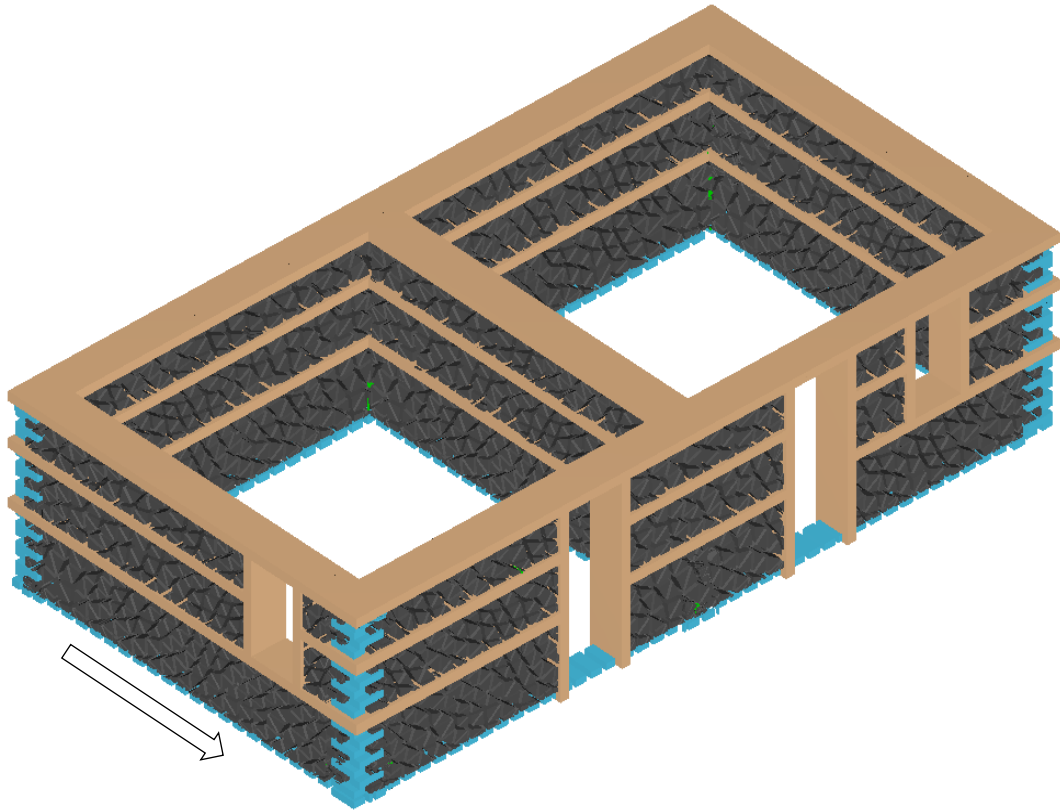
(a) **Operational limit**: Hairline cracks appeared at few corners.

Loading direction
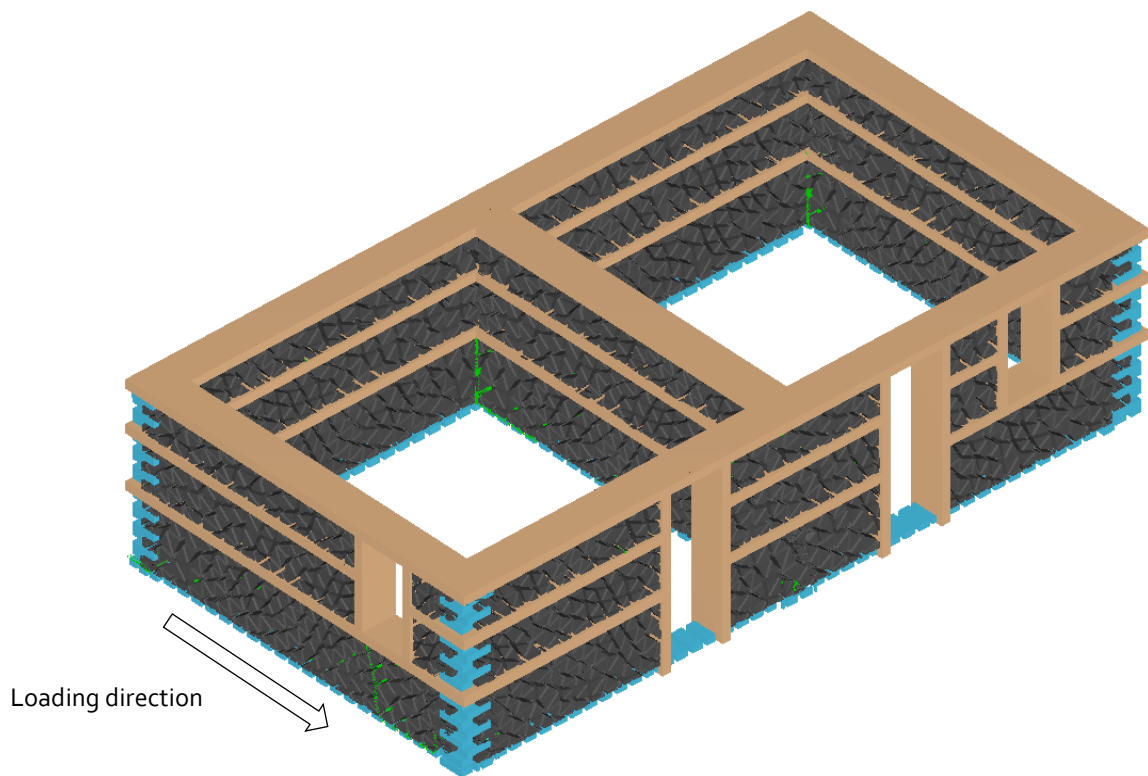
(b) **Immediate occupancy limit**: Hairline to minor cracks on the wall surfaces. Minor shear cracks and shear sliding cracks appear at the bottom most layer. Maximum crack opening is 3 mm.
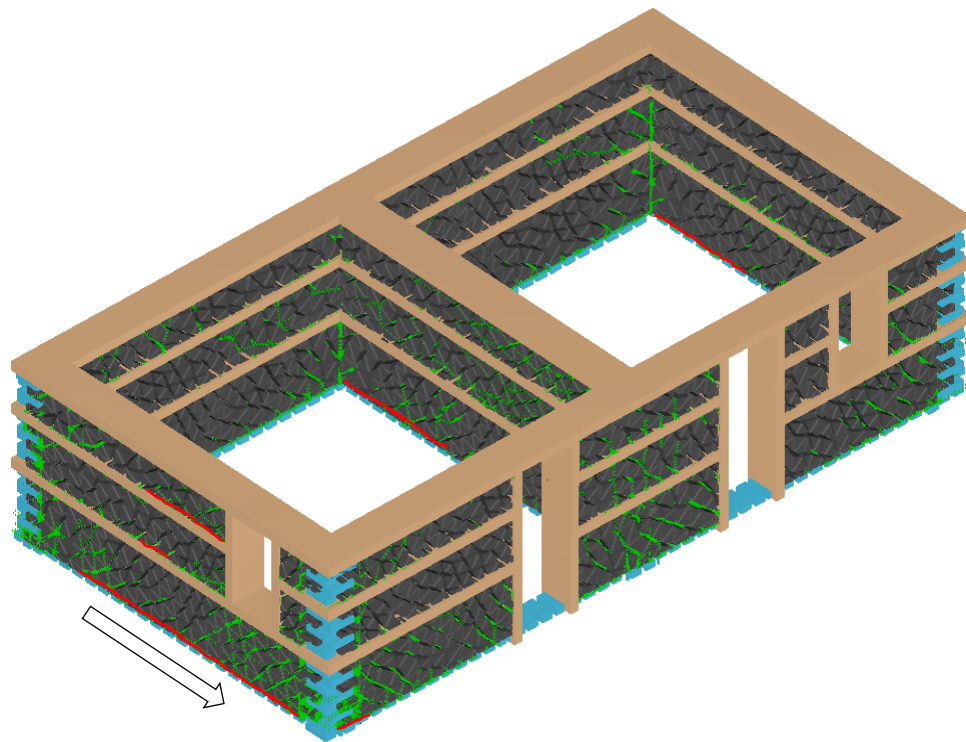
(c) **Life safety limit**: Distributed cracks on all masonry walls. Minor to major sliding shear cracks developed through all the wall-band interfaces. Maximum crack width is about 5 mm.
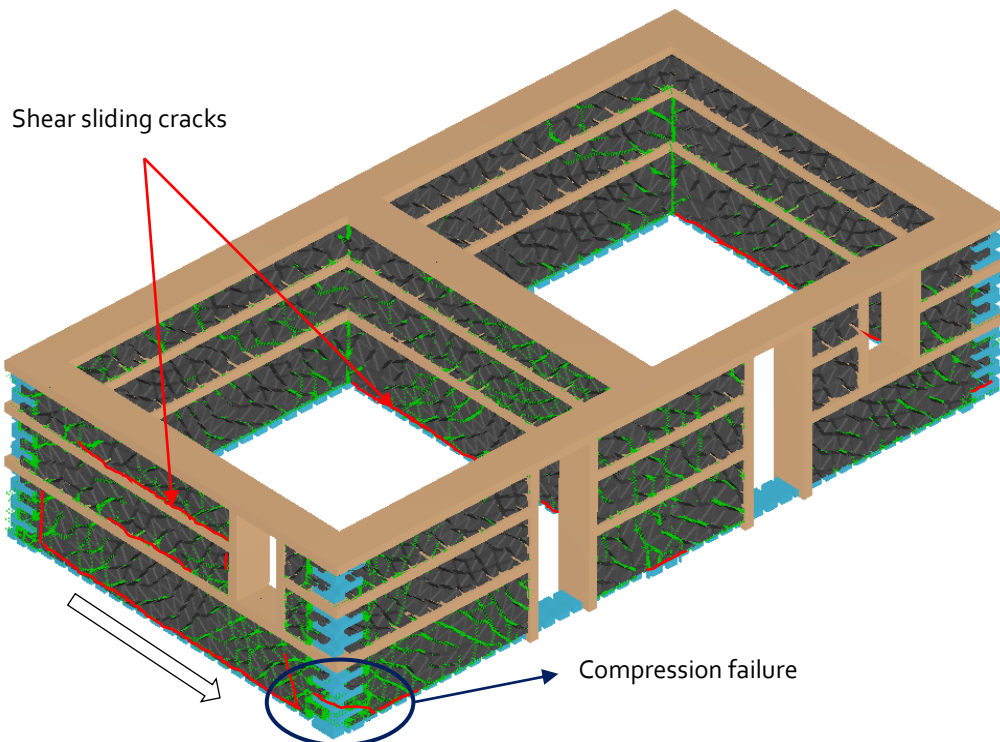
(d) **Collapse prevention limit**: Minor to extensive cracks in all the wall surfaces. The shear sliding cracks extended through full length. Weakest corner on the verge of compression failure. Maximum crack opening of more than 5 mm.

Figure 47. Damage levels in the POST-SMM building at the limits of different performance levels.

7   SEISMIC PERFORMANCE ASSESSMENT AND DERIVATION OF FRAGILITY/VULNERABILITY FUNCTIONS

7.1   Seismic Performance as Per NBC 105: 2019

Since the PRE-SMM buildings were not designed as per seismic design codes, it is important to understand their seismic capacity with respect to the Nepalese seismic design requirements. In this section, the seismic performance assessment of both PRE- and POST-SMM typologies as per the requirements of Nepalese seismic design code (NBC 105: 2019) is conducted. It is worth noting that the seismic design code, drafted initially in 1994, has been revised recently to produce NBC 105: 2019 by incorporating the recent advancements of knowledge in the field of structural engineering and seismic design practice. Table 3 shows the design parameters chosen for characterizing the elastic spectrum which is presented in Figure 48.

Table 3. Parameters chosen for constructing elastic site spectrum as per NBC 105: 2019.

Parameter	Value
Soil type	Type A (Rock site)
Importance factor, I	1 (Residential building)
Seismic zoning factor, Z	0.3 (Chautara, Sindhupalchowk district)
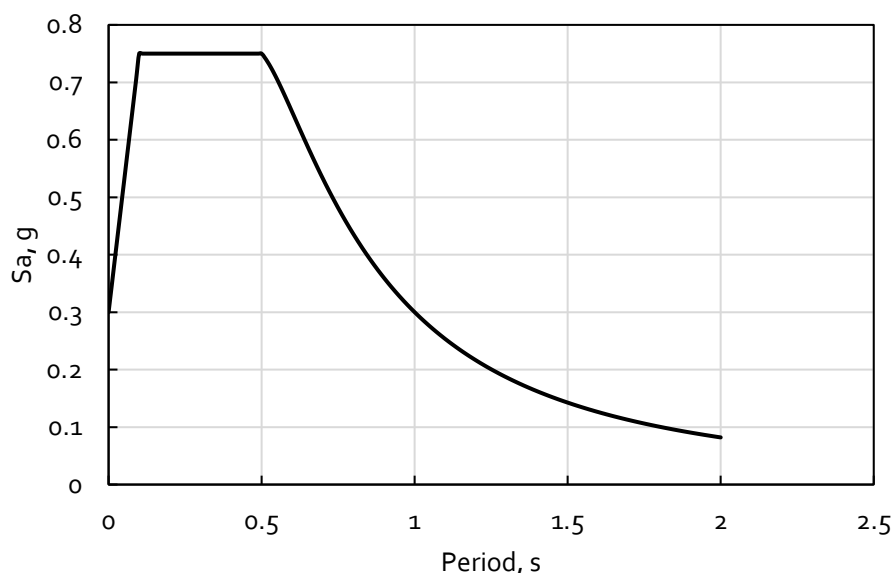
Figure 48. Elastic site spectrum as per NBC 105: 2019.

In order to obtain the performance point, the N2 approach (Fajfar, 2000) is followed by using the NBC 105: 2019 elastic site spectrum (Figure 48) as the seismic demand and intersecting the equivalent SDoF (single degree of freedom system) capacity curve with the inelastic spectrum. Note than in both cases i.e. PRE-SMM and POST-SMM typology, the capacity curves in the transverse (weakest) direction are used for seismic performance assessment.
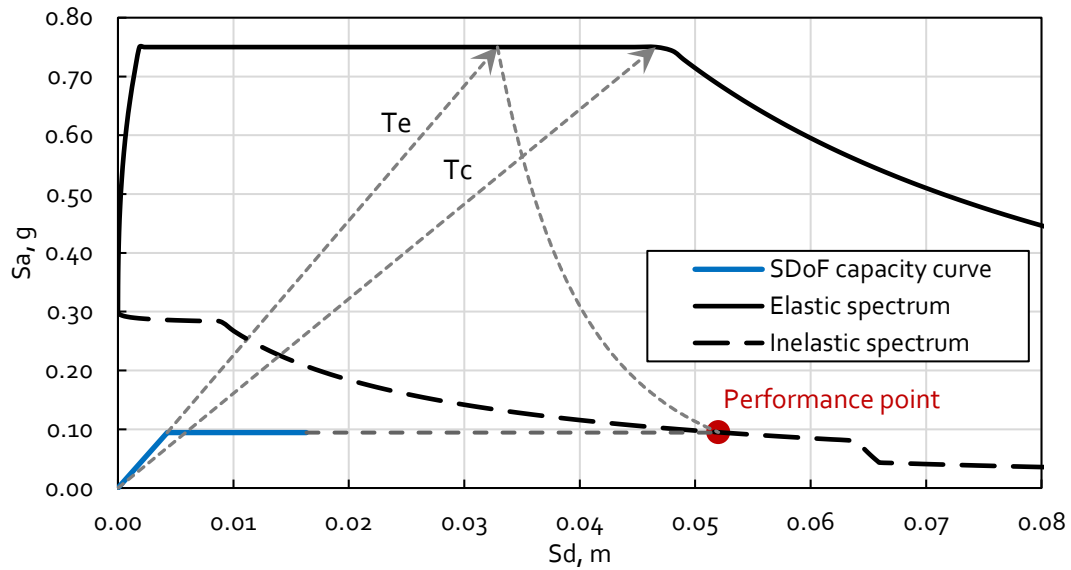
Figure 49. Application of N2 method for seismic performance assessment of PRE-SMM typology (with average quality mortar) using the NBC 105: 2019 elastic site spectrum.
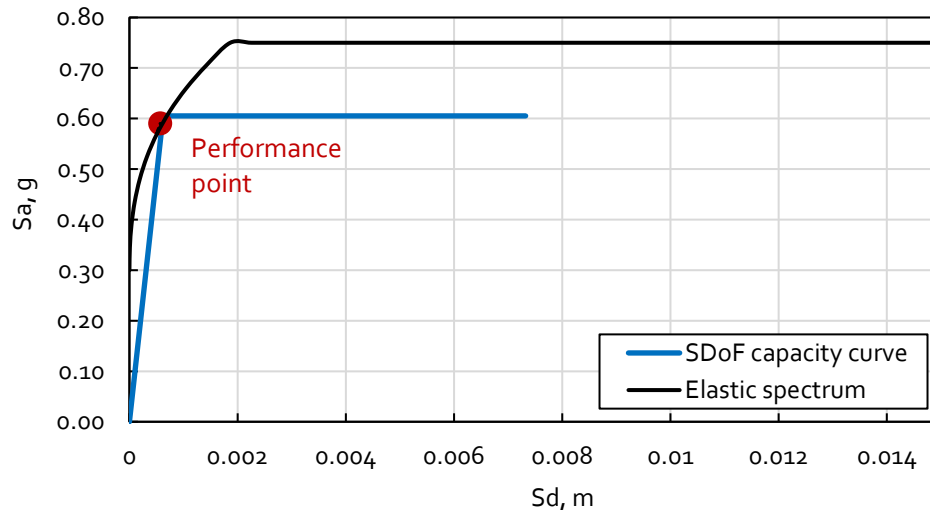
Figure 50. Application of N2 method for seismic performance assessment of POST-SMM typology (with average quality mortar) using the NBC 105: 2019 elastic site spectrum.

For the PRE-SMM typology, the seismic demand is far beyond the 'ultimate' (i.e. Collapse prevention) limit (Figure 49), hence the seismic design level of PRE-SMM typology as per NBC 105: 2019 code can be said to be 'Poor'. On the other hand, the POST-SMM typology, which are designed as per the seismic design code (NBC 203: 2015), performs well within the 'serviceability' (Immediate occupancy) limit (see Figure 50).

In the next section, the same approach (i.e. N2 method) is applied for the seismic performance assessment of both typologies but using a number of natural records instead of code-prescribed design spectrum, in order to consider record-to-record variability in ground motion characteristics.

7.2   Seismic Fragility and Vulnerability Evaluation

Understanding the seismic capacity and failure mechanisms of the two different building typologies (i.e. PRE-SMM and POST-SMM) in section 6.3, this section now advances further to assess the seismic fragility and vulnerability considering the uncertainty in material quality as well as in the ground motions. It should be noted that since the PRE-SMM building is weaker in the transverse direction and POST-SMM building has similar capacity curves in both directions, the fragility and vulnerability functions are generated in the transverse direction for both PRE-SMM and POST-SMM typologies.

A fragility function is a probability-valued function of an intensity measure (IM), that represents the probability of exceeding certain damage state (or limit state) in a building given the value of the IM. On the other hand, a vulnerability function is a loss-valued function of an IM, that represents the distribution of seismic loss given the value of the IM (D'Ayala et al., 2015). These functions can be component or building specific, or even can represent a building class (i.e. typology) and are vital inputs in seismic risk assessments (e.g. see D'Ayala et al., 2015; Yamin et al., 2014).

Mainly, three approaches have been in use for deriving fragility and vulnerability functions: empirical, analytical and hybrid methods, each one with inherent pros and cons (see Calvi et al., 2006). The use of empirical method to derive fragility and vulnerability functions using 2015 seismic damage data is impaired by the poor network of seismic recording stations in the country such that the distribution of ground shaking (i.e. IM) is not known with adequate reliability. Thus, analytical approach outlined in D'Ayala et al. (2015) is followed in this study for which dozens of tools have been proposed in the last three decades, with various levels of complexity and accuracy (Silva et al., 2019). In this study, in order to reduce the uncertainty in modelling approach, validated 3-D element-by-element modelling using the applied element method is followed (see section 6.1). Similarly, 3 different cases of material quality are considered to quantify the resulting dispersion in the fragility and vulnerability functions. As there are very limited ground motion records available from seismic events in Nepal (Goda et al., 2015), a suite of 22 ground motions suggested in FEMA P695 (FEMA, 2009) is used to consider the record-to-record variability. These ground motions contain a considerable dispersion in the main ground motion characteristics such as the total time of shaking, PGA, frequency content, energy content etc. It should be noted that the 22 set of FEMA P695 ground motion set contains 44 components (two horizontal components per recording station) and the stronger component of each ground motion set is chosen for this study. The acceleration spectra of the selected components of the ground motions are plotted in Figure 51 and the event name, year, magnitude and the recording station of the FEMA P695 suite of ground motions are listed in ANNEX A. PGA of these ground motions varies from 0.2g to 0.8g and spectral acceleration in the low period range (i.e. $T_1 < 0.5$ sec, in case of low-rise masonry buildings) also has a considerable dispersion so that the effect of the record-to-record variability can be studied in the fragility functions.
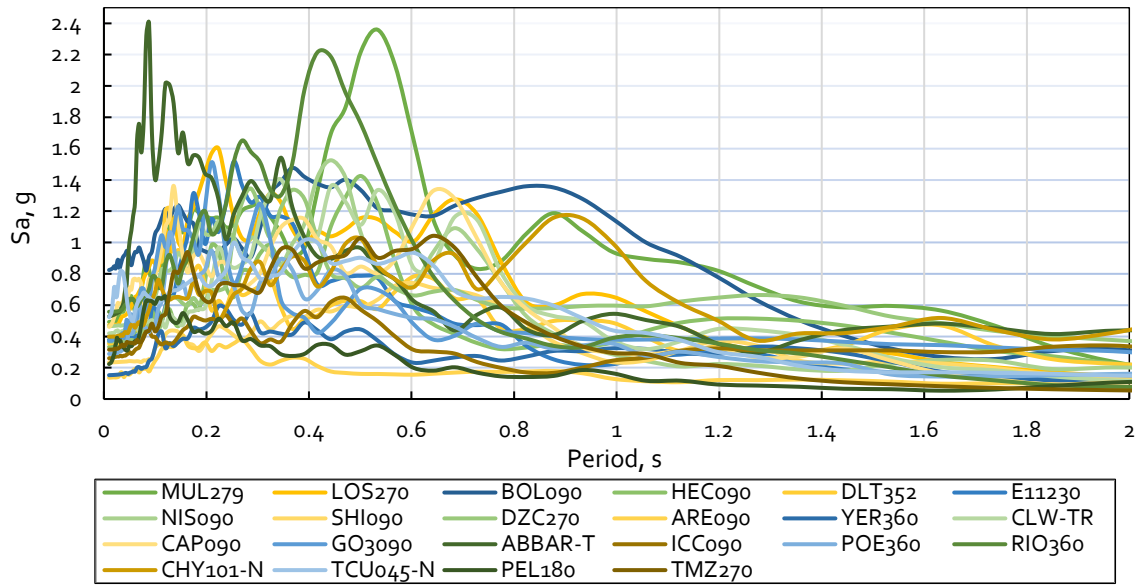
Figure 51. Response spectra of 22 ground motions components from FEMA P695 (FEMA, 2009).

Since the generation of fragility functions requires numerous performance points under several ground motions (and each scaled) so that enough data points for statistical fitting, for all performance levels, can be obtained, non-linear time history analysis (NLTHA) would be highly resource and time consuming, particularly for the modelling approach adopted in this study. Hence simplified but validated method i.e. capacity-spectrum approach following the N2 method (Fajfar, 2000, D'Ayala et al. 2015) which is prescribed in Eurocode 8 (EN 1998-1) is applied for the seismic performance assessment under the suite of FEMA P695 ground motions (each scaled) in order to consider the record-to-record variability. Figure 52 illustrates the application of N2 method to get the performance point of the structure under a spectrum of natural ground motion. Readers are referred to D'Ayala et al. (2015) for detailed procedure on the seismic performance assessment using the N2 method.
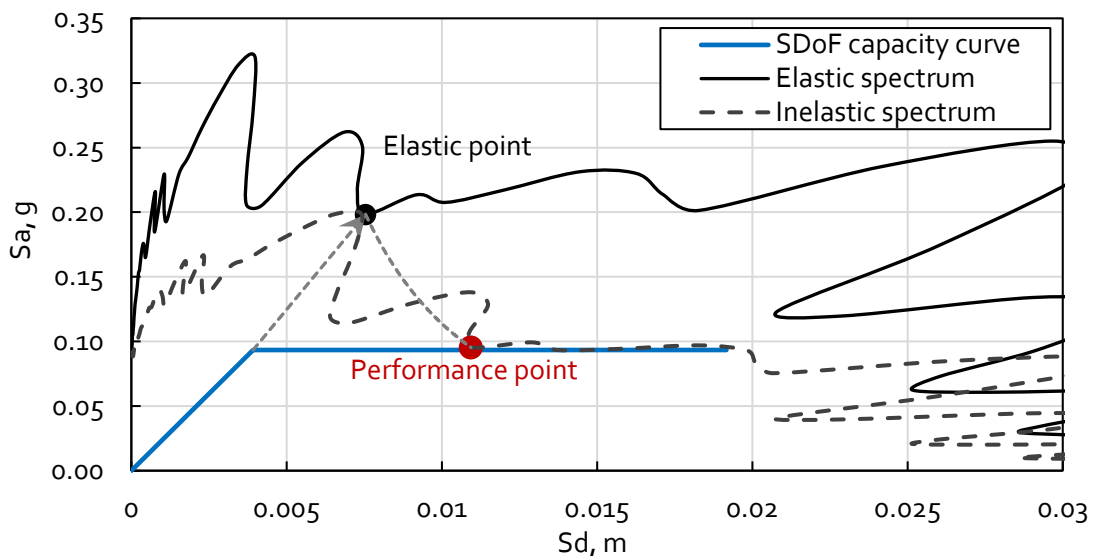
Figure 52. Illustration of seismic performance assessment under a natural record response spectrum using the N2 method.

49
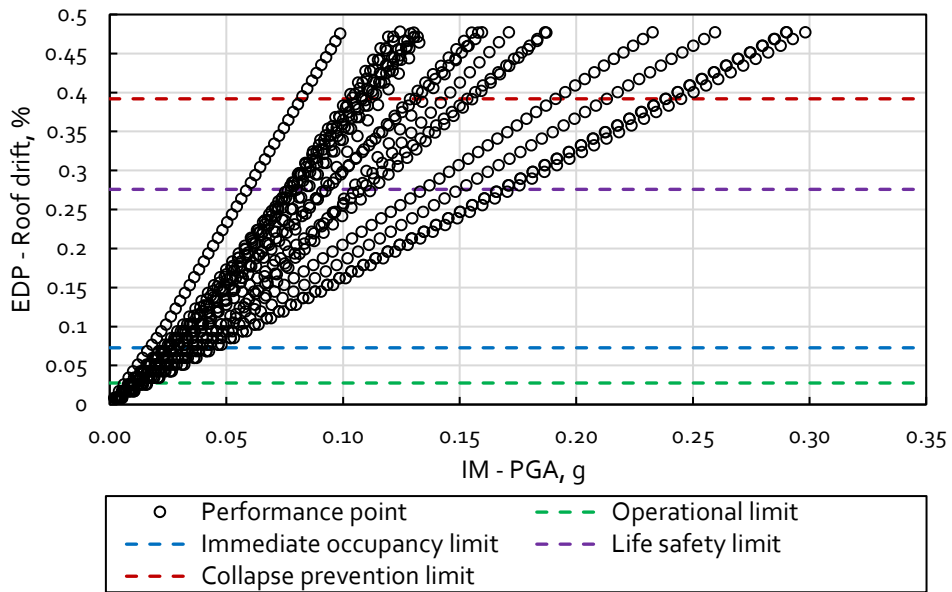
Figure 53. Cloud of performance points for PRE-SMM typology (with average quality mortar) under a suite of FEMA P695 set of 22 ground motions.
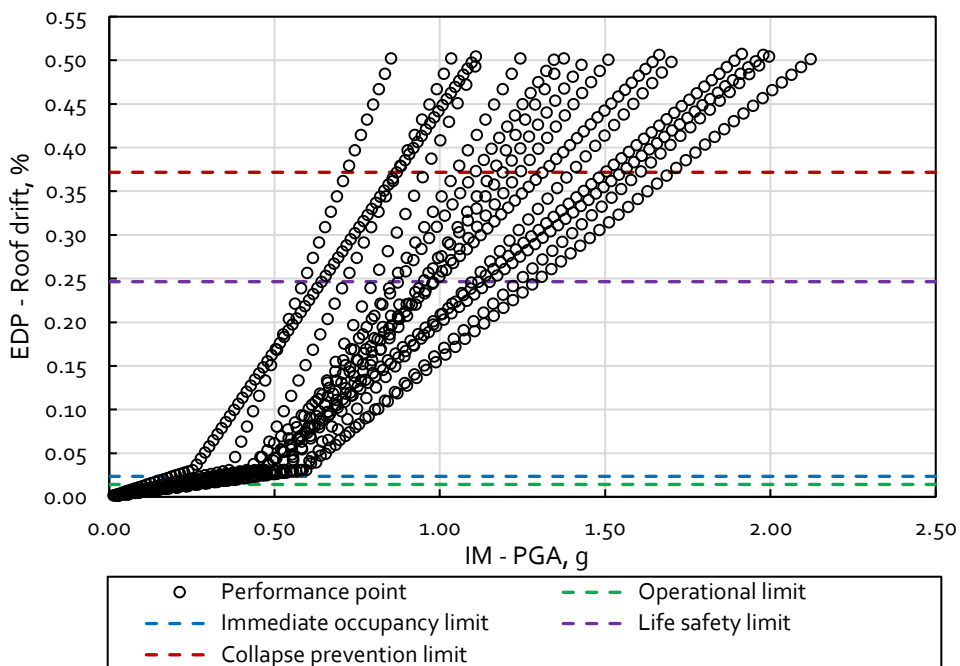
Figure 54. Cloud of performance points for PSOT-SMM typology (with average quality mortar) under a suite of FEMA P695 set of 22 ground motions.

Figure 53 and Figure 54 present the cloud of performance points for PRE-SMM and POST-SMM typologies, respectively obtained with the application of N2 method considering the FEMA P695 set of far-field ground motions. Several hundred performance points are generated by scaling each ground motion records such that the enough points are generated for the entire range performance levels. Also shown in these figures are the thresholds for different performance levels so that one can appreciate the median PGA and dispersion at each performance level resulting from the effect of ground motions with different characteristics. While it is recognised that the use of spectral acceleration (Sa(T1)) as IM produces more dispersion of performance points in the non-linear range ,

50

the use of PGA as the IM in this study is dictated by the fact that these are low-period structures and the comparison of fragility/vulnerability functions for two buildings with substantially different fundamental period becomes meaningful when using the PGA as IM.

Based on the performance point distribution and the thresholds of performance levels presented in Figure 53 and Figure 54, derivation of fragility functions is performed statistically using least square method, as detailed in D'Ayala et al. (2015). Table 4 and Table 5 present the median and dispersion of the PGA for different performance levels for PRE-SMM and POST-SMM typology. The same information is presented in terms of fragility curves in Figure 55 and Figure 56. The 'serviceability' limit state (i.e. Immediate occupancy) is exceeded for the PRE-SMM typology at a median PGA of as low as 0.05g even with good material quality while the same limit state is exceeded for the POST-SMM typology only at a median PGA of about 0.17g even with poor material quality. Similarly, for the PRE-SMM typology, the median PGA for exceeding the 'ultimate' (i.e. Collapse prevention) limit state is very low i.e. about 0.30g even with good material quality while the same for POST-SMM typology is exceeded only at a median PGA of about 0.8g, even with poor material quality. For both building typologies, the fragility curves, particularly for life safety and collapse prevention performance level, present significant dispersion due to the variability in both the ground motions characteristics and material quality.

Table 4. Median and standard deviation (SD) of fragility functions for PRE- SMM typology with poor, average and good material quality.

Performance Level	Poor quality		Average quality		Good quality	
	Median PGA (g)	SD	Median PGA (g)	SD	Median PGA (g)	SD
Operational	0.005	0.567	0.012	0.276	0.016	0.276
Immediate occupancy	0.010	0.569	0.029	0.293	0.052	0.331
Life safety	0.029	0.530	0.097	0.370	0.149	0.468
Collapse prevention	0.074	0.836	0.170	0.676	0.300	0.910

Table 5. Median and standard deviation of fragility functions for POST- SMM typology with poor, average and good material quality.

Performance Level	Poor quality		Average quality		Good quality	
	Median PGA (g)	SD	Median PGA (g)	SD	Median PGA (g)	SD
Operational	0.082	0.306	0.226	0.206	0.338	0.121
Immediate occupancy	0.172	0.364	0.367	0.257	0.600	0.157
Life safety	0.526	0.356	0.948	0.261	1.314	0.181
Collapse prevention	0.799	0.536	1.302	0.352	2.230	0.313

Figure 55. Seismic fragility functions for PRE-SMM typology. Dispersion due to the material quality is also shown.
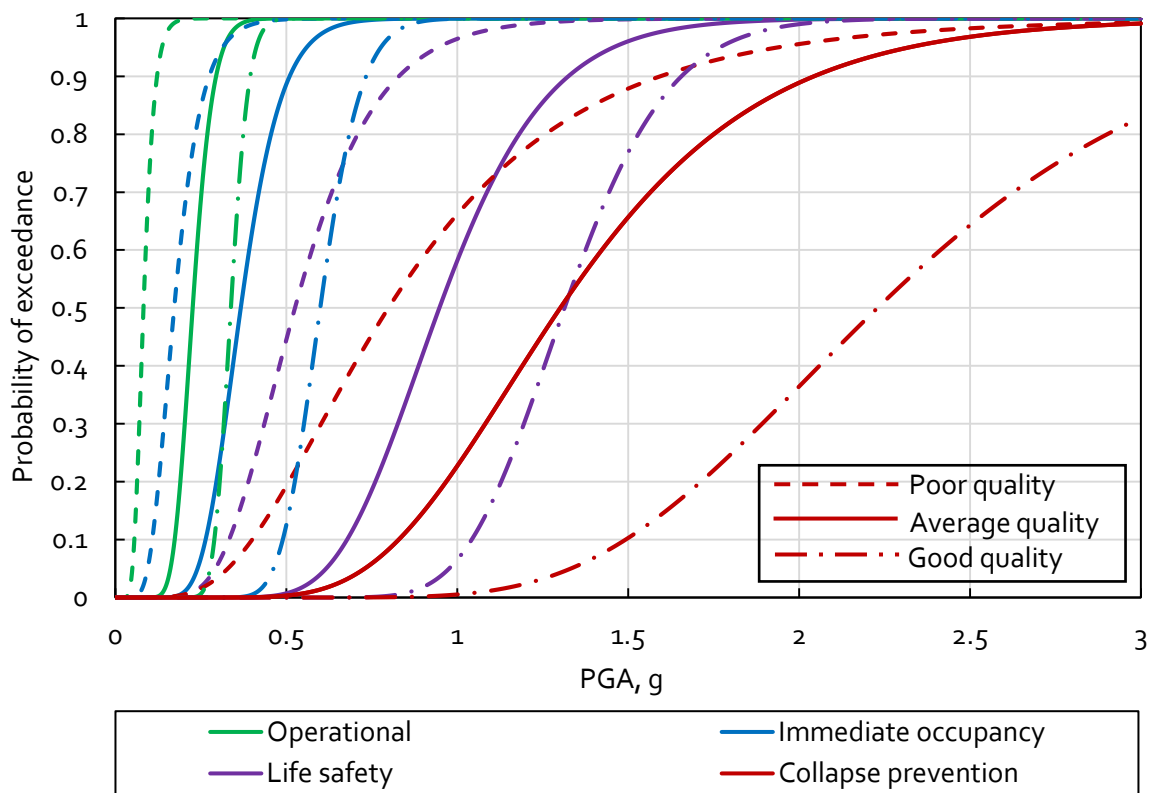
Figure 56. Seismic fragility functions for POST-SMM typology. Dispersion due to the material quality is also shown.

In Figure 57, the fragility functions for the PRE-SMM typology are compared against the fragility functions for similar Nepalese constructions from Guragain (2015). It should be noted that the fragility curves reported in Guragain (2015) represents a broader class of SMM building (single and two-storied) hence the median PGA for exceeding each damage state is generally higher than from the present study. Moreover, the dispersion in the fragility functions for each damage state is also higher except for the collapse fragility.
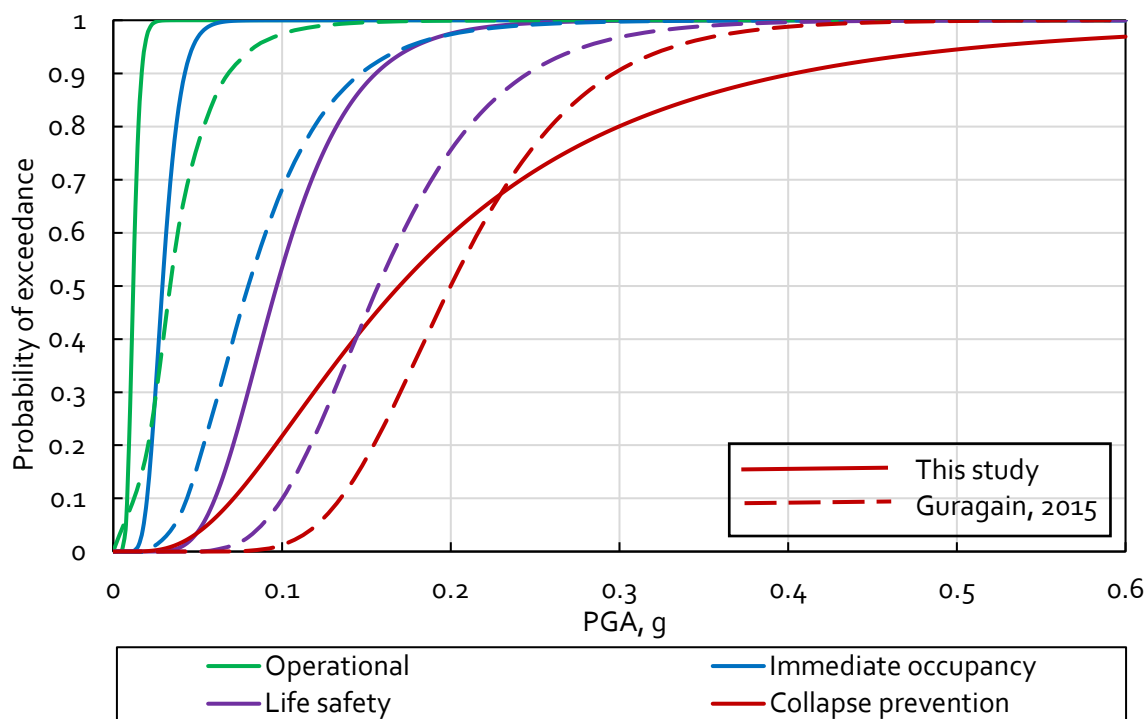
Figure 57. Comparison of fragility curves for PRE-SMM typology from this study with the same from Guragain (2015).

Vulnerability functions for the PRE-SMM and POST-SMM typologies are then generated by computing the damage probabilities for each damage states at a given IM (i.e. PGA) level and then convoluting with the damage to loss function (see Yamin et al., 2014; D'Ayala et al., 2015). HAZUS (FEMA, 2012) consequence model (i.e. damage to loss function) for residential buildings are used in this study which is as follow: 2%, 10%, 50% and 100% mean damage ratios (MDR) for Operational, Immediate occupancy, Life safety and Collapse prevention performance levels, respectively. The MDR represents the ratio of the building repair cost to the replacement cost. This function is selected as country-specific damage to loss functions for Nepalese SMM buildings has not been developed yet and the authors are aware that this depends not only the damage scale but several other factors such as the cost of material, labour, policies etc. (see Hill and Rossetto, 2008; Bal et al., 2008; D'Ayala et al., 2015 etc.). Nevertheless, the HAZUS damage to loss function has been used by other researchers in for seismic loss assessment in developing countries e.g. Pakistan (Ahmad et al., 2014).
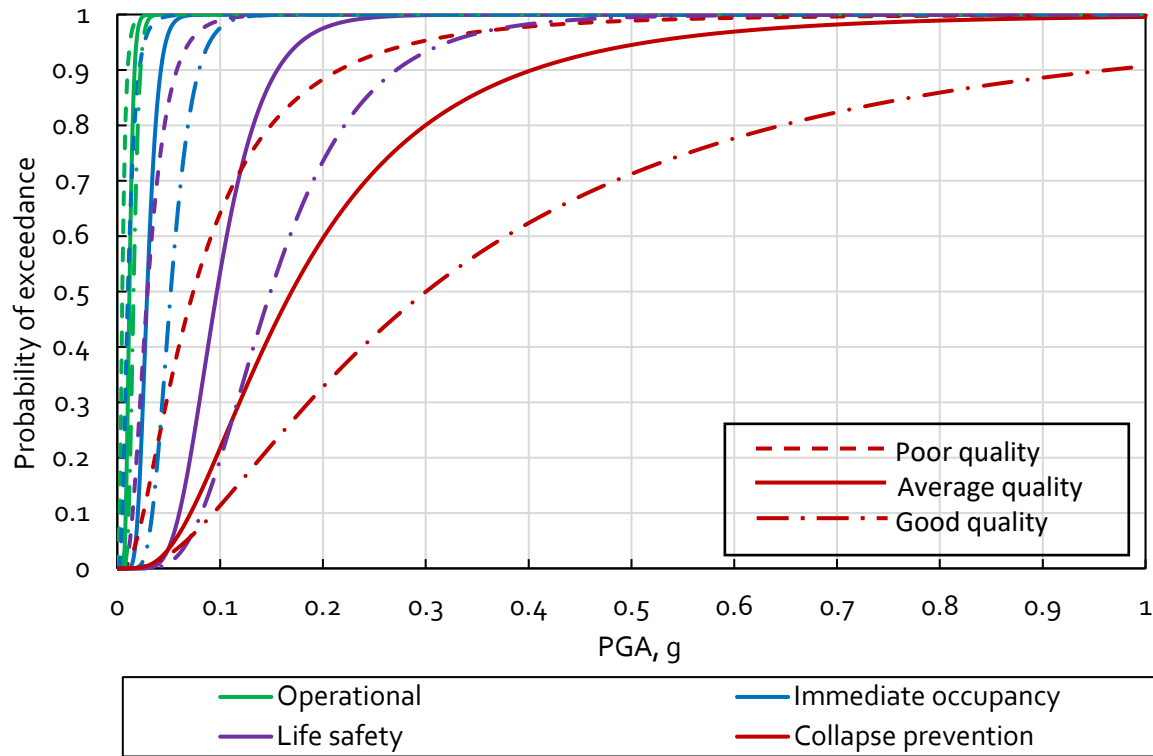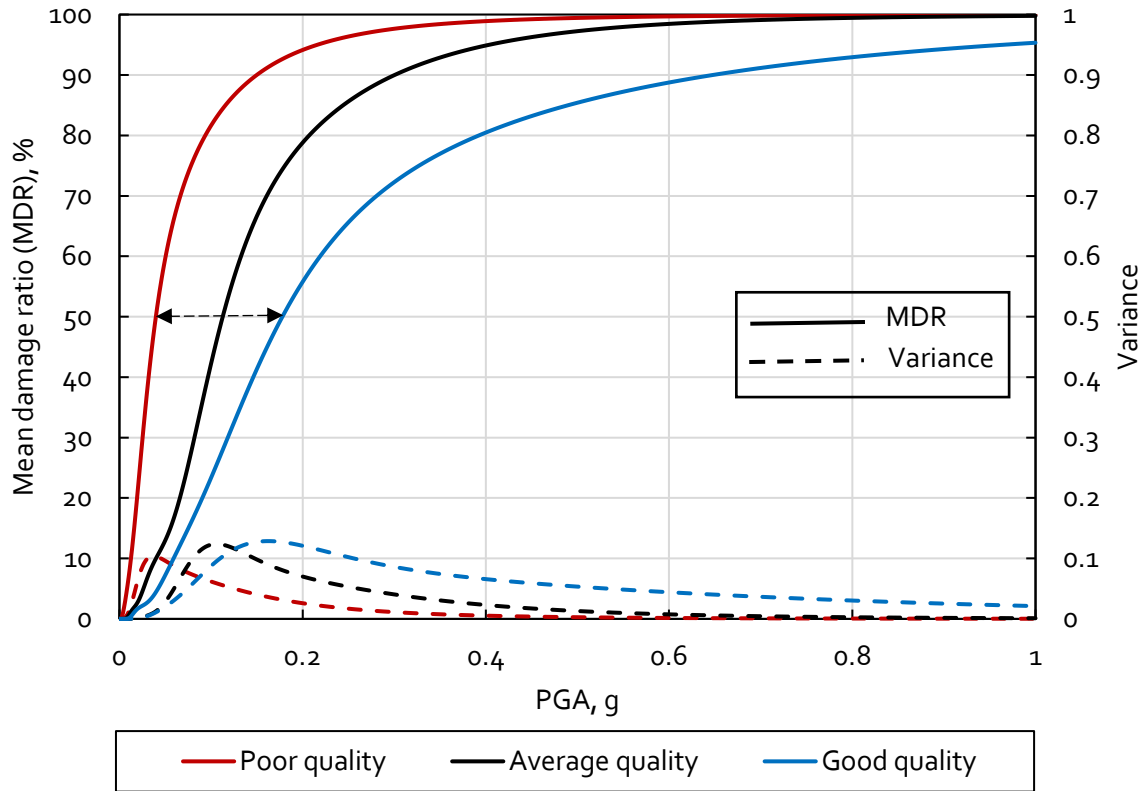
Figure 58. Seismic vulnerability functions for the PRE-SMM typology. Dispersion due to the material quality is also shown.
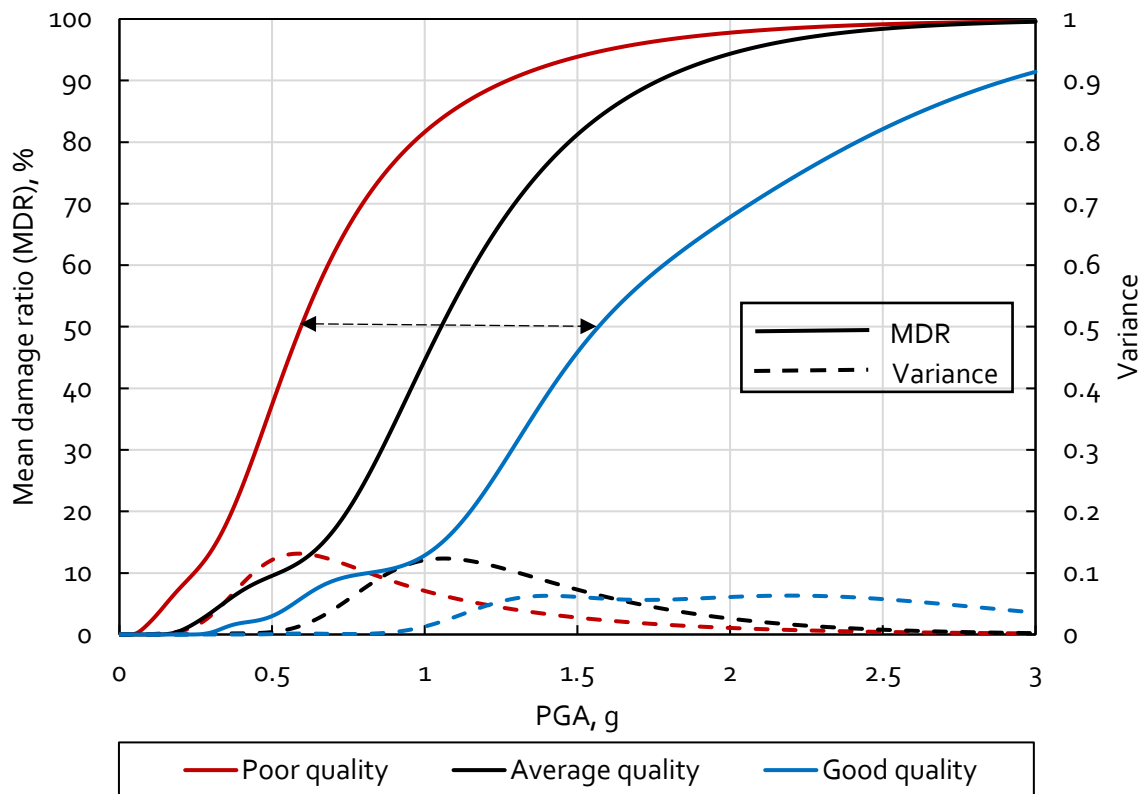
Figure 59. Seismic vulnerability functions for the POST-SMM typology. Dispersion due to the material quality is also shown.

The seismic vulnerability curves for PRE-SMM and POST-SMM typologies are presented in Figure 58 and Figure 59. It is noteworthy that due to the different material quality, the PGA for 50% MDR has a dispersion of more than ±50% in both cases which is very high and shows that the global vulnerability can be substantially reduced using good quality material as well as with proper workmanship in the SMM construction. The vulnerability curves for both PRE- and POST-SMM typologies are compared in Figure 60. For the PRE-SMM typology, a ground motion with PGA of as low as 0.11g can cause 50% mean damage ratio while for the POST-SMM typology, same level of loss is reached at a PGA level of about 1.00g only. Thus, in terms of seismic vulnerability, in average, the PRE-SMM typologies are an order of magnitude vulnerable than the POST-SMM typology.
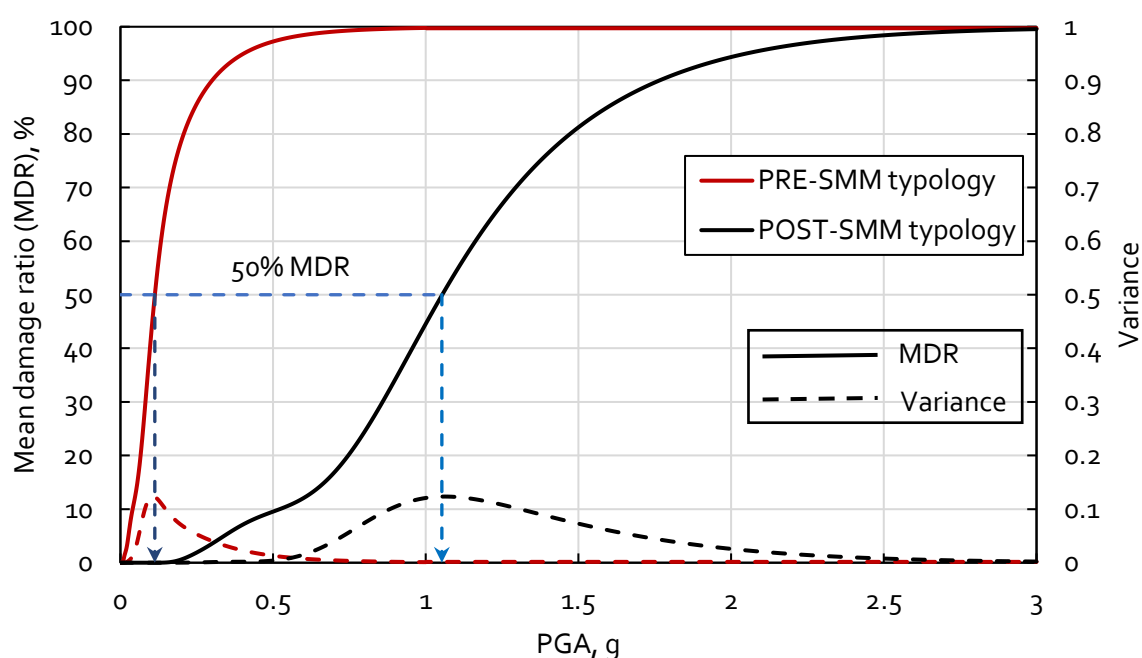
Figure 60. Comparison of seismic vulnerability functions for the PRE- and POST-SMM typologies (with average material quality).

The shake map from the 2015 Nepal earthquake (USGS, 2015) estimated a PGA range of 0.3g - 0.8g in the most affected districts which is far more than 0.11g (IM level for 50% MDR for PRE-SMM typology), hence the heavy damage to the PRE-SMM typology was inevitable. While for same level of intensity, the MDR for POST-SMM buildings would be less than 30% meaning that only repairable damage can be expected.

8   CONCLUSIONS AND FUTURE WORK

From the results and discussions presented in this report, the following main conclusions are drawn.

➢ Main reason of the widespread damage sustained by the residential buildings in the 2015 Nepal earthquake was the poor seismic performance of the most common SMM construction, which lacked adequate seismic resistant features.

➢ There are several pressing issues in the ongoing post-earthquake reconstruction such as: small sized houses affecting the livelihood of the communities, poor inspection of workmanship defects and code-compliance in construction, loss of vernacular construction and architecture affecting the social and cultural values etc. These are urgent issues and NRA needs to implement timely and effective policies in order to correct these and improve the seismic safety and social-cultural aspects of the post-earthquake reconstruction.

➢ Seismic design practice in Nepal has noticeably improved after the 2015 earthquake sequence as seen from the discussion of construction characteristics of newly built post-earthquake houses.

➢ As proven by the results of validation studies, as well as by the comparison of actual and numerical failure modes presented in this study, applied element method can be used as an effective tool to model and study the seismic behaviour of SMM constructions.

➢ The seismic capacity of the PRE-SMM typology is very low in both principal directions, the shorter direction being the weakest. As per the seismic design code of Nepal (NBC 105: 2019), the demand is far beyond the ultimate capacity of these buildings. Thus, the strengthening strategy for these existing SMM buildings should include vertical load resisting elements in order to increase the base shear capacity.

➢ Vertical separation cracks and corner failure triggering the collapse of short walls are the main failure modes in PRE-SMM buildings, as confirmed by the observed damage due to the 2015 earthquake sequence as well as the results of numerical study presented. Strengthening strategies for these buildings should also consider preventing these failure modes.

➢ The POST-SMM construction performs within the serviceability limit against the seismic demand as per NBC 105: 2019. Due to the presence of seismic bands at different levels along the height, the main failure modes in these buildings is shear sliding of masonry walls at the wall-band interfaces. However, addition of vertical confinement at all corners would further improve the global behaviour and ductility.

➢ The PGA capacity for 'ultimate' limit state for the PRE-SMM typology is very low, even with good material quality, compared to the seismic hazard in Nepal. Hence seismic strengthening of these buildings throughout the country (even in the unaffected districts) is urgent.

➢ Sensitivity analysis on the uncertainty related to the material quality shows that the seismic capacity can vary greatly from one building to next due to the lack of quality control in SMM construction. Hence material preparation and workmanship should be given importance in the construction of these buildings.

➢ As the retrofitting of PRE-SMM buildings (both partially damaged and undamaged) is currently ongoing, the future work will focus on the study of comparative improvement in the seismic capacity of these buildings after strengthening.

➢ Also, as a 'consequence model' applicable to Nepalese residential buildings is not currently available, the 2015 damage data and repair/reconstruction cost for different typologies of buildings will be collected and analysed in order to develop a country-specific consequence model for Nepalese constructions.

REFERENCES

Adhikari, R. K., Bhagat, S. and Wijeyewickrema, A. C. (2015). Damage scenario of reinforced concrete buildings in the 2015 Nepal earthquakes, *New Technologies for Urban Safety of Mega Cities in Asia*, USMCA 2015, Kathmandu, Nepal

Adhikari, R. and D'Ayala, D. (2019). Applied Element Modelling and Pushover Analysis of Unreinforced Masonry Buildings with Flexible Roof Diaphragm. *7th International Conference on Computational Methods in Structural Dynamics and Earthquake Engineering*, Crete, Greece

Ahmad, N., Ali, Q., Crowley, H., & Pinho, R. (2014). Earthquake loss estimation of residential buildings in Pakistan. *Natural hazards*, 73(3), 1889-1955

ASI (2018). Extreme Loading for Structures V6. Applied Science International LLC, Durham, N.C., USA.

Bal, İ. E., Crowley, H., Pinho, R. and Gülay, F. G. (2008). Detailed assessment of structural characteristics of Turkish RC building stock for loss assessment models. *Soil Dynamics and Earthquake Engineering*, 28(10-11), 914-932

Bhagat S., Samith Buddika H.A.D., Adhikari R.K., Shrestha A., Bajracharya S., Joshi R., Maharjan R. and Wijeyewickrema A.C. (2018). Damage to cultural heritage structures and buildings due to the 2015 Nepal Gorkha earthquake, *Journal of Earthquake Engineering*, 22(10): 1861-1880

Bothara, J. and Brzev, S. (2011). A tutorial: Improving the seismic performance of stone masonry buildings. Earthquake Engineering Research Institute

Bothara J.K., Giongo I., Ingham J., Dizhur, D. (2018a). Masonry building design for earthquake-affected remote areas of Nepal, *10th Australian Masonry Conference*, Sydney, Australia.

Bothara J.K., Giongo I., Ingham J., Dizhur D. (2018b). Numerical study on partially-reinforced semi-dressed stone masonry for build-back-better in Nepal, *10th International Masonry Conference*, Milan, Italy

Bothara J.K., Ahmad, N., Ingham J., Dizhur D. (2019). Experimental seismic testing of semi-reinforced stone masonry building in mud mortar, *2019 Pacific Conference on Earthquake Engineering and Annual NZSEE Conference*, Auckland, New Zealand

Build Change (2017). Retrofit Type Design Approved: A Turning Point in Nepal's Reconstruction! Available at: https://buildchange.org/retrofit-type-design-approved-a-turning-point-in-nepals-reconstruction/ (Accessed 10/10/2019)

Build Change (2019). Laboratory Test Report on Stone Masonry in Mud Mortar. Build Change Report

Chaulagain, H., Rodrigues, H., Jara, J., Spacone, E. and Varum, H. (2013). Seismic response of current RC buildings in Nepal: a comparative analysis of different design/construction, *Engineering Structures*, 49, 284-294

Chaulagain, H., Rodrigues, H., Spacone, E. and Varum, H. (2015). Assessment of seismic strengthening solutions for existing low-rise RC buildings in Nepal, *Earthquakes and Structures*, 8(3), 511-539

D'Ayala, D. (2004). Correlation of fragility curves for vernacular building types: houses in Lalitpur, Nepal and in Istanbul, Turkey, *13th World Conference of Earthquake Engineering*, Vancouver, Canada

D'Ayala, D. (2013). Assessing the seismic vulnerability of masonry buildings. *In Handbook of seismic risk analysis and management of civil infrastructure systems* (pp. 334-365). Woodhead publishing

D'Ayala D. and Bajracharya, S.S.R. (2003). HOUSING REPORT: Traditional Nawari house in Kathmandu Valley, World Housing Encyclopedia

D'Ayala, D. and Kishali, E. (2012). Analytically derived fragility curves for unreinforced masonry buildings in urban contexts. *15th world Conference of Earthquake Engineering*, Lisbon, Portugal

D'Ayala, D. and Speranza, E. (2003). Definition of collapse mechanisms and seismic vulnerability of historic masonry buildings. *Earthquake Spectra*, 19(3), 479-509

Dizhur, D., Dhakal, R. P., Bothara, J. and Ingham, J. (2016). Building typologies and failure modes observed in the 2015 Gorkha (Nepal) earthquake. *Bulletin of the New Zealand Society for Earthquake Engineering*, 49(2), 211-232

EN 1996-1-1: Eurocode 6 – Design of masonry structures - Part 1-1: General rules for reinforced and unreinforced masonry structures

EN 1998-1: Eurocode 8 – Design of structures for earthquake resistance - Part 1: General rules, seismic actions and rules for buildings

FEMA (2000). FEMA 356: Pre-standard And Commentary for the Seismic Rehabilitation of Buildings, Federal Emergency Management Agency, Washington, D.C., USA.

FEMA (2009). FEMA P695: Quantification of Building Seismic Performance Factors, Federal Emergency Management Agency, Washington, D.C., USA.

FEMA (2012). Multi-hazard Loss Estimation Methodology, Earthquake Model, HAZUS®–MH 2.1 Technical Manual, Federal Emergency Management Agency, Washington, D.C., USA.

Gautam D., Rodrigues H., Bhetwal K.K., Neupane P. and Sanada Y. (2016). Common structural and construction deficiencies of Nepalese buildings. *Innovative Infrastructure Solutions*, 1(1), p.1

Goda, K., Kiyota, T., Pokhrel, R. M., Chiaro, G., Katagiri, T., Sharma, K. and Wilkinson, S. (2015). The 2015 Gorkha Nepal earthquake: insights from earthquake damage survey. *Frontiers in Built Environment*, 1, 8

Guragain, R. (2015), Development of Earthquake Risk Assessment System for Nepal, PhD Thesis, University of Tokyo

Hill, M. P. and Rossetto, T. (2008). Do existing damage scales meet the needs of seismic loss estimation. *14th World Conference on Earthquake Engineering*, Beijing, China

HRRP (2017), District Profile – Sindhupalchok (as of 10 Apr 2017), Housing Recovery and Reconstruction Platform. Available at: https://reliefweb.int/sites/reliefweb.int/files/resources/170410_Sindhupalchok.pdf (Accessed 10/10/2019)

HRRP (2018). Housing Typologies: Earthquake Affected Districts. Housing Recovery and Reconstruction Platform (HRRP), Nepal

Lagomarsino, S., Penna, A., Galasco, A. and Cattari, S. (2013). TREMURI program: an equivalent frame model for the nonlinear seismic analysis of masonry buildings. *Engineering Structures*, 56, 1787-1799

Lemos, J.V. and Campos Costa A. (2017). Simulation of shake table tests on out-of-plane masonry buildings. Part (V): discrete element approach. *International Journal of Architectural Heritage*, 11(1): 117-124

Lourenço, P. J. B. B. (1997). Computational strategies for masonry structures. PhD Thesis, Technische Universiteit Delft

Malomo D., Pinho R. and Penna A. (2018). Using the applied element method for modelling calcium silicate brick masonry subjected to in-plane cyclic loading. *Earthquake Engineering & Structural Dynamics*, 47(7): 1610-1630

MSJC (2019). Building Code Requirements and Specification for Masonry Structures, Masonry Standards Joint Committee

NBC 203 (2015). Guidelines for Earthquake Resistant Building Construction: Low Strength Masonry, Nepal National Building Code, Government of Nepal

NBC 201 (1994). Mandatory Rules of Thumb Reinforced Concrete Buildings with Masonry Infill, National Building Code, Government of Nepal

Nepali Times (2018a). Building homes on a deadline. Available at: https://www.nepalitimes.com/here-now/building-homes-on-a-deadline/ (Accessed 10/10/2019)

Nepali Times (2018b). Lost in reconstruction. Available at: https://www.nepalitimes.com/banner/lost-in-reconstruction/ (Accessed 10/10/2019)

NPC (2015). Nepal Earthquake 2015: Post Disaster Needs Assessment, Volume A: Key Findings, National Planning Commission, Government of Nepal

NRA (2015). Design Catalogue for Reconstruction of Earthquake Resistant Houses: Volume I, Notational Reconstruction Authority, Nepal

NRA (2016a). Structures Damage Grade at 14 Earthquake Affected Districts, National Reconstruction Authority, Nepal

NRA (2016b). Nepal Earthquake 2015: Post Disaster Recovery Framework (2016-2020), National Reconstruction Authority, Government of Nepal

NRA (2016c). Inspection Manual for Houses That Has Been Built Under Housing Reconstruction Programme, National Reconstruction Authority, Government of Nepal

NRA (2017) CORRECTION/ EXCEPTION MANUAL for MASONRY STRUCTURE for houses that have been built under the HOUSING RECONSTRUCTION PROGRAMME, National Reconstruction Authority, Nepal

NRA (2019a). Statistics of reconstruction in Sindhupalchowk district, Central Level Project Implementation Unit, National Reconstruction Authority, Nepal

NRA (2019b). Central Level Project Implementation Unit Official Website. Available at: http://202.45.144.197/nfdnfis/clpiu/index.htm (Accessed 10/10/2019)

NSC (2016), Nepal National Seismological Centre Official Website. Available at: (http://www.seismonepal.gov.np/index.php?listId=161) (Accessed on 10/10/2019).

Parajuli, R. R. and Kiyono, J. (2015). Ground motion characteristics of the 2015 Gorkha earthquake, survey of damage to stone masonry structures and structural field tests. *Frontiers in Built Environment*, 1, 23

Pun, R (2015), Improvement in Seismic Performance of Stone Masonry Using Galvanized Steel Wire, PhD Thesis, University of Technology

Sharma, K., Apil, K. C., Subedi, M., & Pokharel, B. (2018). Post Disaster Reconstruction after 2015 Gorkha Earthquake: Challenges and Influencing Factors. *Journal of the Institute of Engineering*, 14(1), 52-63

Silva, V., Akkar, S., Baker, J., Bazzurro, P., Castro, J.M., Crowley, H., Dolsek, M., Galasso, C., Lagomarsino, S., Monteiro, R. and Perrone, D. (2019). Current Challenges and Future Trends in Analytical Fragility and Vulnerability Modelling. *Earthquake Spectra* In-Press

Spence, R. and D'Ayala, D. (1999). Damage Assessment and Analysis of the 1997 Umbria-Marche Earthquakes, *Structural Engineering International*, 9:3, 229-233

Thapa, D. R. and Wang, G. (2013). Probabilistic seismic hazard analysis in Nepal. *Earthquake Engineering and Engineering Vibration*, 12(4), 577-586

Tomazevic, M. (1999) Earthquake-resistant design of masonry buildings. Imperial College Press, London

USGS (2015), M 7.8 - 36km E of Khudi, Nepal. U.S. Geological Survey Official Website. Available at: http://earthquake.usgs.gov/earthquakes/eventpage/us20002926#general (Accessed 10/10/2019)

Varum, H., Dumaru, R., Furtado, A., Barbosa, A. R., Gautam, D. and Rodrigues, H. (2018). Seismic performance of buildings in Nepal after the Gorkha earthquake. *In Impacts and insights of the Gorkha earthquake* (pp. 47-63). Elsevier

Wang, M., Liu, K., Lu, H., Shrestha, H., Guragain, R., Pan, W. and Yang, X. (2018). In-plane cyclic tests of seismic retrofits of rubble-stone masonry walls. *Bulletin of Earthquake Engineering*, 16(5), 1941-1959

Wilkinson, S., DeJong, M., Novelli, V., Burton, P., Tallet-Williams, S., Whitworth, M., Guillermo, M., White, T., Trieu, A., Ghosh, B. and Datla, S. (2019), The Mw 7.8 Gorkha, Nepal Earthquake of the 25th April 2015: A Field Report By EEFIT, Institution of Structural Engineers

Yamin, L. E., Hurtado, A. I., Barbat, A. H. and Cardona, O. D. (2014). Seismic and wind vulnerability assessment for the GAR-13 global risk assessment. *International journal of disaster risk reduction*, 10, 452-460

ANNEX A

Table A.1. Summary of the 22 ground motion records from FEMA P695 Far-Field record set.

SN	Event name and year	M_w	Recording station	Ground motion ID
1	Northridge, 1994	6.7	Beverly Hills - Mulhol	MUL279
2	Northridge, 1994	6.7	Canyon Country-WLC	LOS270
3	Duzce, Turkey, 1999	7.1	Bolu	BOL090
4	Hector Mine	7.1	Hector	HEC090
5	Imperial Valley, 1979	6.5	Delta	DLT352
6	Imperial Valley, 1979	6.5	El Centro Array #11	E11230
7	Kobe, Japan, 1995	6.9	Nishi-Akashi	NIS090
8	Kobe, Japan, 1995	6.9	Shin-Osaka	SHI090
9	Kocaeli, Turkey, 1999	7.5	Duzce	DZC270
10	Kocaeli, Turkey, 1999	7.5	Arcelik	ARE090
11	Landers	7.3	Yermo Fire Station	YER360
12	Landers	7.3	Coolwater	CLW-TR
13	Loma Prieta	6.9	Capitola	CAP090
14	Loma Prieta	6.9	Gilroy Array #3	GO3090
15	Manjil, Iran	7.4	Abbar	ABBAR-T
16	Superstition Hills	6.5	El Centro Imp. Co.	ICC090
17	Superstition Hills	6.5	Poe Road (temp)	POE360
18	Cape Mendocino	7.0	Rio Dell Overpass	RIO360
19	Chi-Chi, Taiwan	7.6	CHY101	CHY101-N
20	Chi-Chi, Taiwan	7.6	TCU045	TCU045-N
21	San Fernando	6.6	LA - Hollywood Stor	PEL180
22	Friuli, Italy	6.5	Tolmezzo	TMZ270